AD-A156 852 HIGH FLUX CALORIMETRY(U) SCIENCE APPLICATIONS 1/2
INTERNATIONAL CORP MCLEAN VA M MCDONNELL ET AL.
05 MAY 84 SAIC-84/1104 DNA-TR-84-183 DNA001-82-C-0185
UNCLASSIFIED F/G 14/2 NL

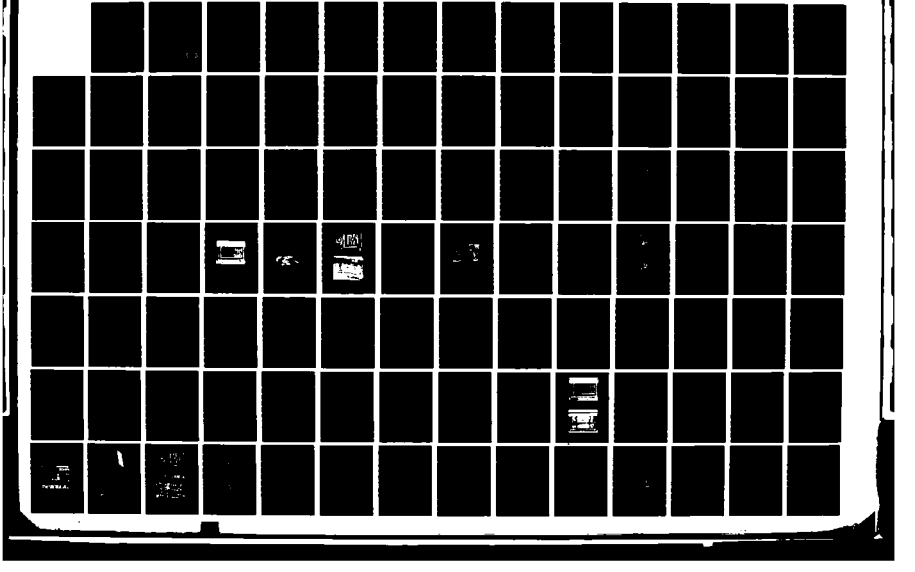

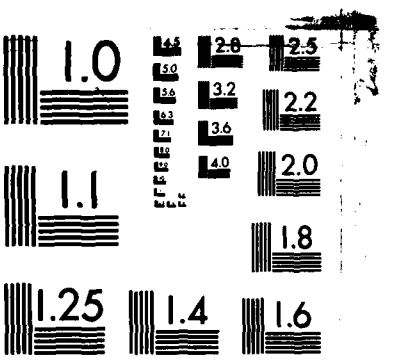

(2)

DNA-TR-84-183

HIGH FLUX CALORIMETRY

M. McDonnell
N. Olson
S. Woods
Science Applications International Corp.
P.O. Box 1303
McLean, VA 22101-1303

5 May 1984

Technical Report

CONTRACT No. DNA 001-82-C-0185

THIS WORK WAS SPONSORED BY THE DEFENSE NUCLEAR AGENCY
UNDER RDT&E RMSS CODE B345083466 G55AMXGR00004 H2590D.

Prepared for
Director
DEFENSE NUCLEAR AGENCY
Washington, DC 20305-1000

Destroy this report when it is no longer needed. Do not return to sender.

PLEASE NOTIFY THE DEFENSE NUCLEAR AGENCY, ATTN: STTI, WASHINGTON, DC 20305-1000, IF YOUR ADDRESS IS INCORRECT, IF YOU WISH IT DELETED FROM THE DISTRIBUTION LIST, OR IF THE ADDRESSEE IS NO LONGER EMPLOYED BY YOUR ORGANIZATION.

UNCLASSIFIED

SECURITY CLASSIFICATION OF THIS PAGE *(When Data Entered)*

REPORT DOCUMENTATION PAGE		READ INSTRUCTIONS BEFORE COMPLETING FORM
1. REPORT NUMBER DNA-TR-84-183	2. GOVT ACCESSION NO. AD-A156852	3. RECIPIENT'S CATALOG NUMBER
4. TITLE *(and Subtitle)* HIGH FLUX CALORIMETRY		5. TYPE OF REPORT & PERIOD COVERED Technical Report 6. PERFORMING ORG. REPORT NUMBER SAI-84/1104
7. AUTHOR(s) M. McDonnell N. Olson S. Woods		8. CONTRACT OR GRANT NUMBER(s) DNA 001-82-C-0185
9. PERFORMING ORGANIZATION NAME AND ADDRESS Science Applications International Corp. P.O. Box 1303 McLean, Virginia 22101-1303		10. PROGRAM ELEMENT, PROJECT, TASK AREA & WORK UNIT NUMBERS Task G55AMXGR-00004
11. CONTROLLING OFFICE NAME AND ADDRESS Director Defense Nuclear Agency Washington, DC 20305-1000		12. REPORT DATE 5 May 1984 13. NUMBER OF PAGES 150
14. MONITORING AGENCY NAME & ADDRESS*(if different from Controlling Office)*		15. SECURITY CLASS *(of this report)* UNCLASSIFIED 15a. DECLASSIFICATION/DOWNGRADING SCHEDULE N/A since UNCLASSIFIED

16. DISTRIBUTION STATEMENT *(of this Report)*

Approved for public release; distribution is unlimited.

17. DISTRIBUTION STATEMENT *(of the abstract entered in Block 20, if different from Report)*

18. SUPPLEMENTARY NOTES

This work was sponsored by the Defense Nuclear Agency under RDT&E RMSS Code B345083466 G55AMXGR00004 H2590D.

19. KEY WORDS *(Continue on reverse side if necessary and identify by block number)*

Calibration
Radiant Thermal Sources
Calorimetry
High Flux Simulation
Flashlamps
Quartz Lamps
Graphite Radiators

20. ABSTRACT *(Continue on reverse side if necessary and identify by block number)*

Four basic radiant energy sensing concepts were examined for applicability to high flux calorimetry measurement. Calorimeters were cross calibrated using five radiant energy sources. Commercial availability was an important criterion. A commercial calorimeter with a specia ly designed and fabricated adapter appears to be an acceptable calorimeter for High Flux Measurements.

DD FORM 1 JAN 73 1473 EDITION OF 1 NOV 65 IS OBSOLETE

UNCLASSIFIED

SECURITY CLASSIFICATION OF THIS PAGE *(When Data Entered)*

SUMMARY

The present work has examined calorimetry concepts for use with a high flux radiant thermal source employing flashlamps. Sensing elements of various calorimeters examined included: thermocouples; photodiodes; thermistors; and, pyroelectric elements. Calorimeters were cross calibrated and characterized using five different radiant sources to provide various fluxes, fluences, thermal pulse shapes or source solid angles. These sources included: a resistively heated graphite element; a quartz envelope tungsten filament lamp bank at the DNA Tri Service Thermal Flash Test Facility; a commercially available portable high intensity tungsten lamp; photographic flashbulbs and; the DNA funded, SAI fabricated, Flashlamp Source (FLS).

The calorimeter concept recommended for use at high fluxes from the FLS is a HyCal calorimeter with a specially designed, fabricated and calibrated attenuator to reduce the flux on the calorimeter to the proper range in a predictable and repeatable fashion. This concept has the advantages of commercial availability, community acceptance of the basic instrument, ease of use, low cost and good response times.

TABLE OF CONTENTS

LIST OF ILLUSTRATIONS

LIST OF ILLUSTRATIONS (Continued)

LIST OF TABLES

SECTION 1 INTRODUCTION

The survivability and vulnerability of equipment threatened by exposure to nuclear weapons effects is a matter of concern to many Defense programs. Much information has been gained on system vulnerability through nuclear weapons tests and, since the nuclear test ban, through high explosive simulations. However, the simulation of the thermal effects of nuclear weapons, especially at high fluxes, has remained a serious problem.

Over the last few years Science Applications, Inc., (SAI) has been developing a high intensity thermal simulator based on the use of flashlamps. (The high directionality and limited spectrum of lasers makes them inferior simulation sources in spite of their high fluxes and intermediate fluences.) The Flashlamp Simulator (FLS) is expected to produce fluxes as high as 2000 cal/cm^2 sec (8.4 KW/cm^2), far in excess of any previous simulators. Since such simulators have not been available, instrumentation capable of characterizing the performance of the flashlamp system does not exist. Consequently, accurate source characterization and testing over the full range of expected flashlamp system capabilities is not presently possible.

In the present work, SAI, which has been developing instrumentation for the defense community for over eight years, has developed preliminary concepts for calorimeters capable of measuring fluxes up to 2000 cal/cm^2 sec. These approaches are based on proven principles which have served the thermal test community well for years. Other concepts hold promise of being able to provide the fast response necessary to characterize the short pulse durations expected during the flashlamp system operation.

The DNA/BMD sponsored high flux nuclear thermal radiation simulator was expected to be ready for first operational testing in April 1982. The system uses high intensity flashlamps to simulate the intense thermal radiation environment produced by the nuclear fireball. Because thermal sources of this intensity have not been available up to now, instrumentation for this regime has not yet been developed.

The thermal test community has developed instrumentation which is quite suitable for the moderate, and relatively constant, flux conditions. However, the standard "high" flux slug type and asymptotic calorimeters do not operate well above 200 cal/cm^2 sec flux ranges and have time constants which are much too long (0.2 sec) for use with the new flashlamp system. Fast response photometers, employing photodiodes, suffer from a limited and non uniform spectral response which precludes their independent use as calorimeters and introduces severe uncertainties even when augmented by spectrometers and energy balance calculations in closed and controllable systems.

Fast response high flux calorimetry therefore presents a serious problem which should be approached initially with a number of techniques each having promise of potential success after a limited initial investigation and each capable of being cross calibrated with existing instrumentation at lower fluxes provided by sources which are better characterized than the new flashlamp system.

Since calorimeters respond to temperature increases in a specific sensing volume, their response to a constant flux is essentially asymptotic. Calorimeters intended for low flux ranges can have small sensing volumes and fast response times. Those used at high fluxes generally have higher thermal inertia and slower responses. One technique for achieving better response times at higher fluxes would be to use a low range fast response calorimeter and attenuate the incident radiation by means of an absorber or collimator. An absorber is not recommended for the flashlamp system since it would absorb in some set spectral region while the spectral form of the flashlamp system output is expected to be time dependent within each simulation, and power density (or input current) dependent for different simulations.

The type of collimator design chosen is shown in Figure 1. The small inlet aperture is shaped to allow acceptance of large angle radiation from the essentially diffuse flashlamp source and the entire collimator is made of a high reflectance material. It is important that the front surface of the collimator also be highly reflective since a high reflectivity will greatly reduce the energy absorbed into the collimator and prevent melting at high fluences.

COLLIMATOR
WITH CONICAL INTERIOR

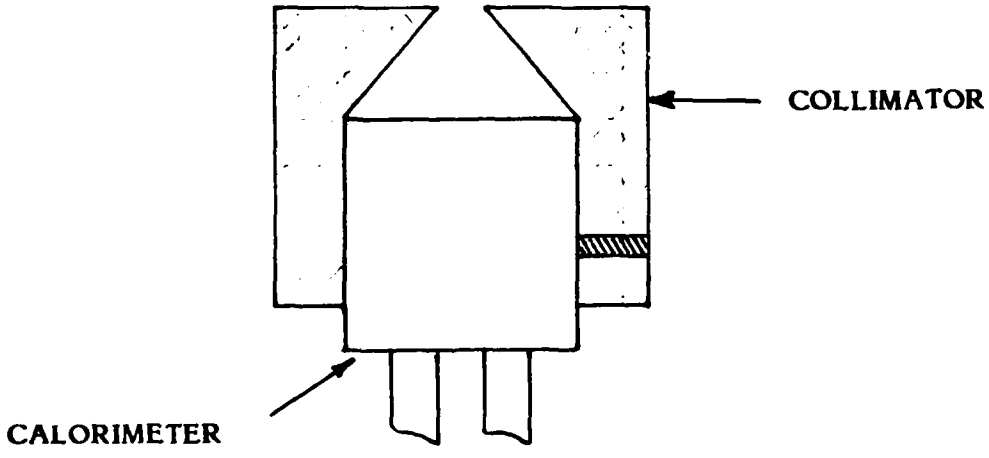

FIGURE 1. COLLIMATOR DESIGN

The internal shape of the collimator is also important. Since flux (as defined and as measured by the calorimeter) is the integral of the perpendicular component of the incident radiation, care must be taken to maintain the diffuse nature of the radiation incident at the aperture. The cavity will attempt to conform to the shape of a truncated cone with its entrance being the internal area of the aperture and its exit being the area of the calorimeter. This should provide a flux uniformity on the detector which is comparable to that at the aperture with a minimum number of reflections and associated reflective losses.

Aside from the fact that the basic calorimeter is readily available this modification approach recommends itself for a number of reasons. First, since the portion of the instrument which faces into the test chamber is not a sensing element, it can be reflectively coated rather than blackened. The maximum rate of heat input to the collimator could then be only 100 cal/cm^2 sec (i.e., 5% absorptivity in a 2000 cal/cm^2 sec flux) and the maximum energy deposition would only be 20 cal/cm^2 based on the maximum phase II system fluence of 400 cal/cm^2. Second, the present thermal test community will have confidence in the performance of an instrument which relies primarily on a well understood and commonly available detector. Furthermore, this will facilitate cross calibration with the types of instruments future flashlamp system users might be expected to own.

In contrast to the above design, Figure 2 shows a simple pin hole attenuator. The relatively small acceptance angle presented by the pin hole eliminates the overall response of the instrument to a large solid angle of diffuse incident radiation. A cylindrical cavity with a small length to diameter ratio results in a non uniform irradiation of the calorimeter while a large L/D spreads the radiation over the calorimeter surface but involves multiple reflections and a further distortion of the initially diffuse radiation into a more direct beam. Under such circumstances even a highly reflective coating cannot significantly improve the design.

Other calorimeter concepts were also examined in the present effort which were based on various sensing elements. These included pyroelectric sensors, thermistors, slug type calorimeters and null point detectors. Each of these will be discussed in the present report as the experimental program is related.

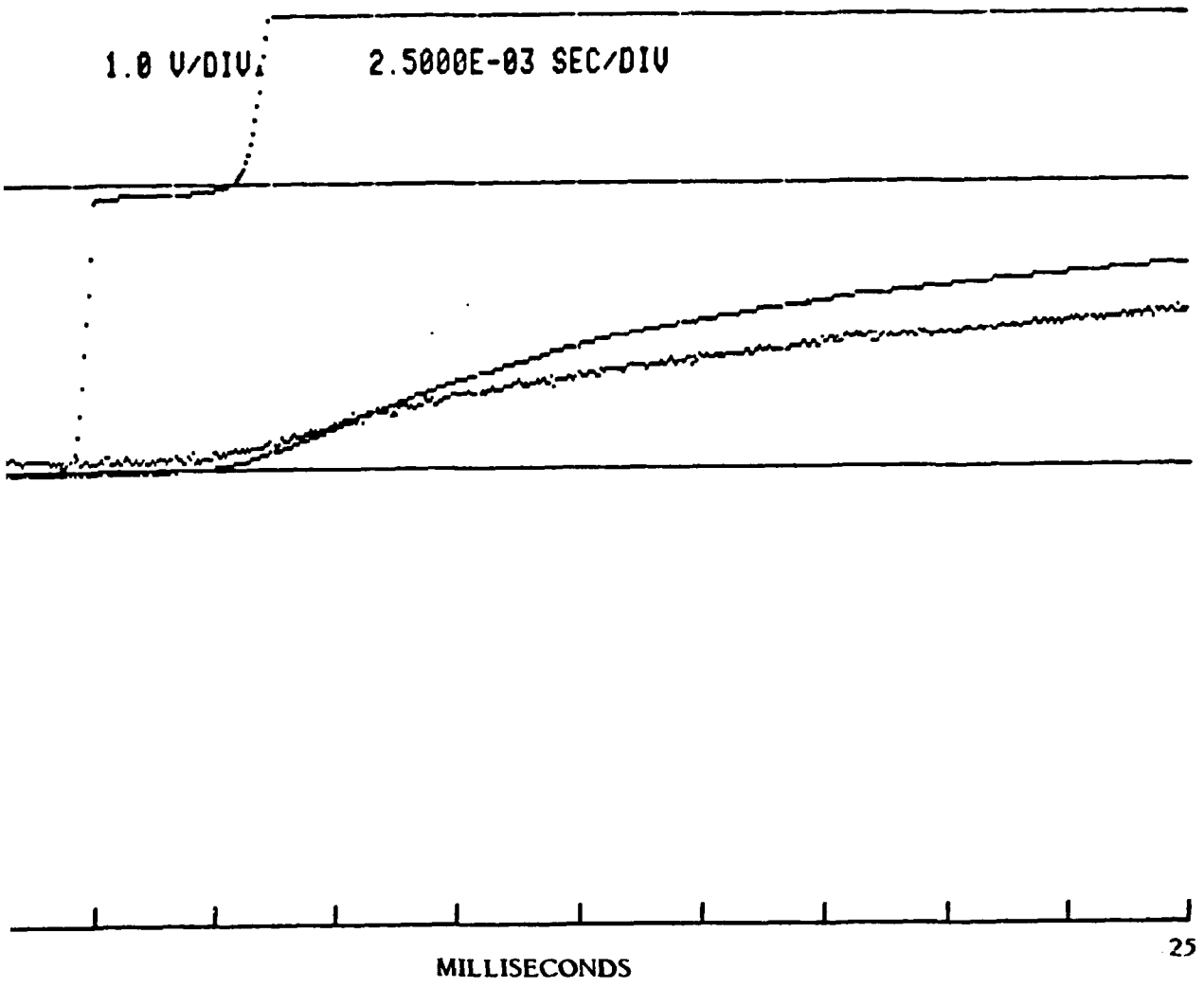

FIGURE 8. EXPANDED VIEW OF FIRST 25 MS OF FIGURE 7

9/2/82
Run #2
5. Batteries

two calorimeters are evident from the traces. The Null Point calorimeter, which possesses a thermocouple attached to a finite thermal mass, registers an ever larger response as it becomes heated while the water cooled Hycal calorimeter asymptotically approaches a fixed response for a fixed input. Ninety percent of the Hycal calorimeter response occurs in approximately 40 ms. Figure 8 is an expanded plot of 7 showing detail in the rise of the shutter and the calorimeter responses. While careful examination of the traces in Figure 8 indicates that the CARRS shutter had fully exposed the calorimeters to the input thermal flux before the calorimeters started to respond it was clear that the shutter opening time was not sufficiently fast to reveal the response of the silicon photodetectors.

2.1.2 Flashbulb Testing

While reasonable fluxes and large fluences are available from the CARRS, the rise time of the thermal output of this source, even when mechanically shuttered cannot approximate that expected from the single lamp pulses developed by the FLS without prohibitive modifications to the shuttering mechanism. Furthermore, there is no capability for repeating the pulse rapidly enough to test the recovery time of the detectors much less to duplicate the firing sequence of the FLS lamp bank.

A fast rising repetitive source was therefore fabricated using standard Sylvania "Blue Dot" photographic flashbulbs with the blue tint removed. Figure 9 shows a schematic of the experimental layout. An Apple II microcomputer was used to trigger the relay which fired the flashbulbs and to simultaneously trigger the LeCroy data acquisition system. A sample output from the one flashbulb is shown in Figures 10 and 11. The upper trace in each case is the reference calorimeter, the lower trace was produced by the photodiode from the IS detector without the integrating sphere. Figure 10 resulted from a blue coated flashbulb while Figure 11 resulted from a flashbulb with the coating removed.

A number of points can be observed in these figures. First one can see the extremely fast response of the photodiode compared to the calorimeter. However when the photodiode is not shielded by the integrating sphere (which provided an

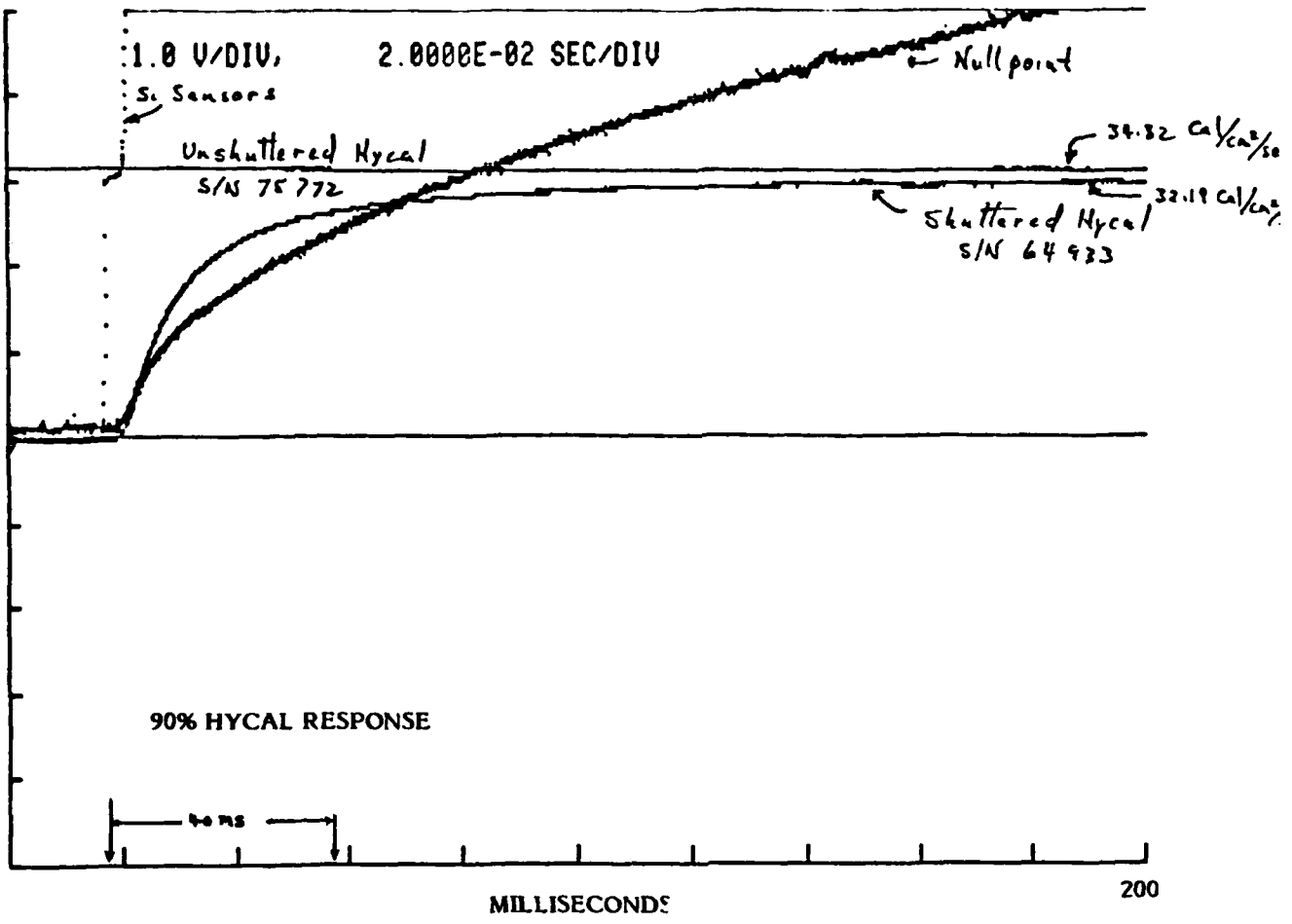

SAMPLE RATE - 20 KHZ

FIGURE 7. HYCAL-NULL POINT CROSS CALIBRATION

9/2/82
Run #2
5 Batteries

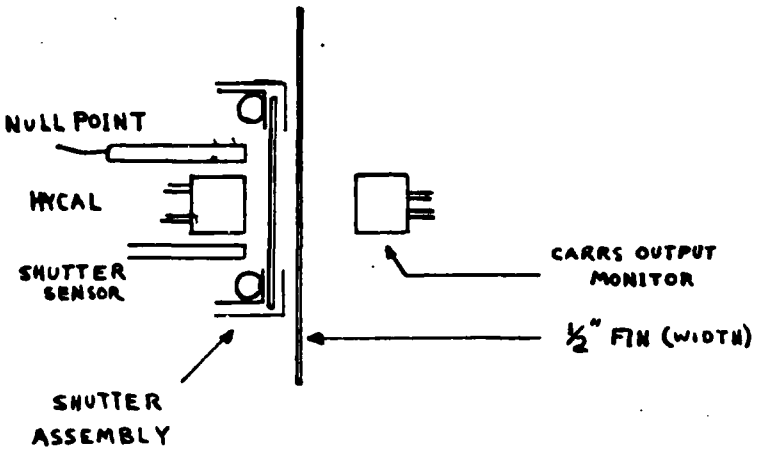

FIGURE 6. SHUTTER ARRANGEMENT

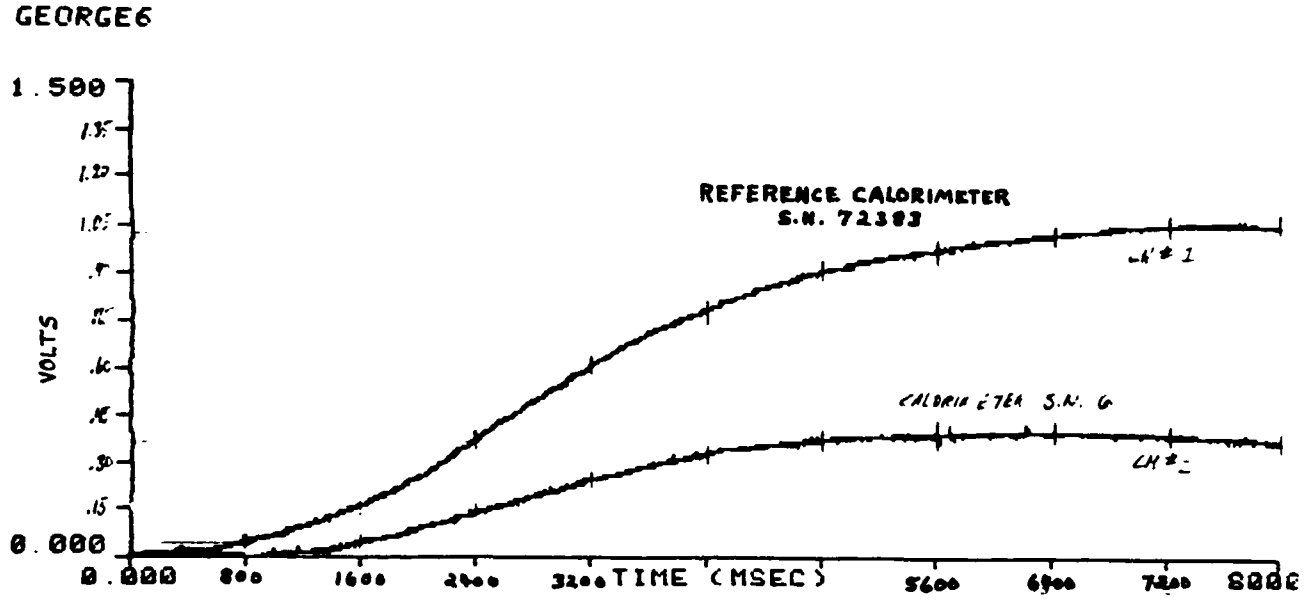

Calorimeters spaced 1.5 mm on center from a 30.1 mm carbon fin

FIGURE 5. CALORIMETER CALIBRATION DATA

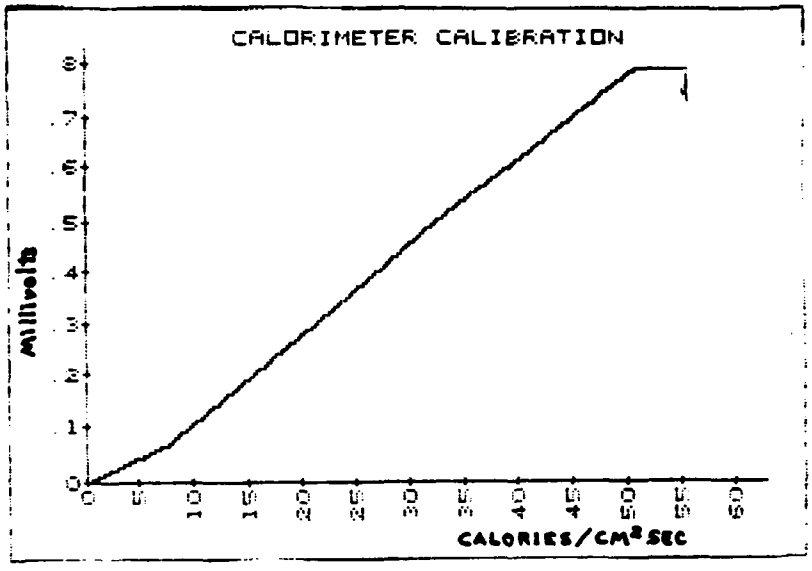

FIGURE 4. SAMPLE CALIBRATION CURVE

TABLE 1

Amplifier Calibration Constants

	A	B
amp # 1, S.N. 41011	- 5.420094E-04	.499553
amp # 3, S.N. 41010	5.788728E-03	.499619
amp # 3, S.N. 41012	1.527294E-04	.498672

A sample calorimeter calibration curve is shown in Figure 4.

The carbon rod used was actually a fin 30.1 mm in width to provide an essentially 2π source to the calorimeters which were positioned 1.5 mm from the fin surface. Figure 5 shows a superposition of two sample outputs from one test. In this case the upper trace is that of the reference calorimeter and the lower trace is that of the Medtherm calorimeter provided by John Dishon.

The CARRS was originally designed to simulate the output of large yield nuclear weapons and the thermal inertia of the relatively massive carbon radiating element allowed it to closely match the slowly varying pulse shape from such weapons. This slow variation was not however useful in estimating the response times of the calorimeters. For this reason a shutter was incorporated into the CARRS design. The shutter was a simple gravity operated blade with a window 10 inches wide. When operated the window moved between the carbon rod and the detectors at a velocity of 179 inches per second. Pulses of variable duration (1 to 20 seconds) could be obtained by opening and closing the shutter. This arrangement is shown in Figure 6 with all other aspects of the system identical to those shown in Figure 3.

Figures 7 and 8 show the results of one such test. In Figure 7 the upper most trace was obtained from the silicon photodetectors used to time the rise of the shutter and mark the onset of the step input thermal pulse. The CARRS was monitored for output variations with a reference calorimeter (SN# 75772). This trace (unshuttered Hycal) appears as an unchanging horizontal line in Figure 7. The remaining traces show the response times of the Accurex Null Point calorimeter (montonically increasing trace) and a Hycal calorimeter (SN# 64933). The different natures of the

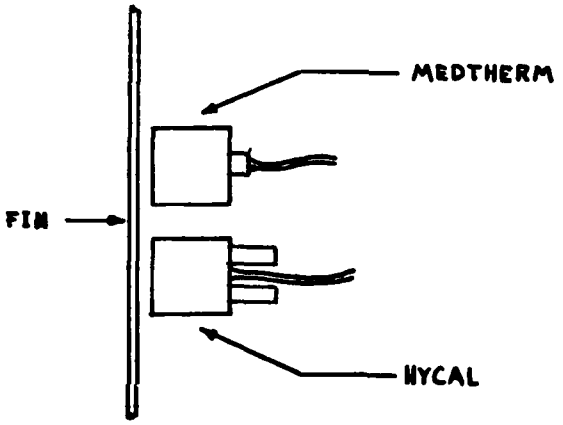

FIGURE 3. CROSS CALIBRATION MOUNTING

However, other sources were used to make specific measurements of certain detector characteristics. Among these were:

- o A collimated high intensity torch lamp whose high directionality allowed determination of the angular dependence of the calorimeter responses. (Section 2.1.4)

- o A photographic flashbulb source whose sharp rise times were useful in determining the response and recovery times of the calorimeters. (Section 2.1.2)

2.1.1 CARRS Testing

These tests employed the SAI designed and fabricated Carbon Rod (or fin) Radiating Source (CARRS) described in Section 2.1.

For cross calibration purposes calorimeters were positioned and connected as shown in Figure 3. The data acquisition system chosen was a LeCroy microcomputer. Two calorimeters were employed in each test, the reference calorimeter (Hycal S.N. 72383, nominally 1000 BTU/ft^{2}sec or 29.81 cal/cm^{2}sec/mv and previously calibrated to 1 mv = 110 BTU/ft^{2}sec) and the calorimeter to be calibrated. Amplifier calibration was of the form

$$F(x) = A + Bx$$

where F(x) is in volts and x, the detector output, is in millivolts.

Three Ectron 500 series D.C. amplifiers were used during the tests. Table 1 identifies them and their respective constants as used in the above equation.

2.1 RADIANT THERMAL SOURCES

The problem of developing a calibrated calorimeter for use with an uncalibrated source (i.e., the new FLS) required the availability of other radiant sources for at least four reasons:

1. The repeatability of the FLS output was unknown

2. The output spectral shape and time dependence was unknown

3. The space and time uniformity of the flux in the exit plane of the FLS was uncertain

4. The FLS was still in shakedown tests and its availability during the test program was expected to be driven by its own, higher priority, development.

It was planned from the beginning to employ other sources in the test program, most notably:

- The SAI designed and fabricated CARRS or Carbon Rod Radiating Source, employing a battery bank to resistively heat a carbon radiating element to a high temperature. (Section 2.1.1)

- The QLB or Quartz Lamp Bank source, used at the DNA Tri Service Thermal Flash Test Facility operated by the University of Dayton Research Institute (UDRI), employing a DC driven bank of tungsten filament, quartz enclosed lamps. The tests performed on the QLB were done under a UDRI subcontract. The UDRI report is contained in a separate appendix (Appendix A). Excerpts from the appendix are included in the main report for the sake of continuity and completeness. (Section 2.1.5)

surface to which the thermocouple is attached follows that of the front surface. The Null Point Detector has been used successfully in temperature measurements of simulated nose cone reentry problems. With a good absorbing coating for broad spectral response and a small sensing volume the ND held promise for a fast response calorimeter. Unfortunately its design stresses temperature measurement rather than flux or fluence and computer interpretation of the output is required for it to be used as a calorimeter. Furthermore, when the duration of the thermal pulse is long enough (greater than .17 seconds for the present detector) to cause the approximation of an infinite front surface to fail, the usefulness of the signal as being representative of the front surface temperature seriously degrades. The ND was provided by Accurex Aerotherm of Mountain View, California.

4. The Pyroelectric Detector (PD) uses the fact that some materials generate an electric field when subjected to a temperature gradient. The output signal is therefore proportional to the flux gradient and must be integrated in order to obtain the flux. The PD is inherently a fast response sensor with a broad and flat spectral sensitivity but they are expensive, especially if purchased in a complete detecting system, and have a reputation for delicacy which has hampered their acceptance not only in field work but even in the laboratory.

5. The Thermistor Detector (TD) is based on the fact that various materials have a strong rapid and reproducible resistivity dependence with temperature and can be produced with a uniform broad band spectral absorbtivity. Theoretically and to a first approximation the temperature increase during irradiation should be relatable to the cumulative incident fluence and hence the flux. The detectors constructed did not perform well and it is assumed that conductive and convective heat phenomena were, and may inherently be, too irreproducible to allow accurate calibration of such devices.

SECTION 2 CALORIMETER CROSS CALIBRATION

The development of any new calorimeter concept first requires the calibration of a standard reference. SAI possesses water cooled Hycal asymptotic calorimeters previously calibrated by the manufacturer with reference instruments traceable to the National Bureau of Standards. Due to the range of sources and fluxes to be used in the calorimeter development and the preference to have a resulting instrument which was based on an off the shelf, and hence community accepted, design, a number of existing calorimeter concepts were cross calibrated with the Hycal standards. These included:

1. The Integrating Sphere (IS) calorimeter currently in use with the Flashlamp System (FLS). It consists of a photodiode mounted in an integrating sphere and was fabricated by SAI for use with the FLS. The response time of the photodiode is excellent but the spectral response is limited. Thus, while pulse shape is well characterized, determination of the total energy in the pulse requires accurate knowledge and stability of the source spectrum. The FLS also uses an SAI designed and fabricated calorimeter employing a large graphite sensing element and standard thermocouple instrumentation but this was too large for use with the sources to be employed in the test program.

2. The Medtherm Calorimeter (MC) which is a commercially available, uncooled, slug type calorimeter. The surface coating on the MC provides a broad spectral response but being uncooled it has a large thermal inertia and a slow response time. This particular calorimeter was supplied by John Dishon of the SAI/Albuquerque office and had been used in conjunction with the SAI developed TRS, a large area thermal simulator which burns aluminum powder and liquid oxygen in a large torch like flame.

3. The Null Point Detector (ND) which is basically similar to a slug type calorimeter in that it uses a thermocouple to measure the back surface temperature of a sensing volume. The main difference in the ND is that the sensing volume is designed so that the temperature history of the

In conclusion, fast response high flux calorimetry is a relatively new field of instrumentation. Modification to existing calorimeters, if feasible, is preferred to enhance the understanding and confidence of the thermal instrumentation community in their operation and calibration but new concepts should be pursued to reach the time responses necessary for characterizing flashlamp outputs. The proposed effort was aimed at producing a reliable high flux calorimeter in order to begin characterization of the flashlamp system and allow the start of meaningful test programs. A second purpose was the examination of new calorimetry concepts which might be developed into instruments particularly suited to the unique environments expected in the flashlamp system and which could be cross calibrated with existing calorimetry and fully accepted by the thermal test community.

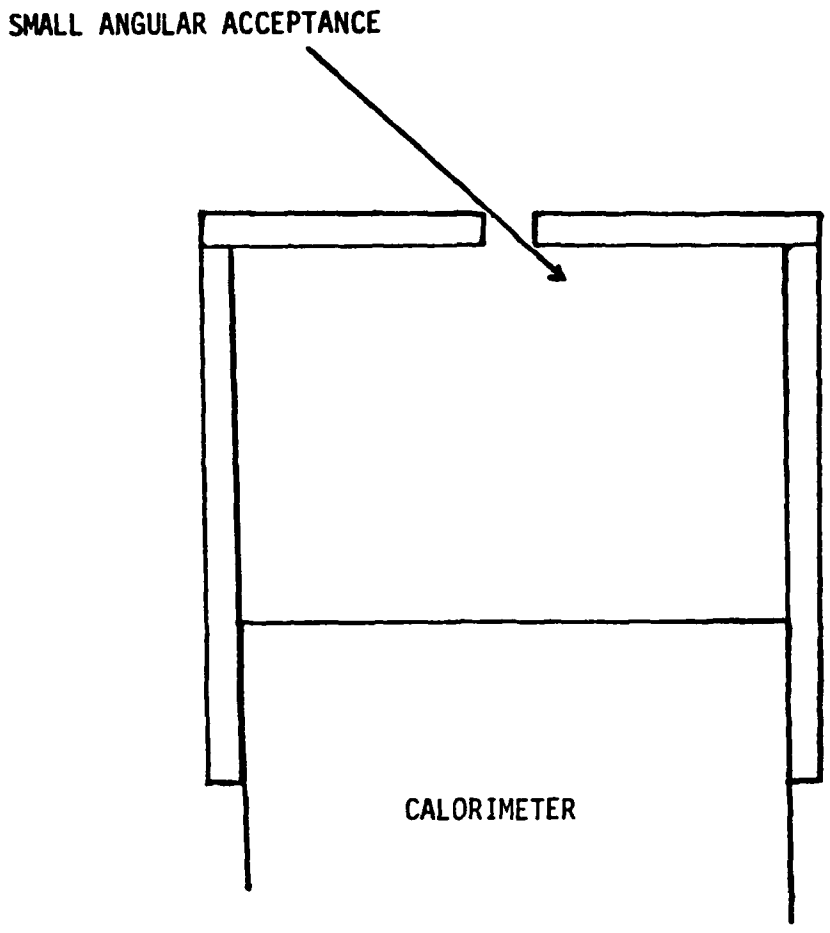

FIGURE 2. Pinhole Collimator

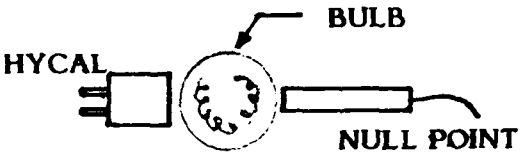

SINGLE BULB ARRANGEMENT

FIGURE 9

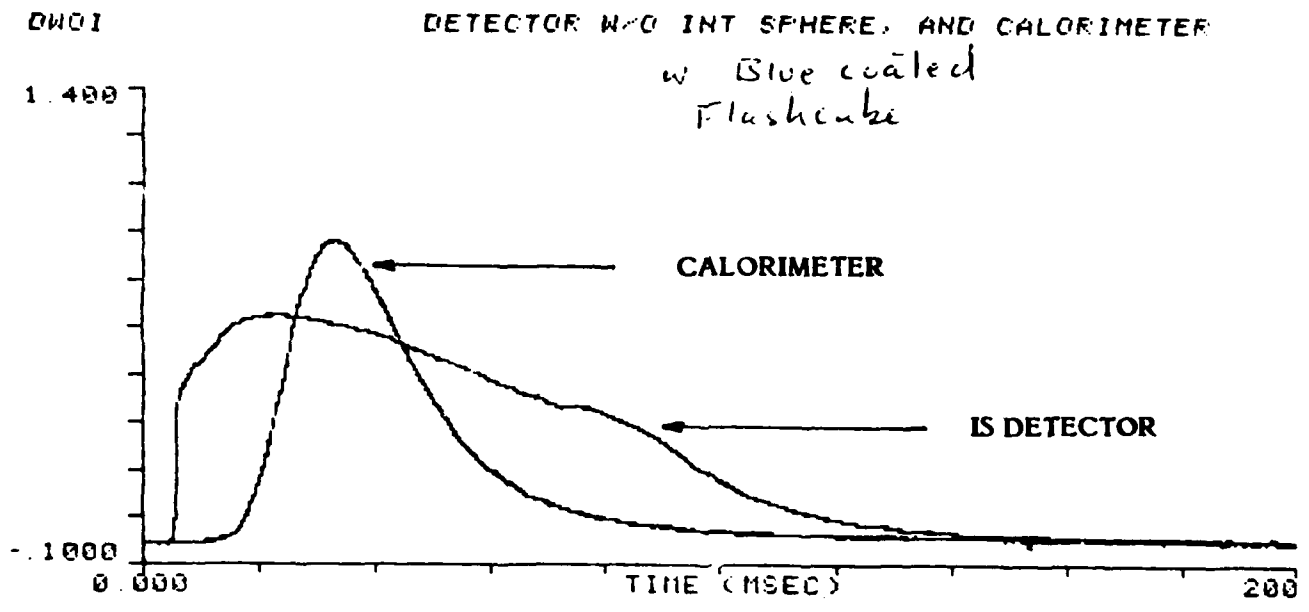

FIGURE 10. CROSS CALIBRATION WITH BLUE FLASHBULB

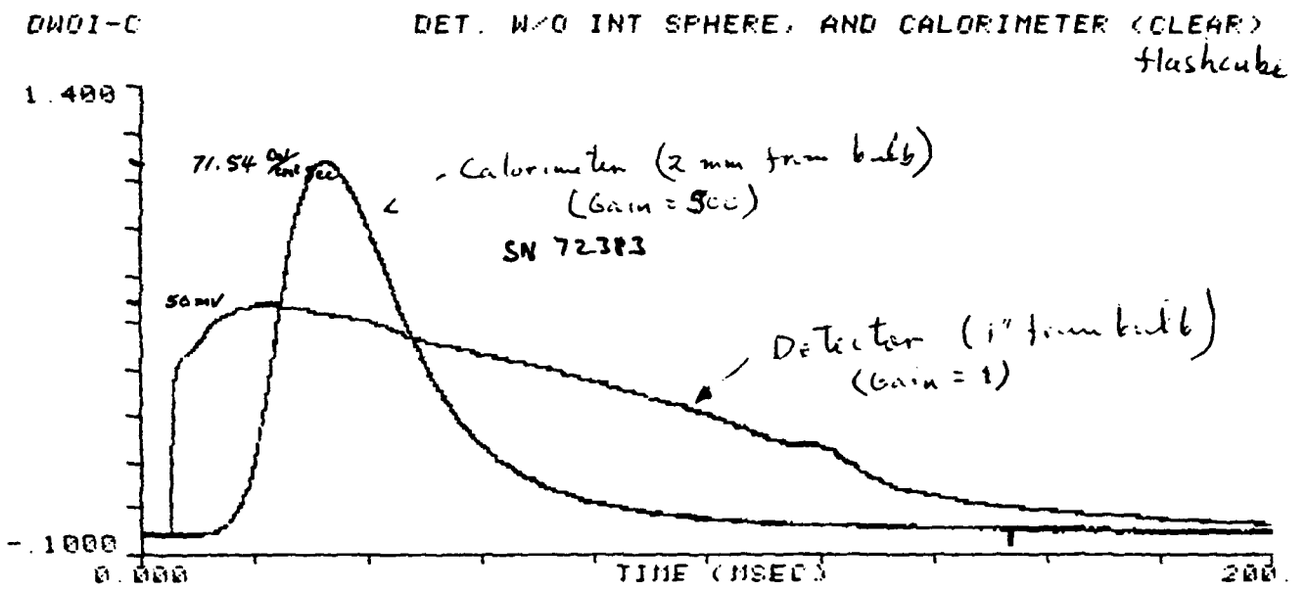

FIGURE 11. CROSS CALIBRATION WITH CLEAR FLASHBULB

attenuation factor of 2.52×10^{-4}) the light levels are so high that the detector cannot recover in a time period comparable to the calorimeter. Figure 12 shows the result when the integrating sphere is used. Now the rise time and the recovery time are better than those provided by the calorimeter.

A second point should be noted in comparing Figures 10 and 11. When the clear flashbulb was used the output of the calorimeter was noticeably higher while there was no change in the photodiode output. This highlights the lack of spectral sensitivity in the photodiode since the components of light filtered out by the blue tint (i.e., the less energetic red and yellow photons) are not detected with any efficiency in the clear flashbulb case.

In order to test the recovery time of the detectors two flashbulbs were fired in sequence using essentially the arrangement as depicted in Figure 13. Initial attempts failed due to sympathetic ignition of the second flashbulb when the first was fired but a simple shield was set up to prevent this. Figures 14 to 16 show the results for two bulbs fired simultaneously, 25 msec apart and 50 msec apart respectively. In each case the photodiode, now in the integrating sphere, shows a faster rise time than either the reference calorimeter (here a Hycal 300 BTU/ft^2/sec S.N. 64933) or the null point detector. However, the recovery time of the IS is generally poorer than the Hycal and the null point detector appears inferior to both in this respect. While computer enhancement of the null point detector output might raise its actual sensitivity, it is unlikely to exceed that of the calorimeter. Obviously the more sensitive, lower range calorimeter used in Figures 14 to 16 has a better response and recovery time than the less sensitive, higher range one used in the single flashbulb tests of Figures 10, 11 and 12.

2.1.3 Flashlamp Testing

The tests performed with the FLS used standard calorimetry to compare the FLS with other thermal sources (CARRS, quartz lamps etc.) and provided ground work for higher flux testing using optical attenuators. Hycal calorimeters from UDRI and SAI and the Null Point calorimeter were placed in known positions about the center of the

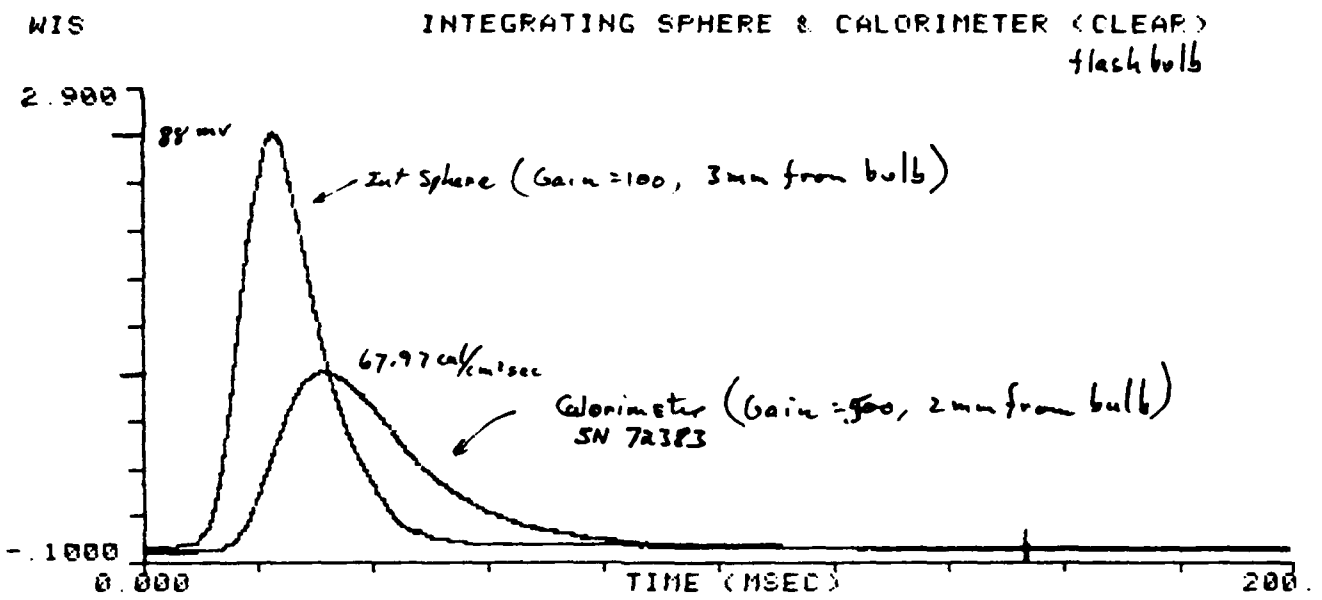

FIGURE 12. CROSS CALIBRATION WITH CLEAR FLASHBULB USING INTEGRATION SPHERE

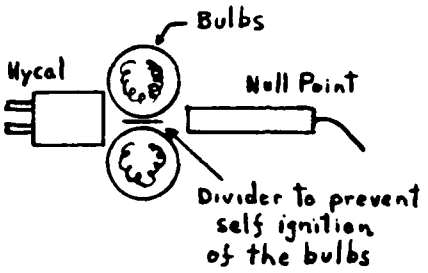

TWO FLASHBULB ARRANGEMENT

FIGURE 13. FLASHBULB ARRANGEMENTS: INTEGRATING SPHERE MOUNTED ABOVE THE BULBS

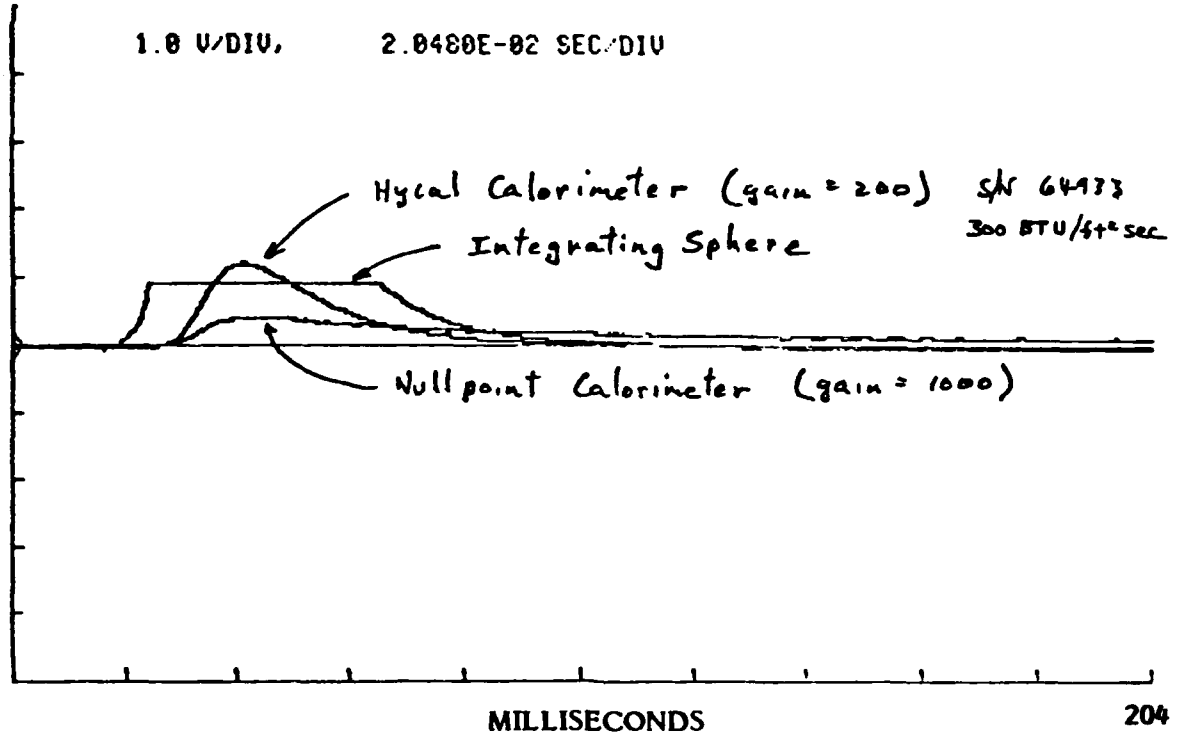

40 KHZ SAMPLE RATE

FIGURE 14. CROSS CALIBRATION: TWO BULBS SIMULTANEOUSLY

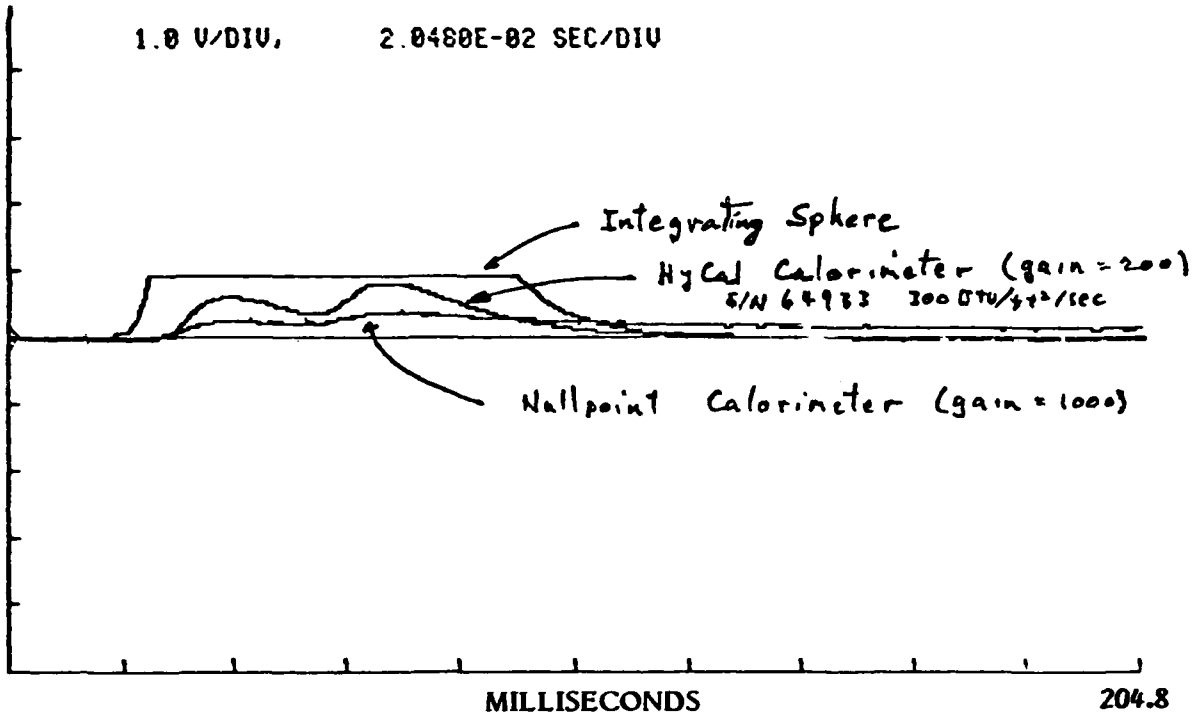

SAMPLE RATE - 40 KHZ

FIGURE 15. CROSS CALIBRATION:
TWO BULBS 25 MS APART

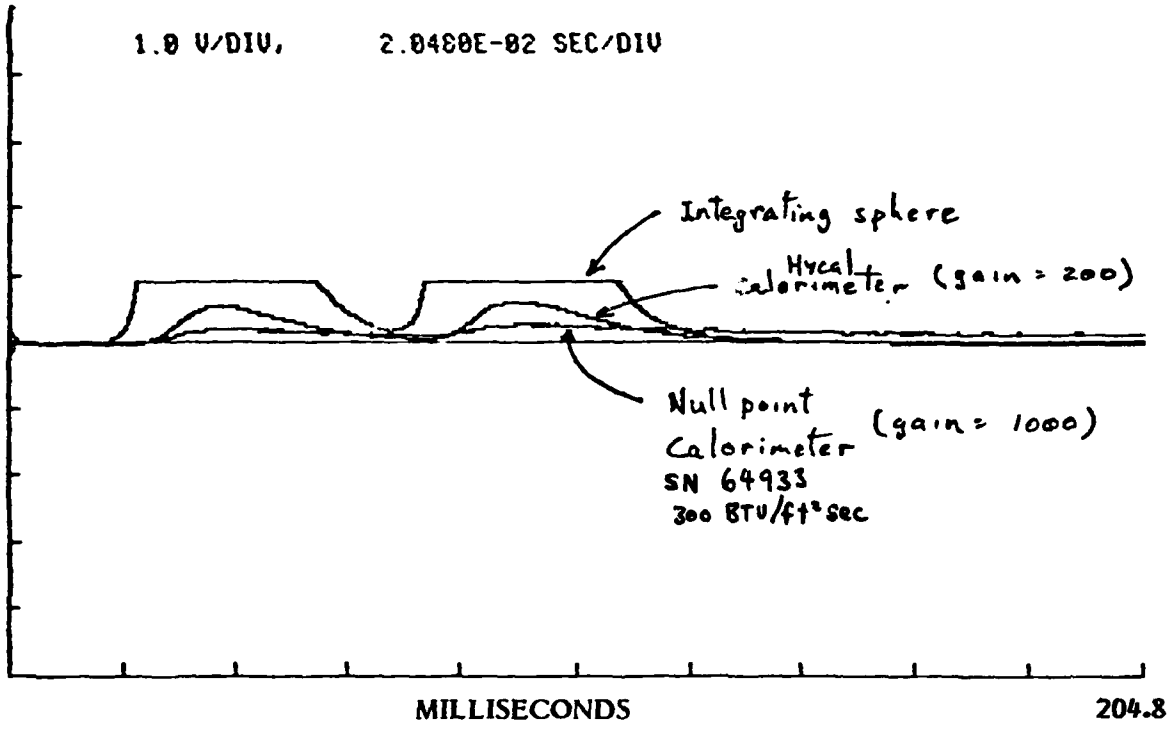

SAMPLE RATE - 40 KHZ

FIGURE 16. CROSS CALIBRATION : TWO BULBS 50 MS APART

exit plane of the FLS output aperture. Data acquisition* was synchronized with the firing of the FLS and simultaneous readings were made on the calorimeters and the total current passing through the Xenon lamps within the FLS. The FLS, which has been constantly evolving towards its final design configuration, possessed 11 separate Xenon flash tubes during these tests. The FLS system controller was programmed to fire the 11 lamps sequentially and repeat once to produce a crude 'square' wave pulse 800 ms in duration. The intensity of the output radiant energy depends upon the amount of overlap in lamp firing and the voltage to which the capacitor bank has been charged (nominally 750 volts). Figure 17 shows a 490 ms pulse at 716 volts while Figure 18 shows an expansion of these results for detail.

The horizontal axis is marked in units of time shown and the vertical axis is scaled in units of flux (calories/cm^{2}sec), millivolts (mv) and amps depending upon the curve under examination (see legend on Figure). The trace consisting of a series of horizontal bumps (CH_4) shows the current flowing to the xenon lamps. Previous work** has shown that the structure of xenon lamp output closely follows the current use, although the absolute intensity of the radiation in the exit plane is not uniform due to the spatial arrangement of the flashlamps. The bumps are roughly 20 ms wide which is half the calorimeter response time.*** It is apparent from the calorimeter traces that the calorimeters had some difficulty in following the current traces although the spacing of the peaks is more important than their magnitude due to geometry considerations mentioned above.

The time lag in calorimeter response leads to a superposition of responses of the individual lamp flashes yielding a waveform with a period of roughly 120 ms. The response of the two Hycal calorimeters are very similar except the UDRI shows less detail. It should be noted that the sudden flattening of response of the UDRI calorimeter and the Null Point calorimeter is due to the signal clipping in the data

---

* LeCroy 3500 system described previously.

** Opinion of Dr. H. Verdun, SAI Electroptics Laboratory.

*** Defined here as 90% of full output.

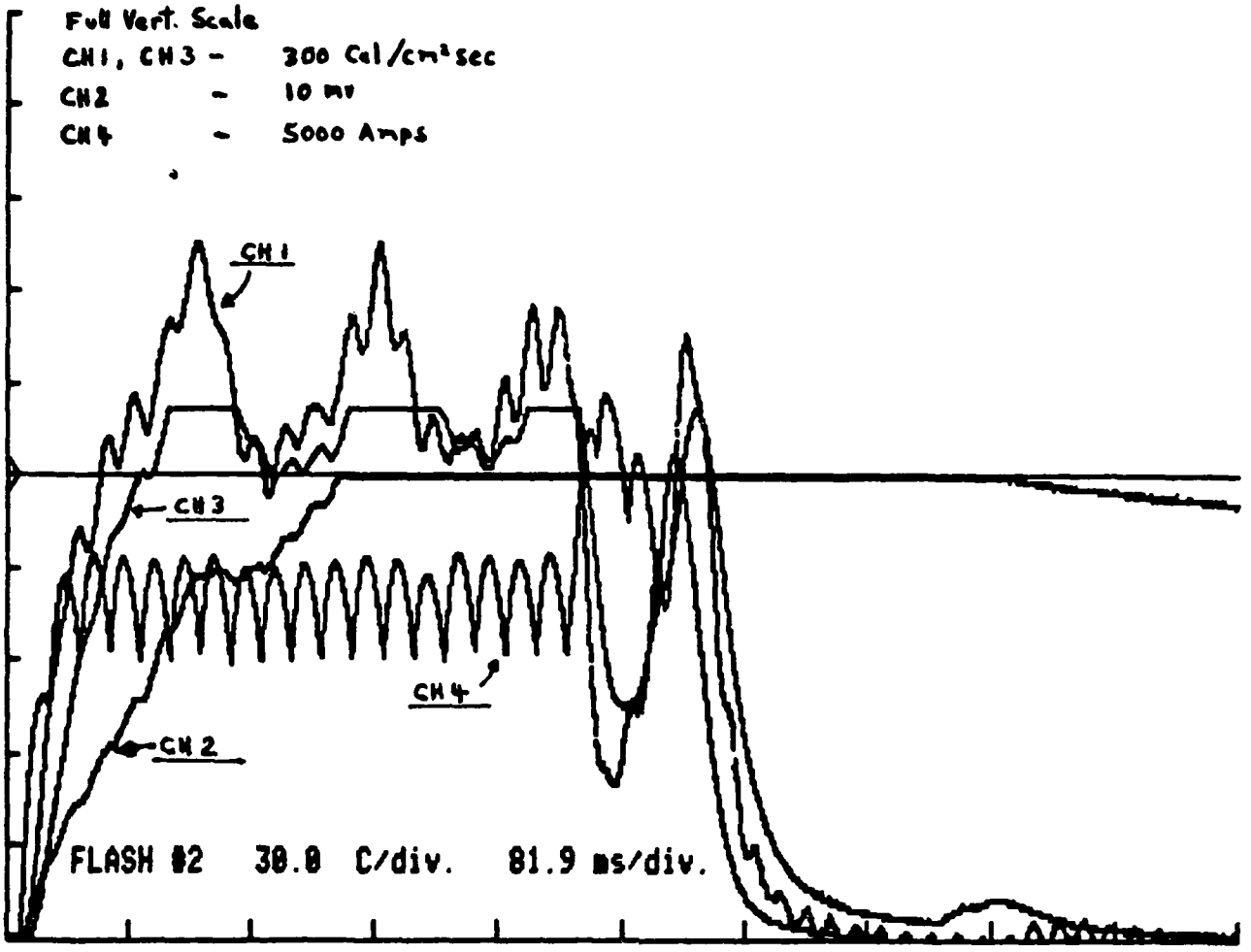

FLASH LAMP TEST # 2 9 SEPT 82

CH 1 = SAI HYCAL (1000 BTU/FT2 SEC)

CH 2 = NULL POINT CALORIMETER

CH 3 = UD HYCAL (750 BTU/FT2 SEC)

CH 4 = CURRENT SENSOR

NOTE: 756.0 VOLT CAPACITOR BANK VOLTAGE. 819.2 MS SHOWS COMPLETE FLASH. CH 3 DATA SHOWS RESULTS OF 8212 DATA LOGGER CLIPPING. & CH2 (-5V TO +5V RANGE)

FIGURE 17. FLASHLAMP CROSS CALIBRATION

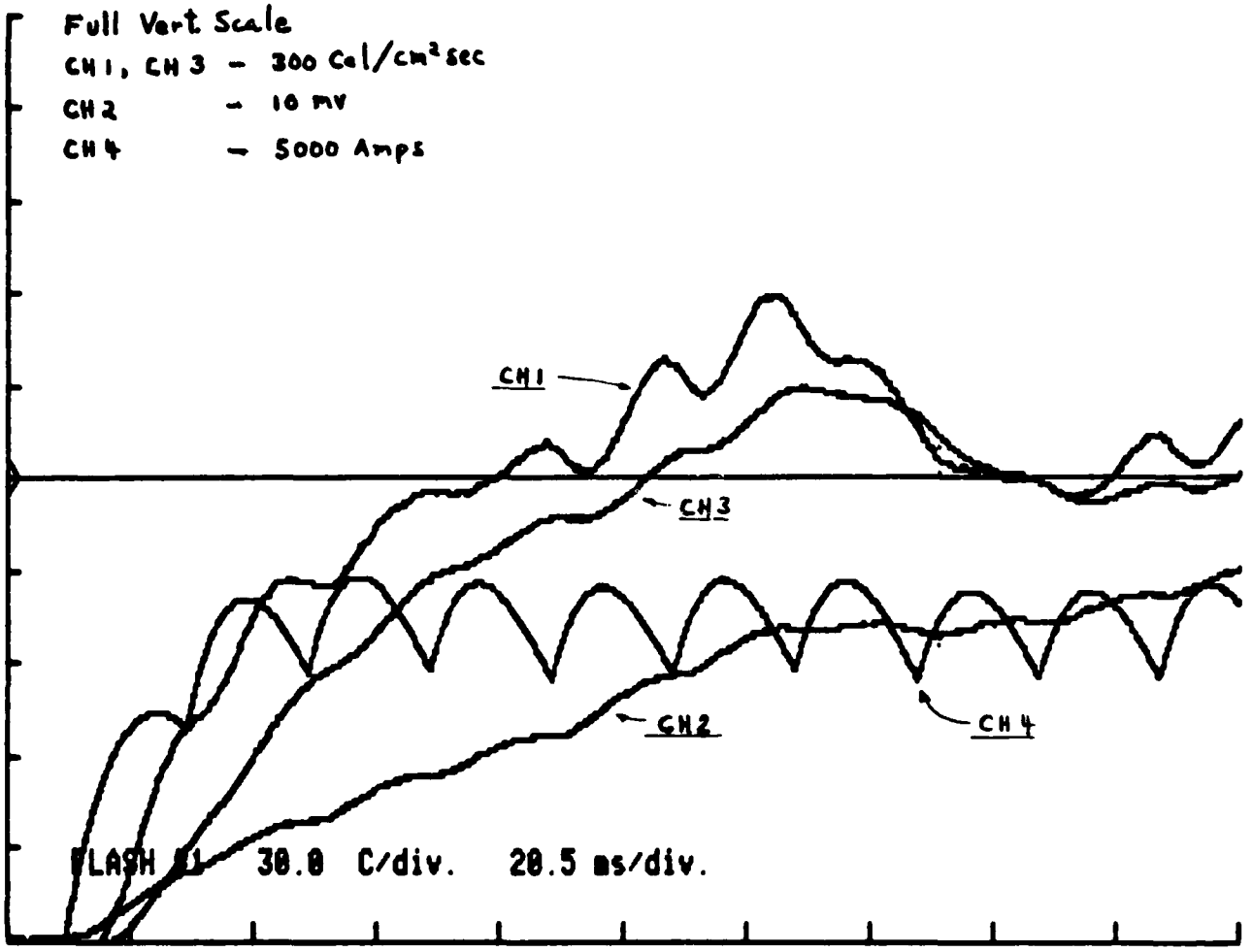

FLASH LAMP TEST # 1 9 SEPT 82

CH 1 = SAI HYCAL (1000 BTU/FT2 SEC)

CH 2 = NULL POINT CALORIMETER

CH 3 = UD HYCAL (750 BTU/FT2 SEC)

CH 4 = CURRENT SENSOR

NOTE: 716.0 VOLT CAPACITOR BANK VOLTAGE. 20SMS SHOWN REPRESENTS FIRST HALF OF FLASH.

FIGURE 18. DETAILED EXPANSION OF FLASHLAMP CROSS CALIBRATION

acquisition system. The Null Point calorimeter seems to reveal less detail than the Hycal calorimeters. Calibration of the Null Point calorimeter is required before flux information can be gathered from this device. Appendix B shows the simulated output of a Null Point calorimeter based on a finite element computer analysis. The average peak fluxes* for two tests based upon SAI and UDRI Hycal calorimeters and FLS capacitor bank voltages are shown in Table 2.

TABLE 2

FLS Test Results

	Test 1	Test 2
Average Peak Flux (cal/cm^2 sec)	207.0	213.3
Bank Voltage (volts)	716	756

Figure 17 is interesting due to the sudden drop in calorimeter responses and a sudden surge in current approximately 400 ms into the test. This corresponds to the failure of a xenon lamp and arcing to the reflective chamber side walls during the test. Since these calibrations were performed during the checkout of the new FLS such problems were common.

2.1.4 Angular Dependence of Detectors

Many detectors possess an angular dependence in their output which may effect the manner in which energy radiated at angles other than normal to the detecting surface is recorded. Both the Hycal calorimeters and the Accurex Null point probe possess a flat detecting surface which is normally exposed to a 2π solid angle of incoming energy. The surface behaves much like a blackbody absorber with emissivities ranging from .89 to .95. However the Integrating Sphere (IS) and the collimator for the calorimeters both possess pinhole apertures which do not permit

* The hycal calorimeter output is accurate to $\pm$ 5%.

total 2π angular acceptance of energy. The angular dependence of the collimator - calorimeter system was tested at UDRI and results are given in the UDRI report. The results of test upon the SAI IS are presented here.

A high intensity lamp with a 1000 watt (Smith Victor Corp. TL2 formula) collimated output was moved in 15 degree angular increments in one plane and at a fixed distance from the input aperture (see Figure 19) .

This procedure was repeated along another axis perpendicular to the first. The resultant outputs for the two axes are shown in Figure 20 plotted against the angular position. Collimated light falling on a perfect absorbing surface at different angles would exhibit a cosine dependance with the maximum intensity recorded with the lamp normal to the absorbing surface. Figure 20 plots the output normalized to the light detected with the lamp in the normal position and divided by the cosine of the angle of the lamp from vertical. This is done to show any deviation from perfect cosine dependance which is illustrated by a dashed line in Figure 20. From the plot we see that for the plane containing Axis 1 at increasingly oblique angles to the input aperture, the IS response deviates ever more from perfect cosine dependence. This is due to blockage at the input aperature similar to the depiction showing in Figure 19. A second plane, containing Axis 2 was selected to fall above the detector. At angles where the light falls directly upon the detector, rather than diffusely from reflections on the internal surface of the integrating sphere, a highly peaked response is observed (see Figure 20). These deviations from the preferred cosine response of the detector, together with its lack of spectral sensitivity, invalidate its use as a calorimeter regardless of its utility as a monitor of the temporal output of the FLS.

2.1.5 Quartz Lamp Testing

Calorimeters were also crosscalibrated at the DNA Tri Service Thermal Flash Test Facility (TFTF). The source used consists of a bank of 24 GF Q6M/T3/CL/HT "Quartzline" lamps, rated 6000 watts at 480 volts each, in two rows of 12 lamps each mounted horizontally with their quartz envelopes in contact forming a pack approxi

Table 5

Results of Angular Dependence Measurements at TFTF

Configurations: (Calorimeter No. 75771)

a) w/o attenuator
b) with attenuator face at inside wall plane (Fig 35a)
c) with attenuator, with calorimeter face at inside wall plane (Fig 35b)

face-to-lamp angle	Flux (cal/cm^2-sec)(Figs 36-50) a)	b)	c)
0°	53.3	14.4	14.2
5° right	53.3	13.9	13.9
10° right	52.5	14.0	13.7
5° up	53.3	14.2	13.1
10° up	52.8	14.6	13.5

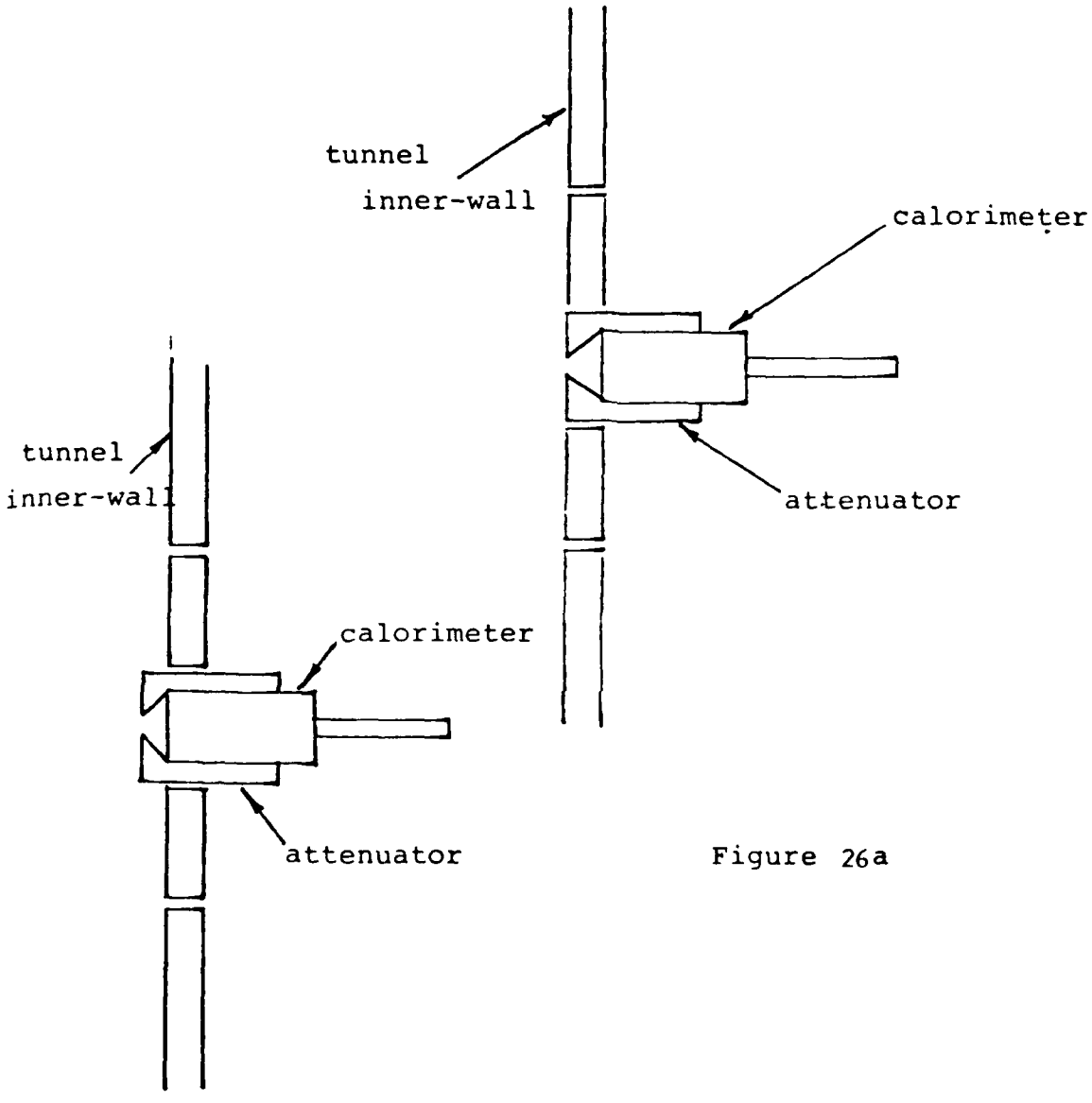

Figure 26a

Figure 26b

FIGURE 26 CALORIMETER/ATTENUATOR/TUNNEL WALL

differences in the cosine effect of the incident radiation and the still limited acceptance angle.

This attenuator was also calibrated in the holder described in Figure 26 at various angles with results presented in Table 5.

Complete details of the UDRI calibrations are presented in Appendix B.

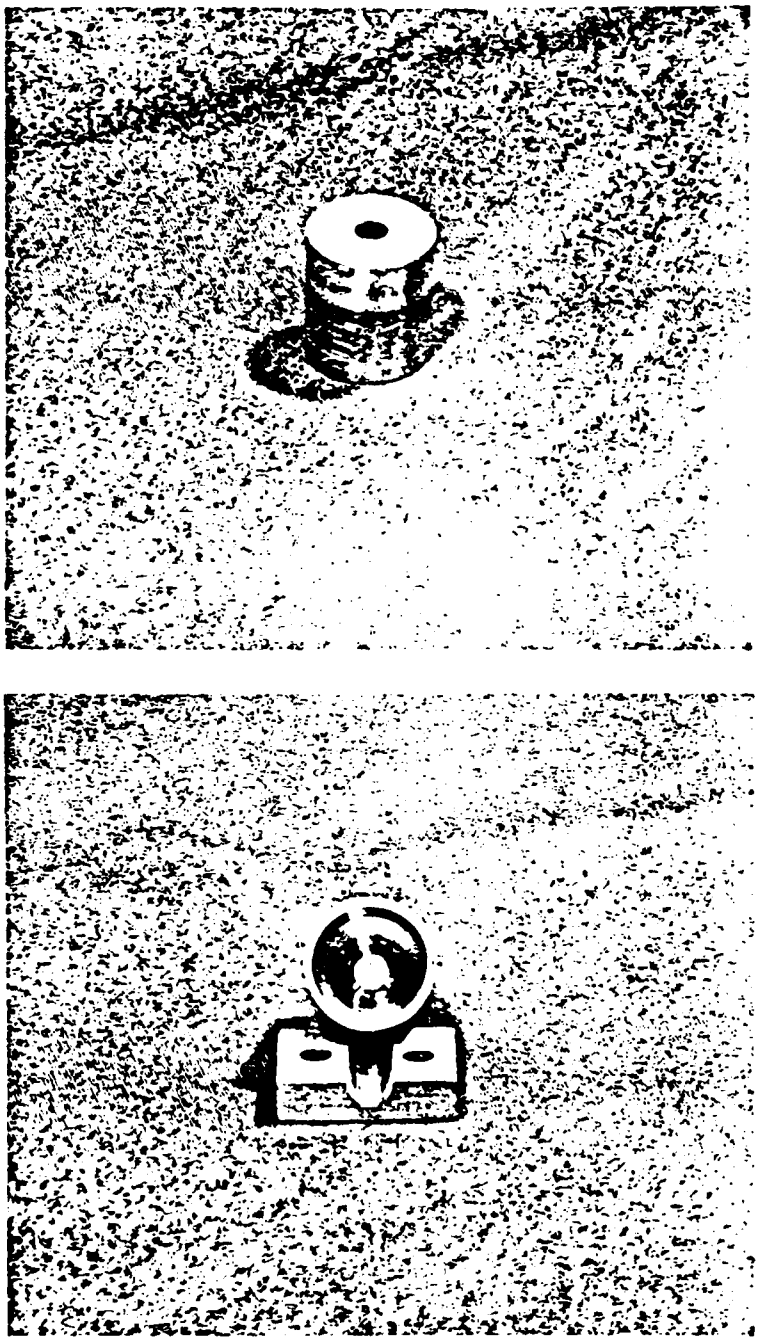

ALUMINIUM COLLIMATING ATTENUATOR

FIGURE 25

Table 4 (Continued)

Results of Tests at Three Flux Levels at TFTF

LEVEL 3

HDLB2 without reflector. 60% power. Full-window, single-unit calorimeter holder with blackened face.

	Flux (cal/cm^2-sec)			
Ser. No.	group 1	group 2	group 3	Average
55199	17.4	17.4	17.2	17.3
95301	17.0	16.9	17.0	17.0
75771	17.4	17.6	17.4	17.5
36002	17.2	17.2	17.0	17.1
72383	18.3	18.3	18.0	18.2

Table 4

Results of Tests at Three Flux Levels at TFTF

LEVEL 1

HDLB2 with gold-plated aluminum reflector. Full-power, full-window, single-unit calorimeter holder with polished face.

	Flux (cal/cm^2-sec)			
Ser. No.	group 1	group 2	group 3	Average
55199	63.3	63.3	63.7	63.5
95301	62.6	62.6	62.7	62.6
75771	64.1	64.1	64.1	64.1
36002	64.2	64.2	64.2	64.2
72383	66.7	66.7	67.1	66.8

LEVEL 2

HDLB2 without reflector. Full power, full-window, single-unit calorimeter holder with blackened face.

	Flux (cal/cm^2-sec)			
Ser. No.	group 1	group 2	group 3	Average
55199	37.4	37.2	37.2	37.3
95301	36.7	36.5	36.7	36.6
75771	37.7	37.5	37.5	37.6
36002	37.1	36.9	36.9	37.0
72383	39.3	38.9	38.9	39.1

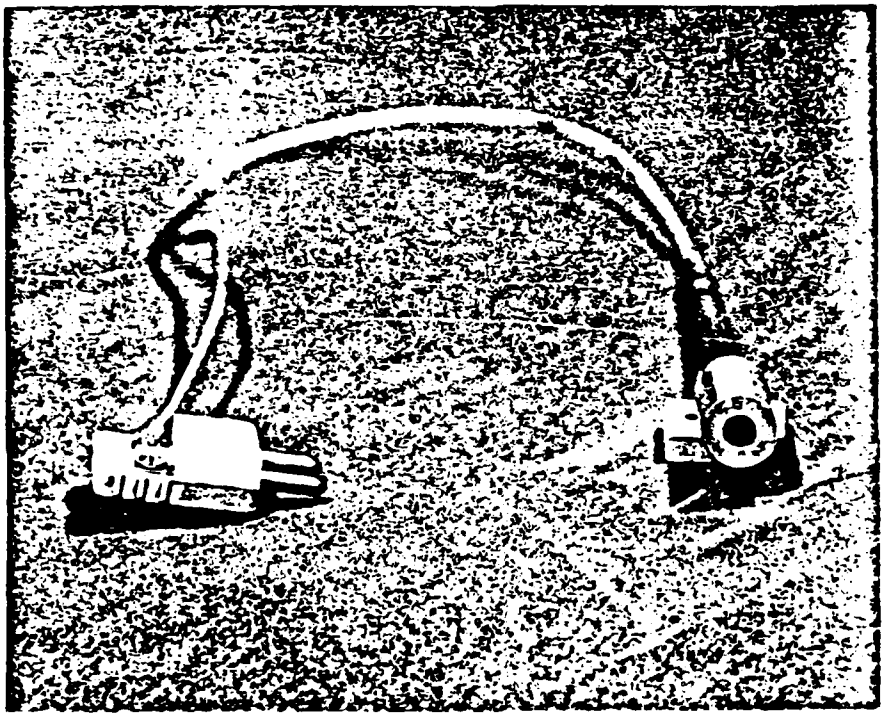

NULL POINT CALORIMETER ADAPTER

FIGURE 24

Table 3

Operational Parameters of HyCal Detectors

Used at TFTF

Ser. No.	Calibration Date	BTU Range	Conversion Factor $(cal/cm^2\text{-}sec)/mv$	Response, ms (time constant)
55199	02-21-83	300	9.170	70
36002	"	750	24.592	40
95301	"	300	8.191	70
72383	"	1000	32.716	30
75771	"	300	10.475	70

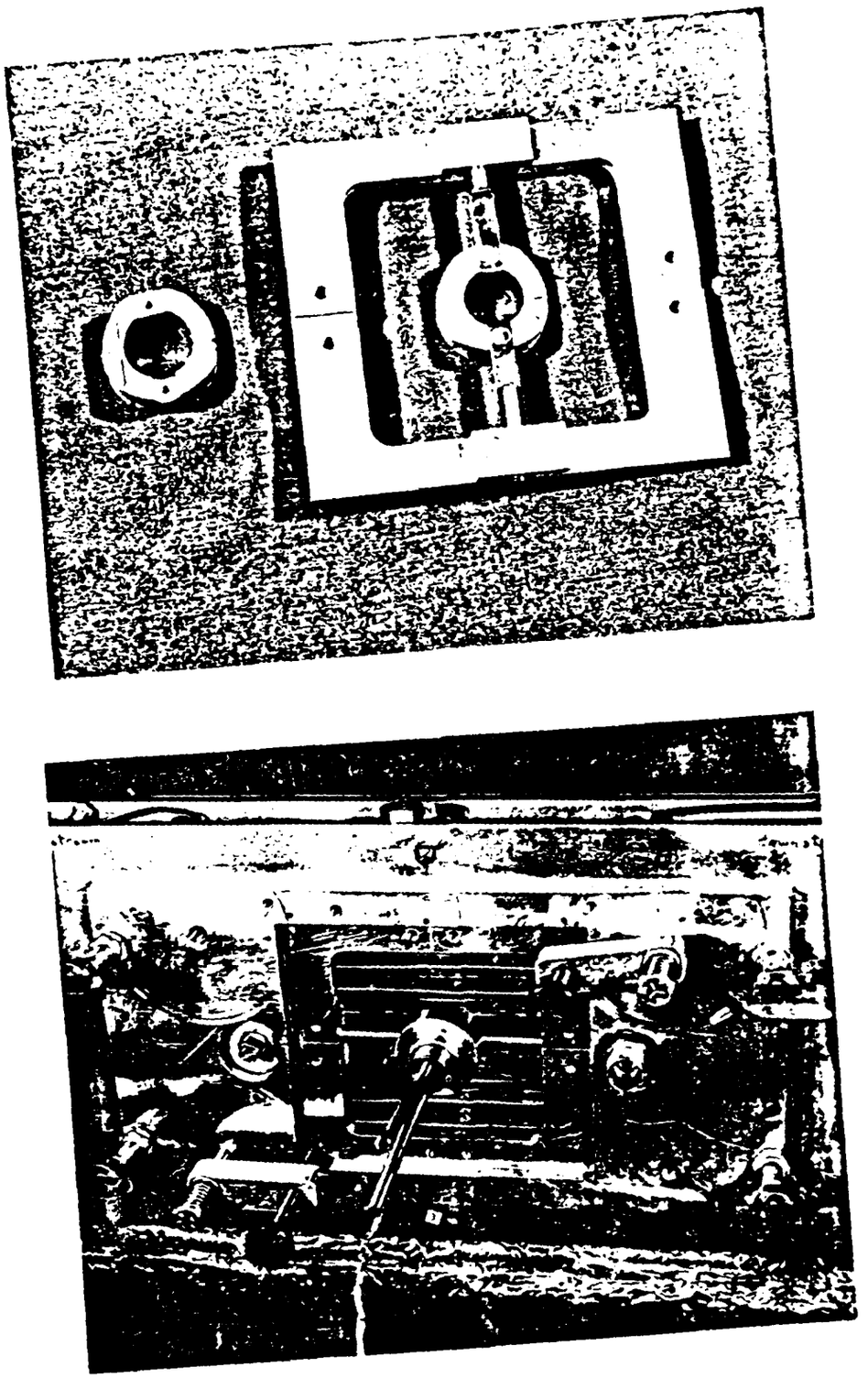

FIGURE 23
CENTER-MOUNT-PIVOT HOLDER

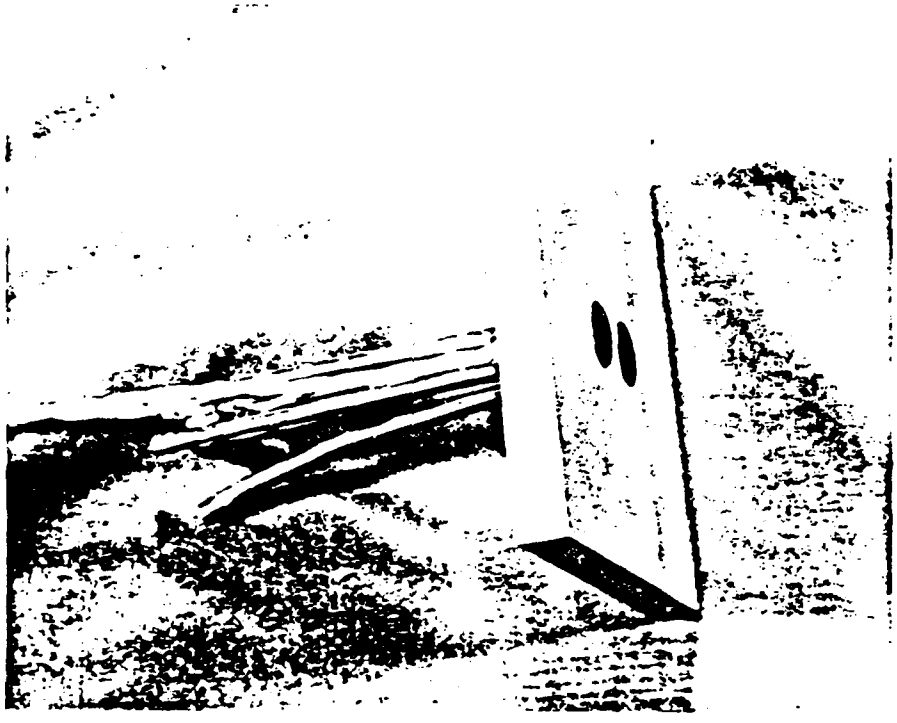

FULL-WINDOW DUAL UNIT HOLDER

FIGURE 22

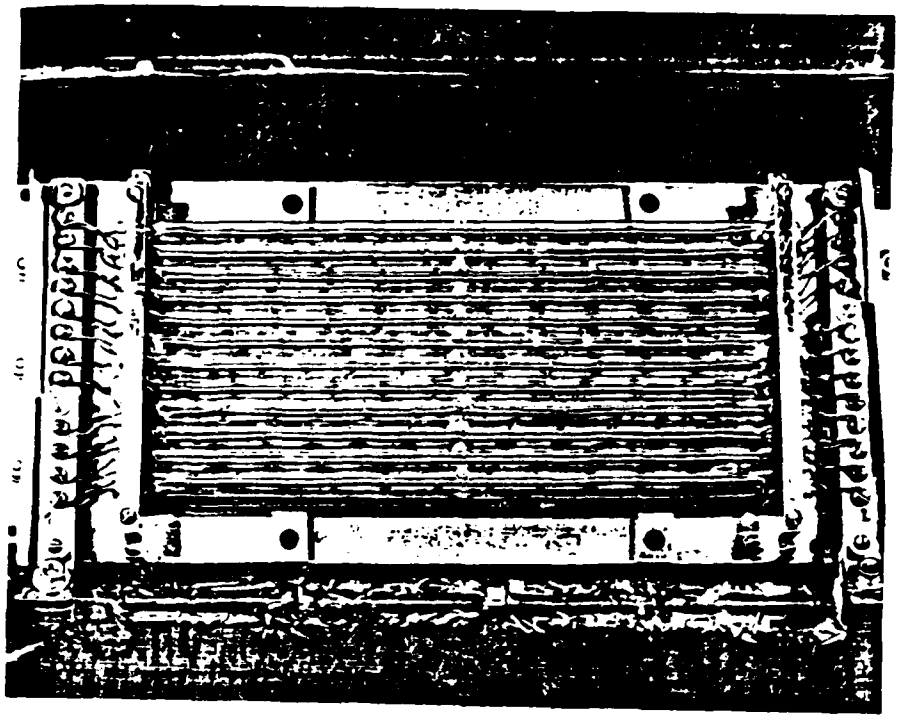

HIGH DENSITY LAMP BANK No. 2

FIGURE 21

mately 5" high, 7/8" deep with 10.5" between retainers (Figure 21). Most calibrations were performed at full power voltage which improved pulse repeatability. Three different source configurations were employed to vary the radiant energy rates. A gold plated aluminum reflector fits around the bank at a 1.5" separation to provide the highest flux. Lower fluxes are achieved by a gold plated stainless steel reflector with a 2" separation and still lower fluxes are generated without a reflector. Pulses are shaped by a gold plated aluminum shutter moved by a pneumatic solinoid opening at 224 in/sec and closing at 75 in/sec.

Calorimeters can be cross calibrated using a full window dual unit which fills the 4" x 4" test window and holds two calorimeters above and below each other on the vertical centerline of the test window and 0.362" off the horizontal centerline (Figure 22). Another holder (Figure 23) fits into the test window and holds one calorimeter in a ring mount which can rotate on a vertical axis. Data collection was by a Hewlett/Packard model 7046A dual-pen platen recorder.

Six calorimeters were used in the cross calibration. Five were Model C-1312-A Asymptotic calorimeters manufactured by Hy-Cal Engineering (Table 3). Manufacturers specifications indicate that this model has an accuracy $\pm$ 3%, a repeatability of $\pm$ 0.5% and a linearity of $\pm$ 2.0%. The sixth calorimeter was the null point calorimeter, mentioned previously, held in a special adapter (Figure 24) to allow its use with the above mentioned calorimeter holders.

Calorimeters were cross calibrated at the three flux levels produced by the different configurations mentioned above using the dual unit and, in the case of the null point detector, the special adaptor. Results are presented in Table 4.

An attenuator (Figure 25) was fabricated from aluminum to press fit snugly on the standard 5/8" o.d. HyCal instrument. The design of the attenuator followed that shown previously in Figure 1 with an inner core surface of 45° and a high polish on both the interior surface and the front face to reduce the heat load on the adaptor. The input aperture is 0.198" yielding an input aperture to HyCal surface ratio of 10:1. The actual measured attenuation factor was however 3.7:1 resulting from

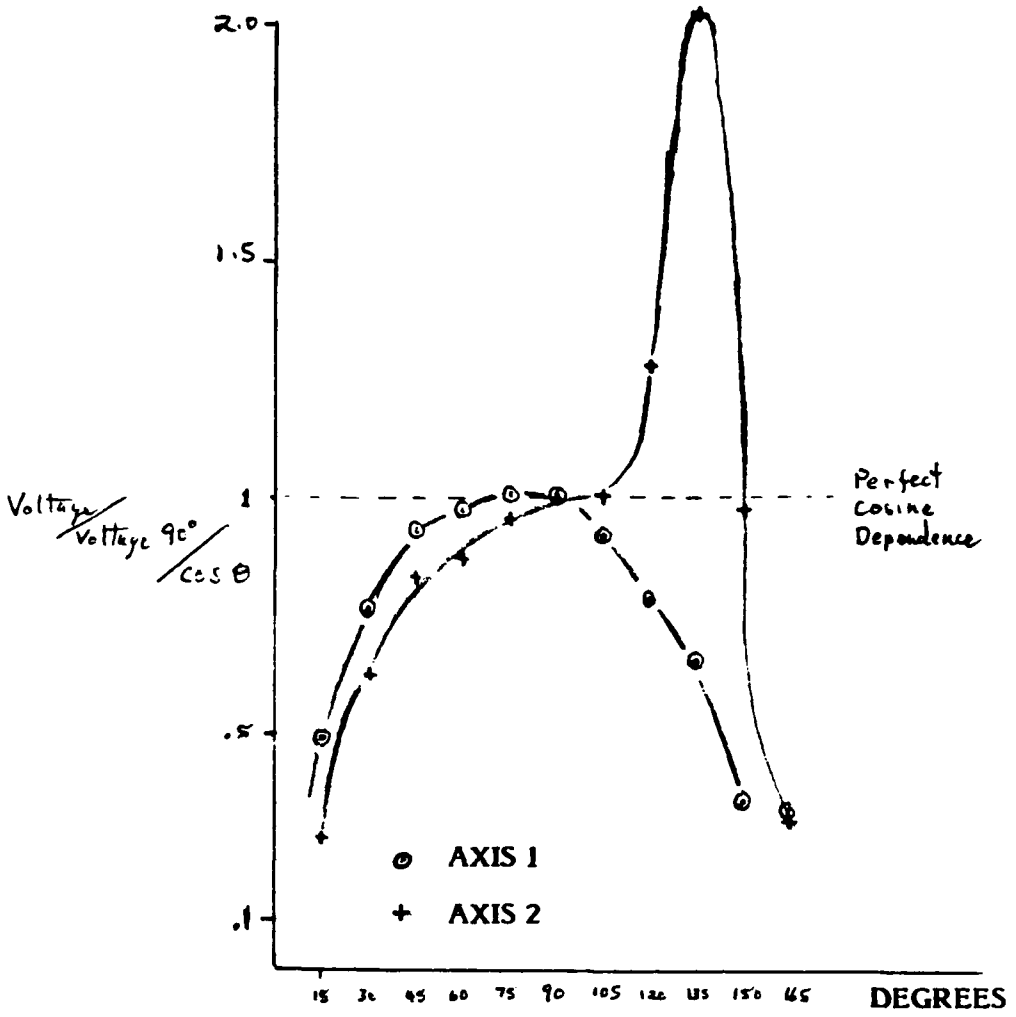

FIGURE 20. ANGULAR DEPENDENCE OF SAI INTEGRATING SPHERE

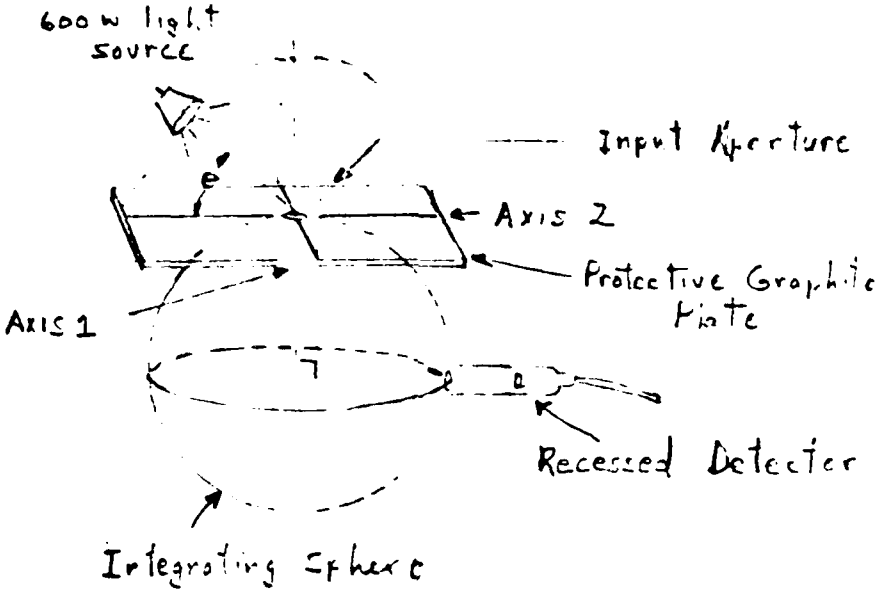

LIGHT BLOCKAGE AT IS APERTURE

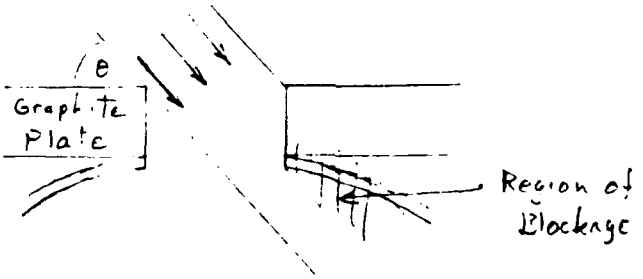

FIGURE 19. GEOMETRIC RELATIONSHIP OF LIGHT SOURCE TO INTEGRATING SPHERE

SECTION 3 CONCLUSIONS

The present effort has cross calibrated four basic calorimeter types:

- o Watercooled Hycal asymptotic calorimeter
- o Slug Type Medtherm calorimeter
- o Null point calorimeter
- o SAI Integrating sphere

Four different sources were used:

- o SAI designed CARRS
- o Flashbulbs
- o DNA Tri Service Thermal Flash Test Facility
- o SAI Flashlamp System

Two other calorimeter concepts based on thermistor and pyroelectric sensors were examined but could not be developed into useful calorimeters within the restrictions of the present contract. Thermistors examined did not have acceptable response characteristics and the pyroelectric sensor was extremely delicate and failed before testing was completed.

The calorimeter concept recommended for near term use with the flashlamp system is a specially designed and fabricated attenuator to allow use of a lower range, fast response, commercially available Hycal. Being based on a community accepted calorimeter it is felt that this concept will allow ease of operation, ready relatability to other efforts and user confidence in the instrument.

APPENDIX A

UDRI REPORT

CALIBRATION TECHNIQUES
using the
UDRI/DNA
THERMAL FLASH TEST FACILITY

PREPARED FOR: Michael McDonnell, Phd
Experimental Sciences Division
Science Applications Inc.

BY: Nicholas Olson
Chief Technician
UDRI/DNA Thermal Flash Test Facility

TABLE OF CONTENTS

PART I
THERMAL FLASH TEST FACILITY
SOURCE

The primary radiant energy source of the UDRI/DNA Tri-Services Thermal Flash Test Facility (TFTF) consists of a bank of 24 GE Q6M/T3/CL/HT "Quartzline" infrared lamps rated 6,000 watts at 480 volts each. The lamps have an envelope outside diameter of 3/8" and are 11-3/4" in overall length with an effective radiating filament length of 9-3/4". At rated power 100% of the relative intensity of the lamp is at 0.9 micron with a usable spectral distribution of 0.4 micron to 5 micron (Fig. 1). The Facility has several configurations of lamp mountings, one of which is called the High Density Lamp Bank No. 2 (HDLB2) and was used exclusively for the calibration program resulting in this report. Two rows of 12 lamps each are mounted horizontally with their quartz envelopes in contact forming a pack approximately 5" high, 7/8" deep with 10-1/2" between retainers (Fig. 2). The HDLB2 is attached to the side of the Wind Tunnel test section, 1/8" away from the 4-1/2"x9" quartz window that forms one wall of the tunnel. The lamps are wired in three groups of eight to a three-phase SCR type power controller capable of supplying any balanced AC voltage to the lamps up to a maximum of 480 vac. Full power voltage was used for the major portion of this calibration program with the exception of the Level 3 DETECTOR CROSS CALIBRATION where power was reduced approximately 40% to generate a low flux level for a third level of comparison. It should be noted that repeatable flux levels are difficult to maintain at reduced power levels. Current and voltage were closely monitored to maintain reasonable repeatability. Three source configurations were employed to establish three radiant energy rates (flux in calories/cm^2-sec). A gold-plated aluminum reflector (GPAR) fits around the bank within 1-1/2" of the back of the lamps (Fig. 3) yielding the highest flux. Lower flux levels are achieved with a similar

reflector of gold-plated stainless steel (GPSS) 2" from the lamps, while the lowest level of flux was generated without a reflector.

SHUTTER

The aluminum shutter, gold-plated on both sides, locates in slots in the center of the floor and ceiling of the 1" wide wind tunnel test section. Moved by pneumatic solenoid, the shutter opens at a speed of 224 in/sec and closes at 75 in/sec. The tunnel downstream edge of a standard 4-1/2" wide sample will be exposed for 0.06 sec longer than the upstream edge. The shutter effectively blocks the lamp radiant energy to the sample side of the tunnel. The gold plate reflects the energy back to the lamps when the shutter is closed lessening heat buildup in the shutter. The energy reflected back to the lamps from the shutter increases the lamp filament temperature which increases the filaments resistance and a correspondingly lower current flow results. Current flow is further reduced when a reflector is in place around the lamps reflecting radiant energy back to the filaments. With either the reflector or shutter removed, energy escapes in the open direction allowing the filaments to cool to normal operating temperature. When the shutter opens with a reflector in place, the higher filament temperature produces a higher flux. As the temperature drops to normal, the flux also drops. In order to produce a square wave pulse of energy available to the sample, the timing of delay between initial lamp current flow and shutter opening is critical. If the delay is short, the rise time of the pulse will be slow to a stable level following the stabilizing lamps (Fig. 4). If the delay is long, the lamps will have stabilized but at the higher energy level dictated by the reflected radiance trapped between the reflector and shutter. When the shutter does open, the higher level will cause the leading edge of the pulse to overshoot before stabilizing (Fig. 5). With the correct delay timing the energy pulse will be a square wave (Fig. 6).

GENERATING A SQUARE-WAVE PULSE

Two exposures on the same graph (Fig. 7), one after the other under as repeatable conditions as reasonable using the HDLB2 w/GPAR compare pulse shapes with and without shutter. Lamp "on" time for the two exposures is the same as well as lamp current at shutdown. With use of the shutter a square wave pulse is indicated with a delay of 1.4 secs. In the second exposure the shutter is held open and a plot of lamp radiant energy indicates the peak flux is not achieved during the "on" time. Lamp current is also affected being slightly lower when the shutter opens than at the same time with the shutter blocked open. Comparison of these two plots clearly indicates the stable flux levels available in a shorter time as a result of the lamp radiant energy being reflected back into the lamps by the shutter/reflector combination.

CALORIMETER HOLDERS

Part of the wall of the wind tunnel test section opposite the lamp bank is formed by a removable aluminum plate which contains the 4"x4-1/2" sample opening or "window" (Fig. 8). The aluminum holders that support the calorimeters fit into the sample window with the inside face of the holder on the same plane as the inside wall of the tunnel. There are three such holders: One called Full Window Single Unit (FWSU) which fills the test window completely while centering a single calorimeter with its sensing face flush with the holder face (Fig. 9a). This holder is used in two configurations. For the highest levels of indicated flux the holder face is highly polished. For all other flux levels the holder face is coated with 3M Nextel flat black paint. One called Full Window Dual Unit (FWDU) which also fills the test window completely and places two 5/8" OD calorimeters above/below each other on the vertical centerline of the test window and 0.362" above/below the horizontal centerline so that the two units are 0.725" center-to-center (Fig. 9b). The face of the FWDU holder is neither coated nor polished but is left in its "as-milled" state. A third holder is called Center Mount Pivot (CMP) which fits into the test window as the others but does not fill the window (Fig. 10). The outer frame supports two opposite extensions from a 1-1/4" OD aluminum ring into which the calorimeter is mounted. The extensions may be mounted to the frame vertically allowing the ring to pivot on a vertical axis across the calorimeter face. Mounting the extensions on a horizontal plane allows the calorimeter a horizontal pivot. The calorimeter supporting ring is chamfered on either side of the pivot plane to prevent blocking incoming radiant energy from that side which is turned away when the calorimeter face is at some angle to the lamps other than 0°.

A second ring identical in outside dimensions and location to the frame replaces the first ring when the aluminum collimating attenuator (see "Task 2") is used. The

attenuator (Fig. 11) fits snugly over the calorimeter requiring the larger bore of the second ring for proper fit and location. Once in place over the calorimeter, the distance between the face of the attenuator and the face of the calorimeter remain fixed but the entire assembly may be moved in/out of the second ring to allow either the attenuator face or calorimeter face to be on the same plane as the wind tunnel wall.

INSTRUMENTATION

A Hewlett/Packard model 7046A dual-pen platen recorder was used for all data collection. The recorder was calibrated on 11-23-82 and checked at completion of this program (Fig. 12). Except when indicated, lamp current was monitored on channel 1 (black) at a slower response to prevent off-scale pen travel at the initially high lamp current. For all other applications channel 1 was at a normal response of 30 in/sec. A current transformer with a ratio of 400/5 fed a conditioning module which converted the current signal to a DC level of 1 volt/400 amps. Using 0.1 v/in scale on the recorder yielded 40 amps/in. Channel 2 (red) monitored calorimeter output direct at ranges of 0.5 mv/in and 1 mv/in where indicated.

Lamp voltage was monitored visually using a Digital Voltage Panel Meter (DVPM) that was calibrated using a standard laboratory source.

CALORIMETERS

Six calorimeters were used to gather the information contained in this report. Five of the devices are Model C-1312-A Asymptotic type manufactured by Hy-Cal Engineering, 12105 Los Nietos Road, Santa Fe Springs, Calif., 90670. Manufacturers specifications indicate this model calorimeter to have an accuracy of $\pm$3%; repeatability $\pm$0.5% and linearity of $\pm$2.0%. The Sensing surface has a colloidal graphite coating with an absorptivity of 0.89 flat across the spectral range from 0.2 microns to 30 microns. Distilled water was used for cooling with flow rates greater than 1 gpm at pressures greater than 80 psi. Four of the asymptotic calorimeters were hand-carried to the manufacturers facility and recalibrated consecutively along with a fifth unit that was purchased at the facility. Calibration of the five units was observed by the Tri-Services Thermal Flash Chief Technician to assure as repeatable conditions as reasonably possible. The devices are supplied with calibration certificates (Figs. 13-17) that are NBS traceable in (BTU/ft^2-sec)/mv and must be converted to (cal/cm^2-sec)/mv. The factor for this conversion works out to 0.27236 x (BTU/ft^2-sec) = (cal/cm^2-sec). The operational parameters of the four Hy-Cal calorimeters are as follows:

Ser. No.	Calibration Date	BTU Range	Conversion Factor (cal/cm^2-sec)/mv	Response, ms (time constant)
55199	2-21-83	300	9.170	70
36002	"	750	24.592	40
95301	"	300	8.191	70
72383	"	1000	32.716	30
75771	"	300	10.475	70

The sixth device is referred to as a Null-Point Calorimeter (NPC). Very little information is available about this device except that it functions much like a copper-slug calorimeter using a Type K thermocouple. The output was corrected

for room temperature using an Omega model MCJ type K compensator. An adaptor (Fig. 18) was fabricated to fit the NPC in the three different holders allowing proper location of the device relative to the other calorimeters.

PART II
TASKS, DEFINITIONS, AND ACCOMPLISHMENTS

Task 1. DETECTOR CROSS CALIBRATION

Request:

A. Cross calibrate SAI Hy-Cal (1000 BTU range) and UDRI midtherm detectors using Quartz Lamp Bank. Provide response curves for at least 3 fluence levels at each of three flux levels between the maximum available and around 300 cal/cm^2-sec. In all instances use maximum shutter speeds.

B. Cross calibrate SAI Hy-Cal (300 BTU) and UDRI midtherm detectors at 3 flux levels between 10 cal/cm^2-sec. and 50 cal/cm^2-sec. Choose at least one flux level in common with those selected above.

Explication:

A. The UDRI midtherm detectors are no longer used for calibration in the Thermal Flash Test Facility (TFTF) due to slow response times and restricted view angles. The devices now used for calibration are model C-1312-A asymptotic calorimeters manufactured by Hy-Cal engineering.

Fluence is generally considered to be the total energy delivered while flux is the rate-of-delivery. Since the calorimeters to be compared are primarily flux measurement devices the length of time each is exposed need only be enough to allow the asymptotic devices to stabilize.

Three flux levels were used in the fulfillment of this request but a maximum level of near 60 cal/cm^2-sec is the upper limit of the TFTF.

The shutter was not used as this request is only concerned with identifying stable output levels not the rise or decay of those levels.

B. Both the 300 BTU and 1000 BTU SAI Hy-Cal units were compared with the three UDRI/DNA units consecutively at each of three flux levels of approximately 15, 30 and 60 cal/cm^2-sec.

Action:

Two Hy-Cal model C-1312-A calorimeters belonging to Science Applications Inc. (SAI) and three same model units belonging to the UDRI/DNA Thermal Flash Test Facility were exposed consecutively to the radiant energy pulses of three configurations of the High Density Lamp Bank No. 2 under as repeatable conditions as reasonably possible. Each group of five calorimeters was exposed three times consecutively and in repeated order to allow a realistic mean to be derived for each unit. The sequence was repeated for each of the three flux levels for a total of 45 exposures.

Level 1 (Figs. 19-23)

HDLB2 with gold-plated aluminum reflector. Full-power, full-window, single-unit calorimeter holder with polished face.

	Flux(cal/cm^2-sec)			
Ser. No.	group 1	group 2	group 3	Avg.
55199	63.3	63.3	63.7	63.5
95301	62.6	62.6	62.7	62.6
75771	64.1	64.1	64.1	64.1
36002	64.2	64.2	64.2	64.2
72383	66.7	66.7	67.1	66.8

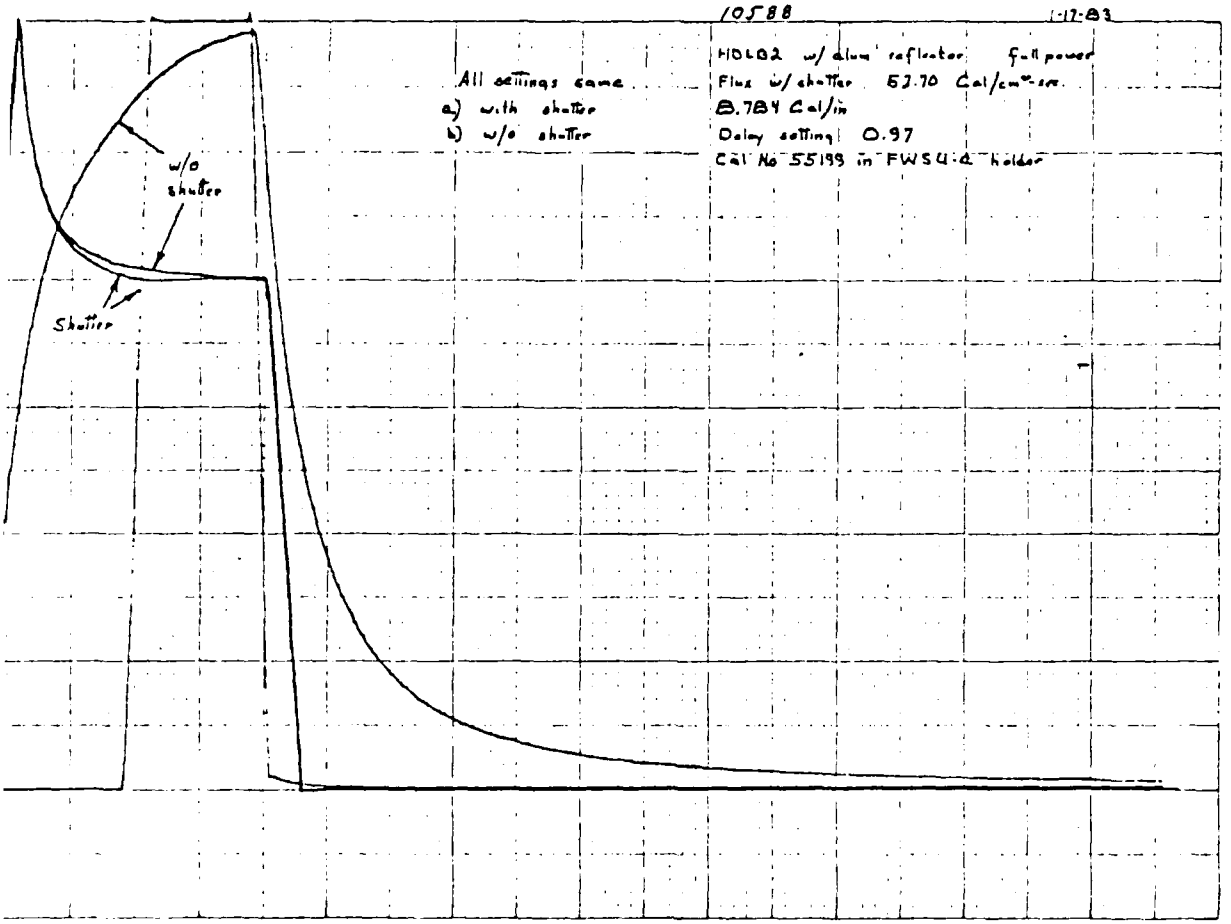

Figure A7.

PULSE WITH AND WITHOUT SHUTTER

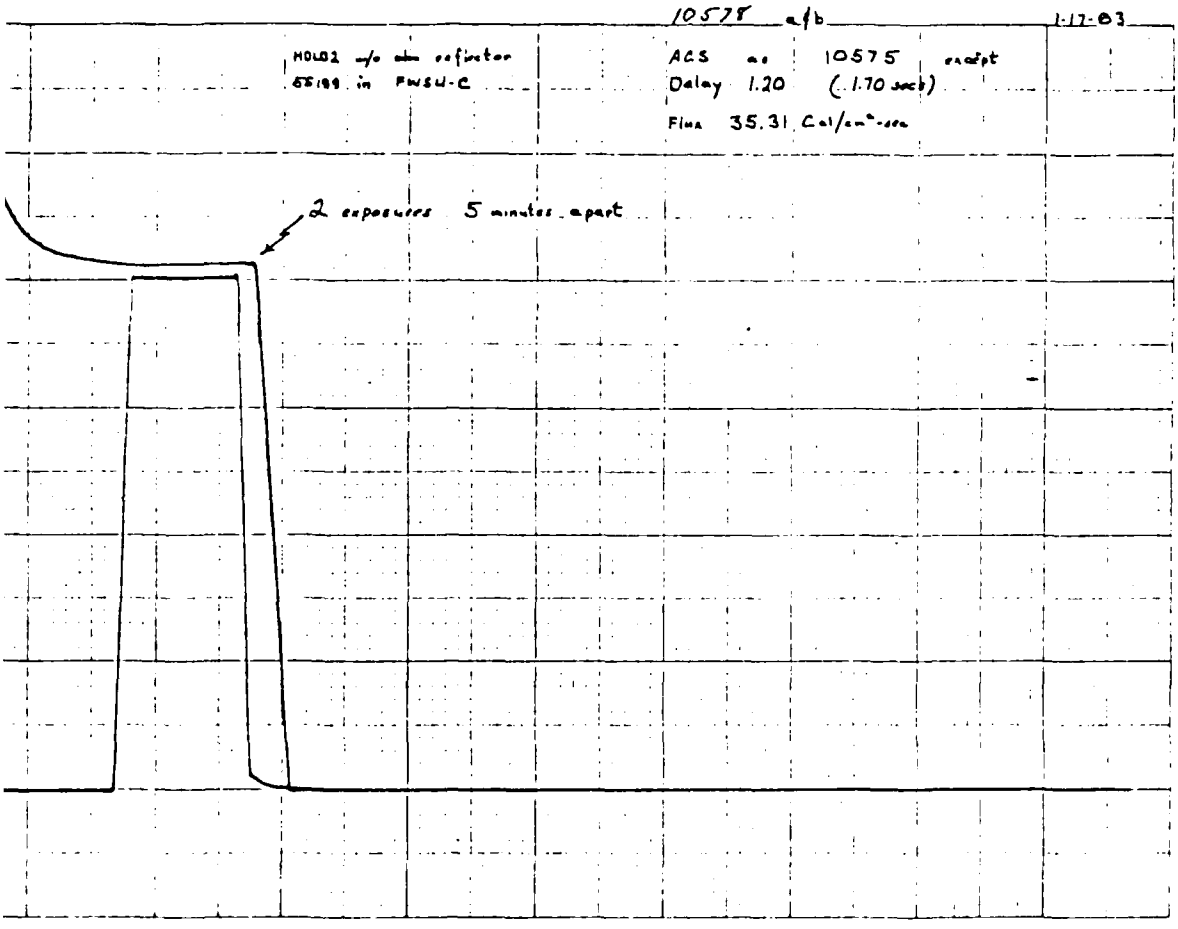

Figure A6.

PULSE WITH CORRECT DELAY

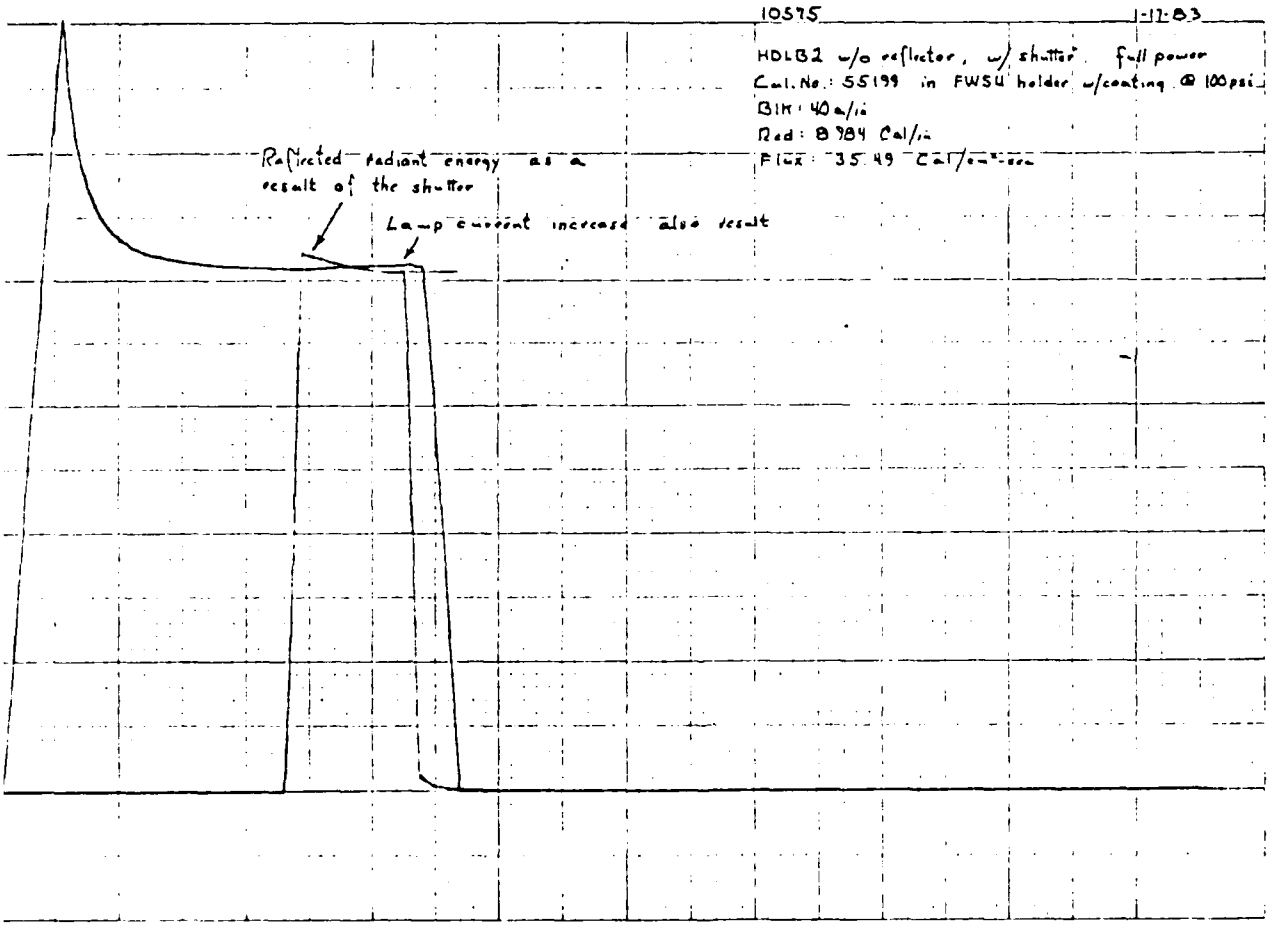

Figure A5.

PULSE WITH LONG DELAY

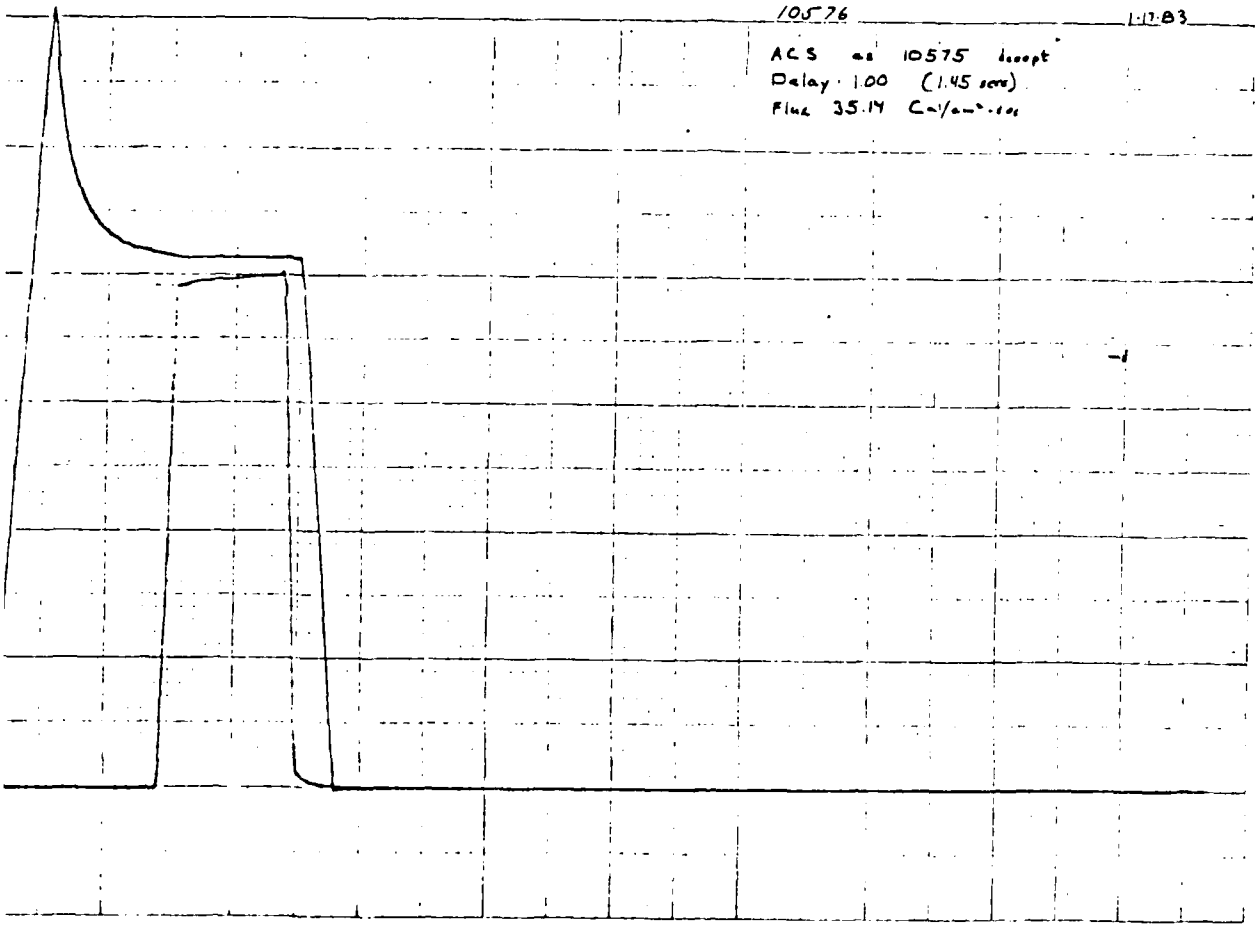

Figure A4.

PULSE WITH SHORT DELAY

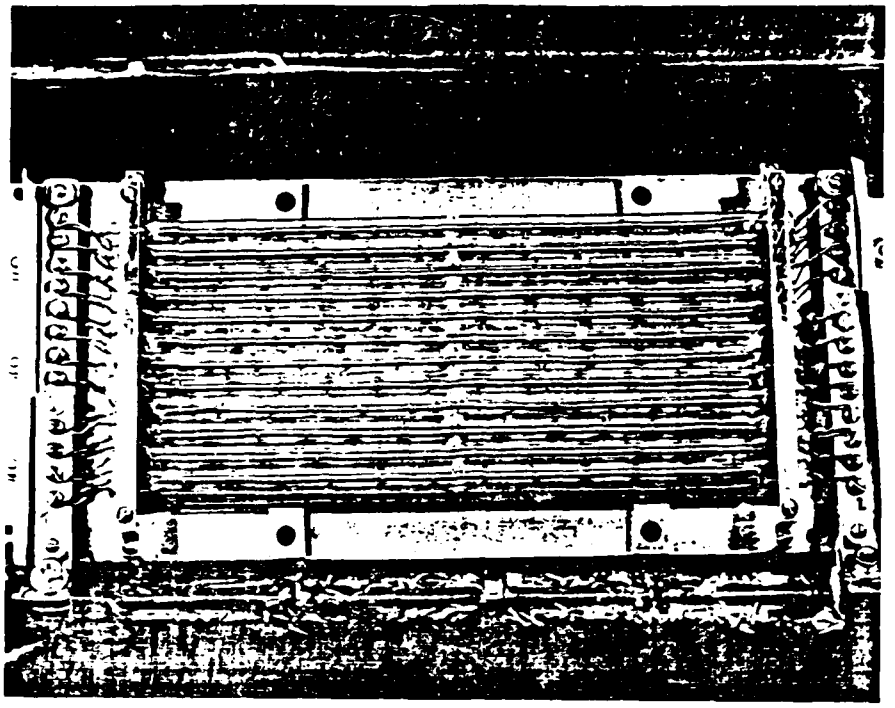

Figure A2.
HIGH DENSITY LAMP BANK No. 2

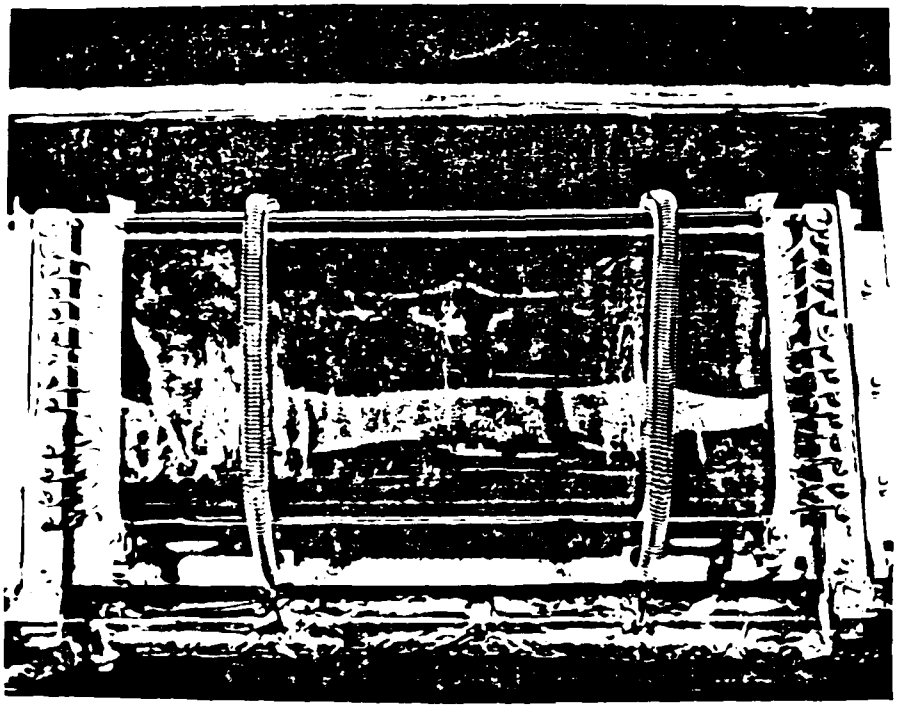

Figure A3.
HDLB2 GOLD-PLATED REFLECTOR

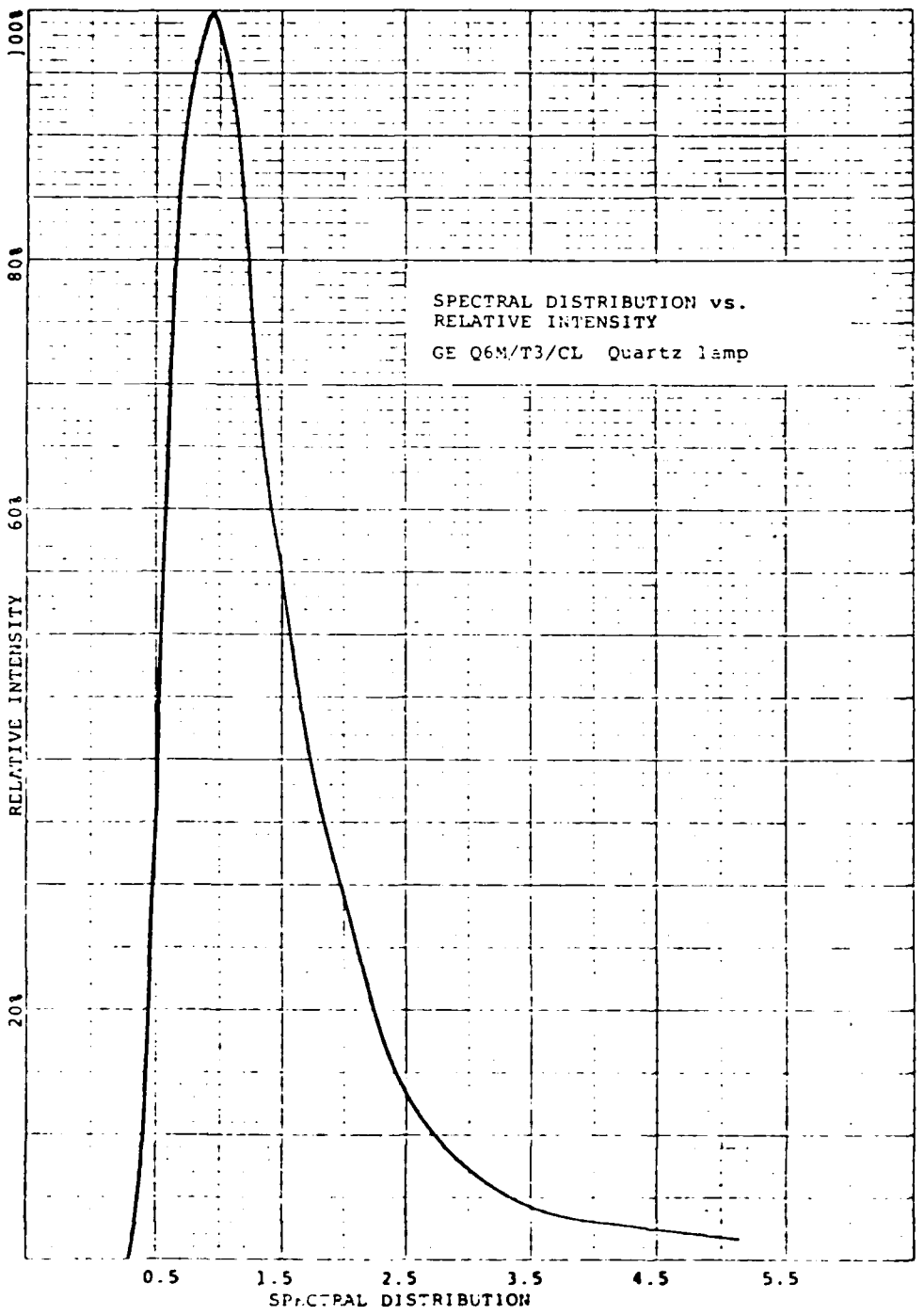

Figure A1.

QUARTZ LAMP SPECTRAL DISTRIBUTION

Task 4. PYROELECTRIC DETECTOR CHARACTERIZATION

Request:

Complete breadboard of Pyroelectric Detector. Since Pyroelectric element is sensitive to rate of change of flux, absolute peak flux level is not important but cross calibration with a good Hy-Cal is still required. Variable shutter speeds would be desirable in this case.

Action:

Several circuits similar to those suggested by the manufacturer were tried in an effort to generate some relative voltage or current change as a function of a change in light level at the surface of the Pyroelectric Detector. Intensity levels no greater than a 100 watt unfrosted light bulb at distances no closer than 3 inches did not result in any discernible change in the out put of the detector. If the detector could be made to function, it is a rate-of-change device and therefore should not be calibrated against an equilibrium device such as an asymptotic calorimeter. Variable shutter speeds would not produce a variable rate-of-change, only the relocation of a fixed level of radiant energy from one point to another, i.e.: from the face of the shutter to the face of the detector.

Note: this task was completed prior to the resurfacing and recalibration of Hy-Cal ser. no. 36002. The new calibration factor is 24.592 (cal/cm^2-sec)/mv versus the old factor of 24.0 representing an increase of 2-1/2% in indicated apparent flux.

1) Comparing the NPC against calorimeter 36002 in Full Window Dual Unit Holder using HDLB2 @ full power

a) with gold-plated aluminum reflector

1 sec exposure

NPC	above	peak temperature	186°F	(Fig. 51)
36002	below	flux	68.4 cal/cm^2-sec	
NPC	below	peak temperature	187°F	(Fig. 52)
36002	above	flux	67.7 cal/cm^2-sec	

2 sec exposure

NPC	above	peak temperature	223°F	(Fig. 53)
36002	below	flux	68.6 cal/cm^2-sec	
NPC	below	peak temperature	223°F	(Fig. 54)
36002	above	flux	67.7 cal/cm^2-sec	

b) without reflector

1 sec exposure

NPC	above	peak temperature	143°F	(Fig. 55)
36002	below	flux	42.2 cal/cm^2-sec	
NPC	below	peak temperature	147°F	(Fig. 56)
36002	above	flux	42.1 cal/cm^2-sec	

2 sec exposure

NPC	above	peak temperature	170°F	(Fig. 57)
36002	below	flux	42.8 cal/cm^2-sec	
NPC	below	peak temperature	170°F	(Fig. 58)
36002	above	flux	42.4 cal/cm^2-sec	

2) Determining effects of angle on the NPC in Center Mount Pivot Holder using HDLB2 @ full power with gold-plated reflector

face-to-lamp angle	peak temperature	
0°	173°F	(Fig. 59)
10° down	174°F	(Fig. 60)
10° up	173°F	(Fig. 61)
10° left	171°F	(Fig. 62)
10° right	174°F	(Fig. 63)

Task 3. NULL POINT CHARACTERIZATION

Request:

Simultaneously expose the null point calorimeter and the 1000 BTU Hy-Cal to a flux level of 40 cal/cm^2-sec. normal flux and fastest shutter speeds. Expose to at least four angles with respect to the constant normal flux and at each angle expose to one test duration equal to 1.0 sec.

Explication:

The full-window, dual unit calorimeter holder (Fig. 9b) was used to simultaneously expose the Null Point Calorimeter and the 750 BTU Hy-Cal calorimeter ser. no. 36002 to flux levels of approximately 30 and 60 cal/cm^2-sec. The 750 BTU unit was used because it was mounted in the holder and had been the lab reference unit. Two flux levels were chosen to display differences in the slope of the curve generated by the NPC. Exposure times (with shutter) of both 1 and 2 seconds confirmed the slope shape.

Action:

The Null Point Calorimeter (NPC) is a device that seems to act much like a copper slug calorimeter using a type K thermocouple. The output of the device was compensated to room temperature although it is believed that only the Δt/time is of importance. An adapter was fabricated to allow the device to be used in the various holders that were developed for the Hy-Cal calorimeters.

Observation:

Angle relationship between calorimeter sensing surface and source does not seem to have a severe effect on indicated flux with a worst-case w/o attenuator of only 1.5% down at 10°. With attenuator face at normal pace, the worst-case is 3.5% down and a loss of near 8% is indicated when the attenuator is used, but the calorimeter face is at the normal plane (inner tunnel wall). More importantly the attenuator seems to have about a 3.7:1 reduction factor (73%).

at four different angles plus straight on the highest flux level available using the HDLB2 at full power with the gold-plated aluminum reflector.

Configurations: (Calorimeter no. 75771)

a) w/o attenuator

b) with attenuator face at inside wall plane (Fig. 35a)

c) with attenuator, with calorimeter face at inside wall plane (Fig. 35b)

Flux (cal/cm^2-sec)(Figs. 36-50)

face-to-lamp angle	a)	b)	c)
0°	53.3	14.4	14.2
5° right	53.3	13.9	13.9
10° right	52.5	14.0	13.7
5° up	53.3	14.2	13.1
10° up	52.8	14.6	13.5

Note: this task was completed prior to the resurfacing and recalibration of Hy-Cal ser. no. 75771. The new calibration factor is 10.475 (cal/cm^2-sec)/mv versus the old factor of 9.309 (cal/cm^2-sec)/mv representing an increase of 12-1/2% in indicated apparent flux.

Task 2: ATTENUATOR DEVELOPMENT

Request:

Produce sample attenuator as shown in Fig. 34 to provide a factor of 10.0, reduction of incident flux. Use attenuator on high flux calorimeter and cross calibrate with low flux calorimeter to determine actual attenuation factor. Expose attenuated calorimeter to at least four angles with respect to a constant normal incident flux to estimate conformance to sine dependence. Fastest shutter speeds should be used in all cases.

Explication:

All indicated dimensions of the collimator were adhered to with the exception of outside diameter which was reduced from 1" to 3/4" to minimize surface area exposed to radiant energy.

The collimator was used on the high flux calorimeter (ser. no. 75771-1000 BTU) but the attenuation factor was determined directly by exposing the calorimeter to similar radiant energy pulses both with and without the collimator.

Action:

A pinhole collimating attenuator was fabricated from aluminum as per dimensions (Fig. 34). The attenuator was constructed to press-fit snugly over a standard 5/8" o.d. Hy-Cal calorimeter. The inner cone surface is at a 45° angle and highly polished. The face is also polished. The input aperture is 0.198" yielding an area ratio of 10:1. The attenuator and calorimeter in three configurations were held in the Center Mount Pivot (CMP) holder (Fig. 10) and exposed

Level 2 (Figs. 24-28)

HDLB2 without reflector. Full power, full-window, single-unit calorimeter holder with blackened face.

Ser. No.	Flux (cal/cm^2-sec) group 1	group 2	group 3	Avg.
55199	37.4	37.2	37.2	37.3
95301	36.7	36.5	36.7	36.6
75771	37.7	37.5	37.5	37.6
36002	37.1	36.9	36.9	37.0
72383	39.3	38.9	38.9	39.1

Level 3 (Figs. 29-33)

HDLB2 without reflector. 60% power. Full-window, single-unit calorimeter holder with blackened face.

Ser. No.	Flux (cal/cm^2-sec) group 1	group 2	group 3	Avg.
55199	17.4	17.4	17.2	17.3
95301	17.0	16.9	17.0	17.0
75771	17.4	17.6	17.4	17.5
36002	17.2	17.2	17.0	17.1
72383	18.3	18.3	18.0	18.2

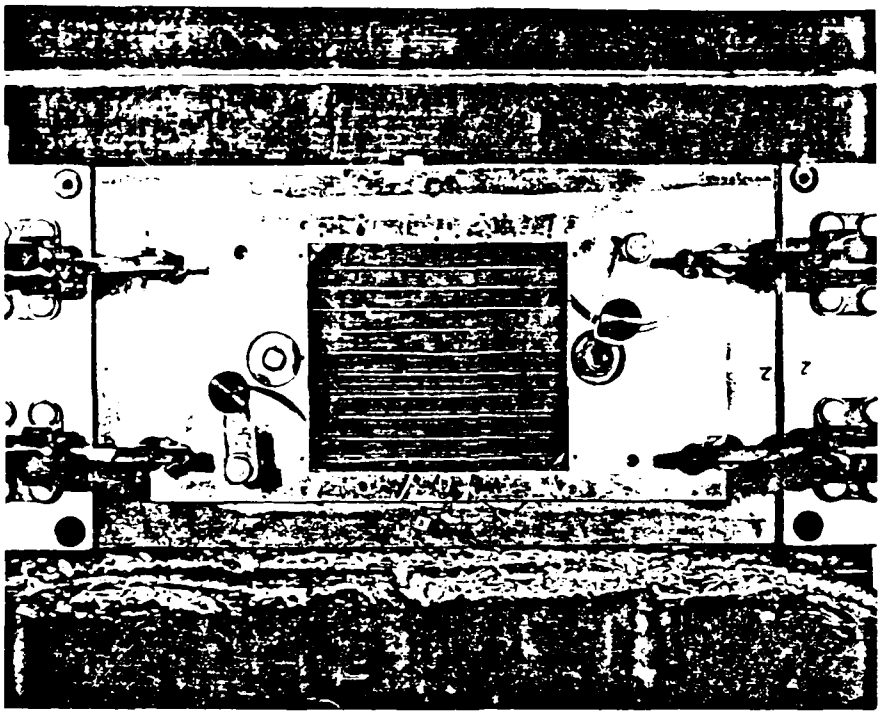

Figure A8.

SAMPLE WINDOW

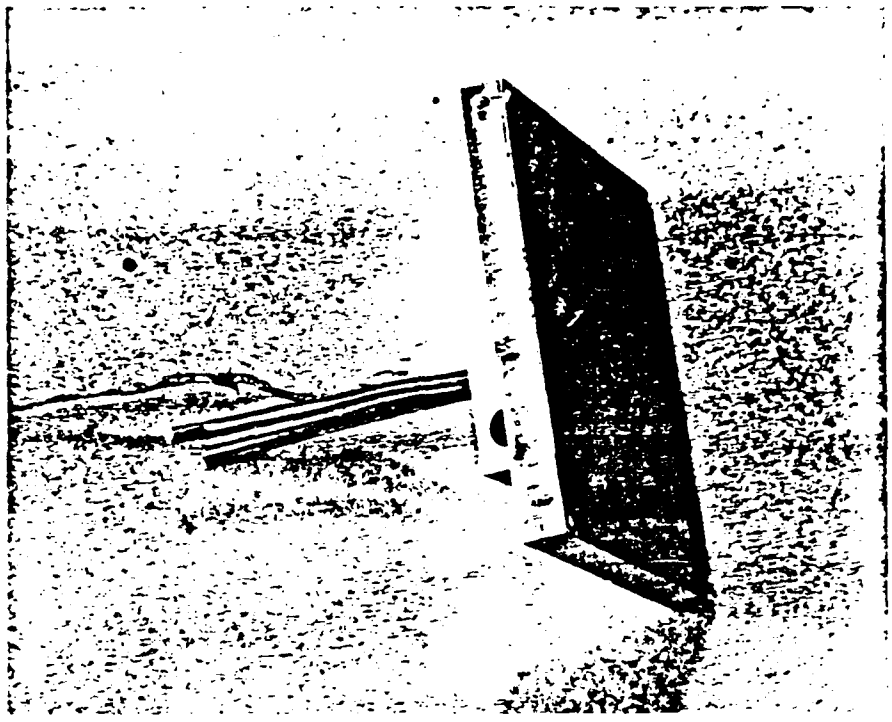

Figure A9a.
FULL-WINDOW SINGLE UNIT HOLDER

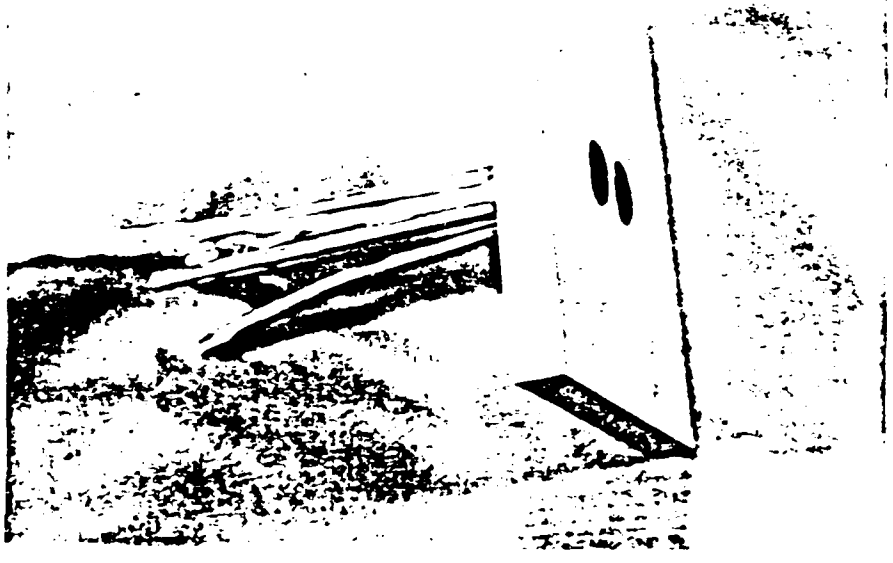

Figure A9b.
FULL-WINDOW DUAL UNIT HOLDER

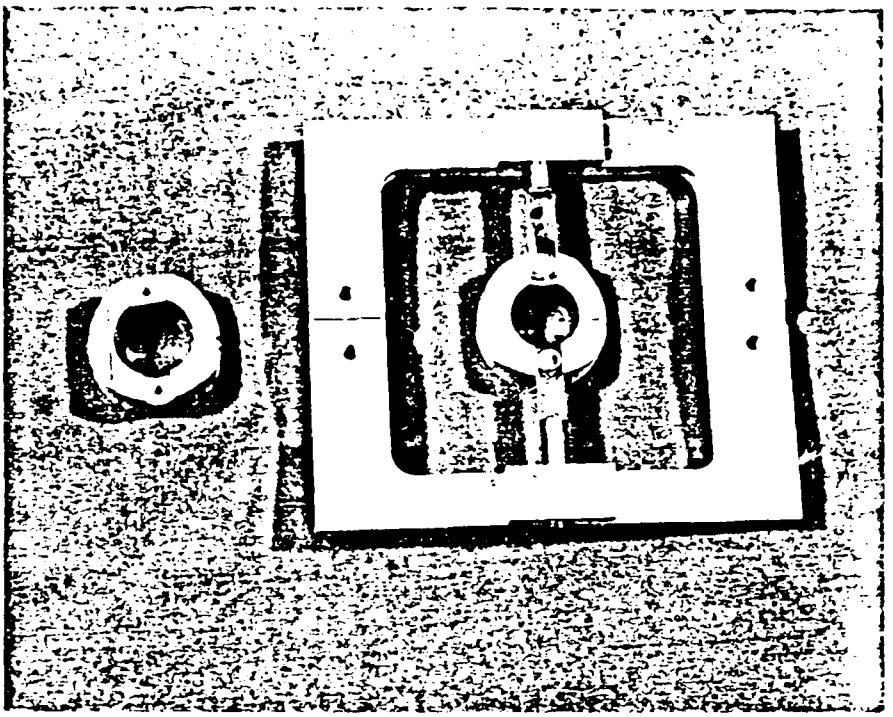

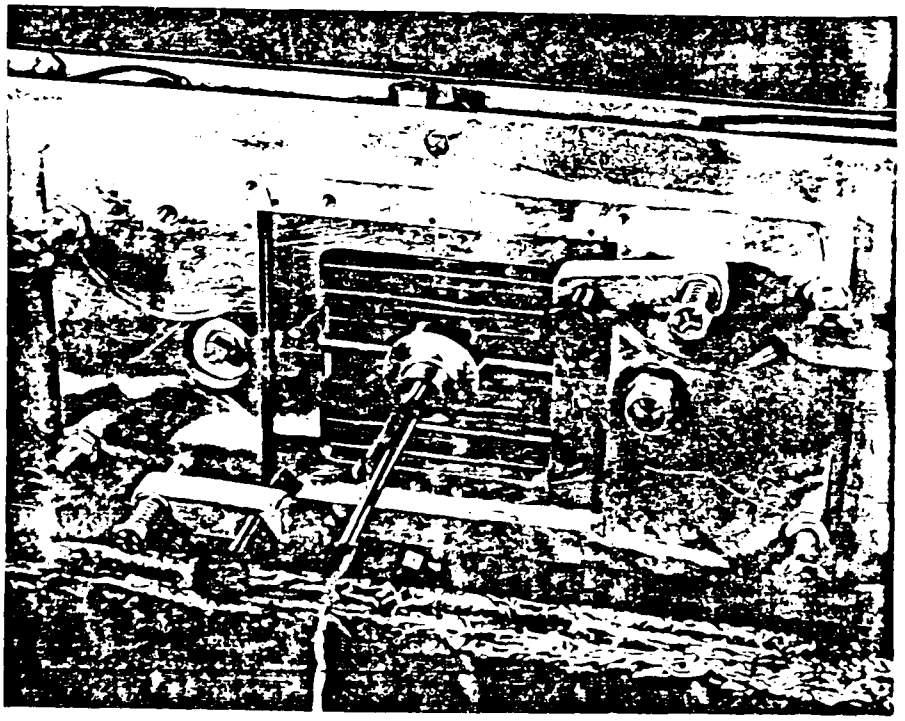

Figure A10.
CENTER-MOUNT-PIVOT HOLDER

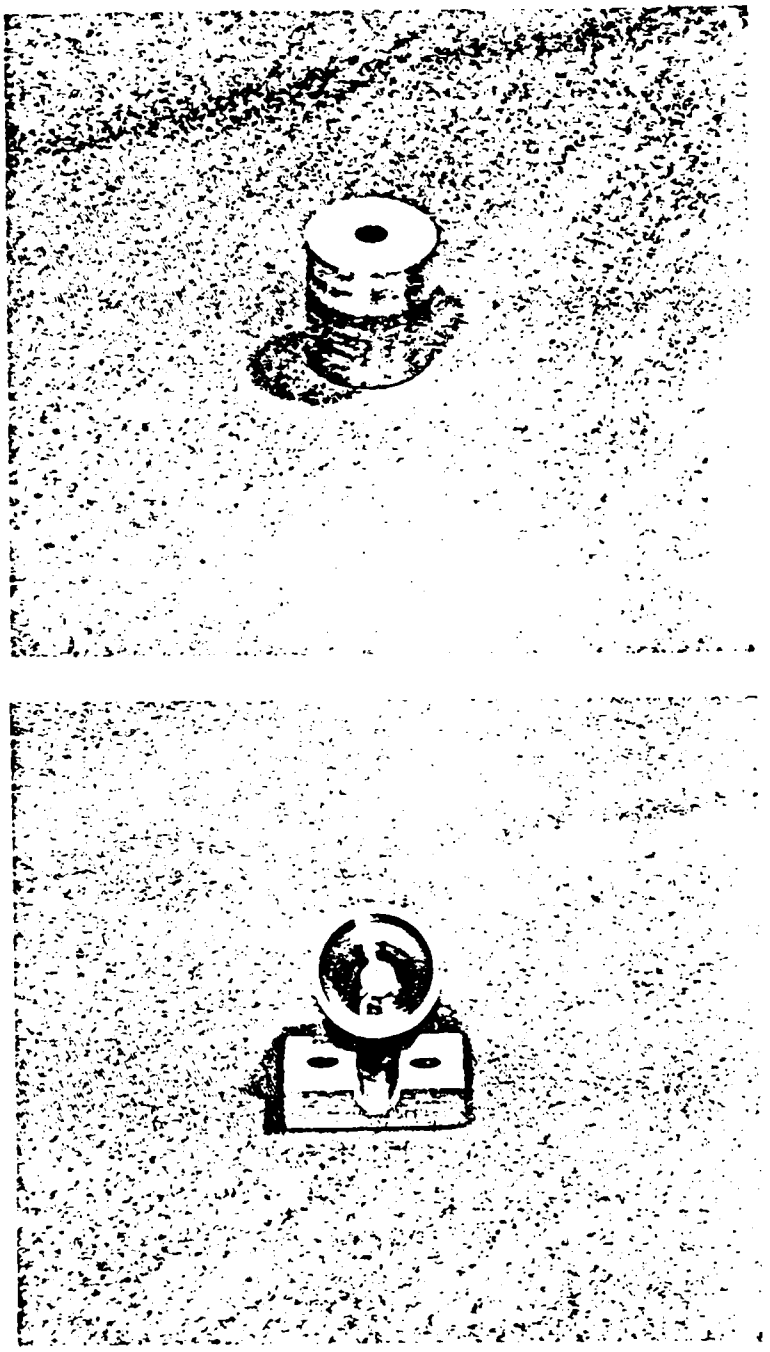

Figure A11.

ALUMINIUM COLLIMATING ATTENUATOR

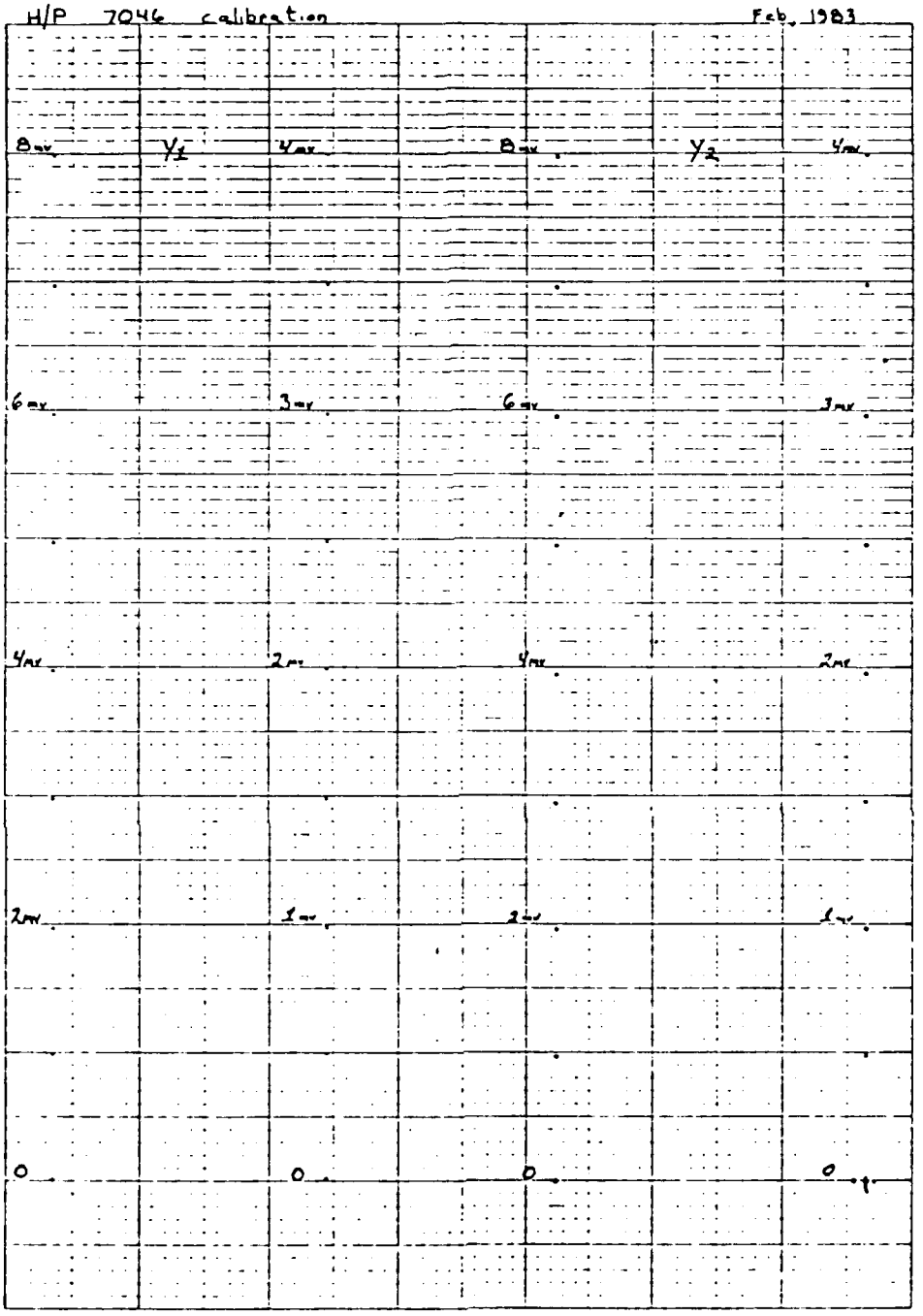

Figure A12.

H/P Recorder Calibration.

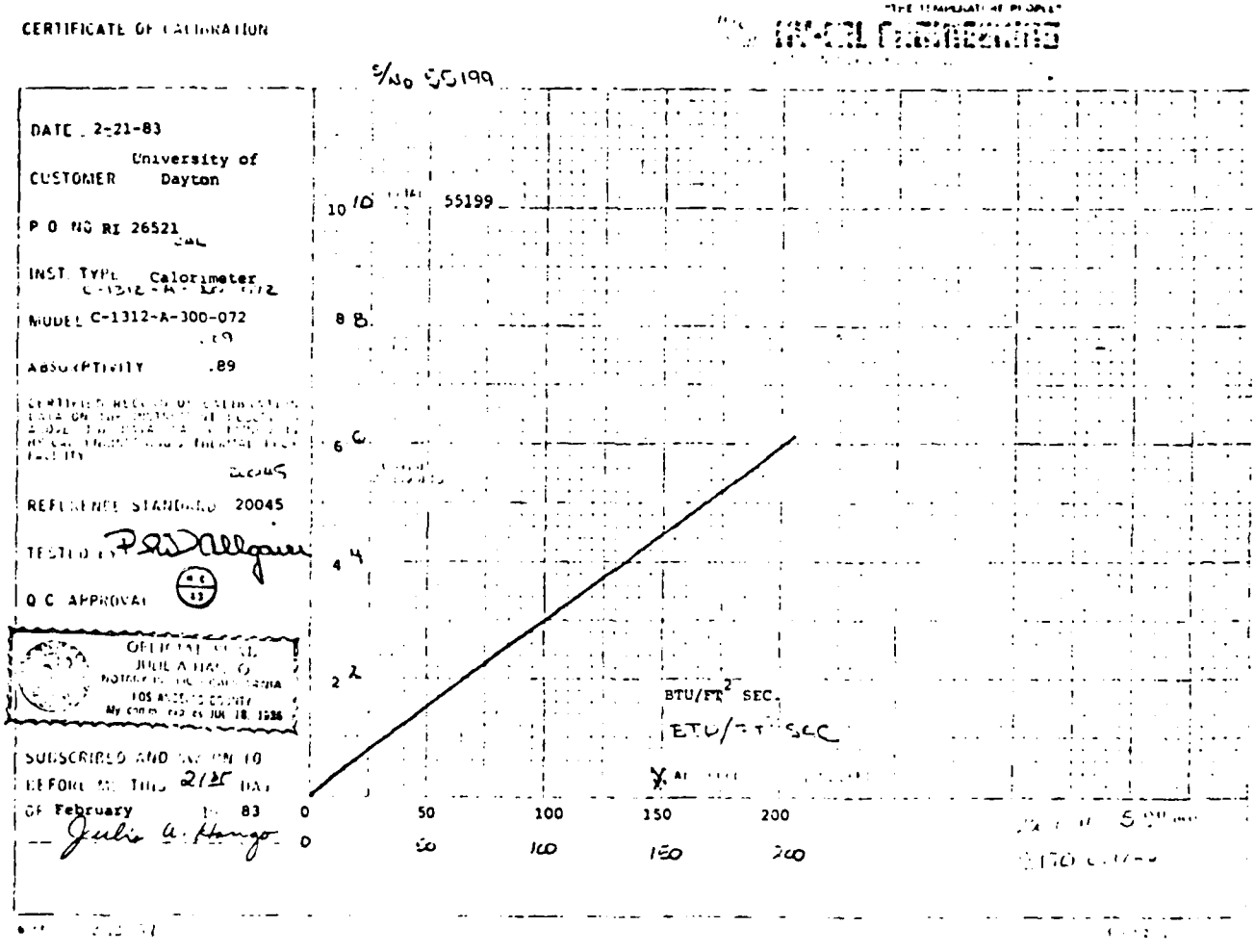

Figure A13.

HY-CAL CALIBRATION CERTIFICATE Sr. no. 55199

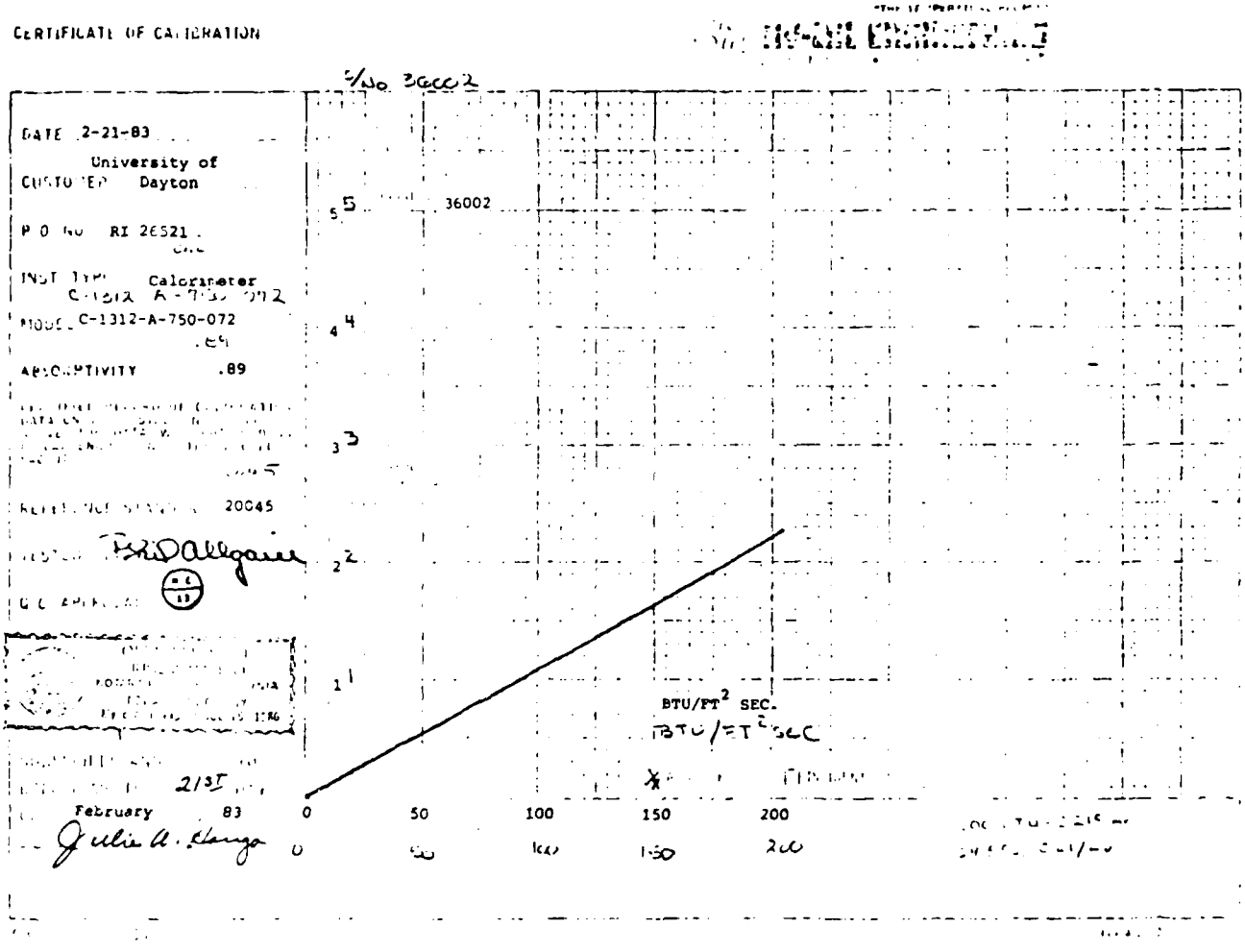

Figure A14.

HY-CAL CALIBRATION CERTIFICATE Sr. no. 36002

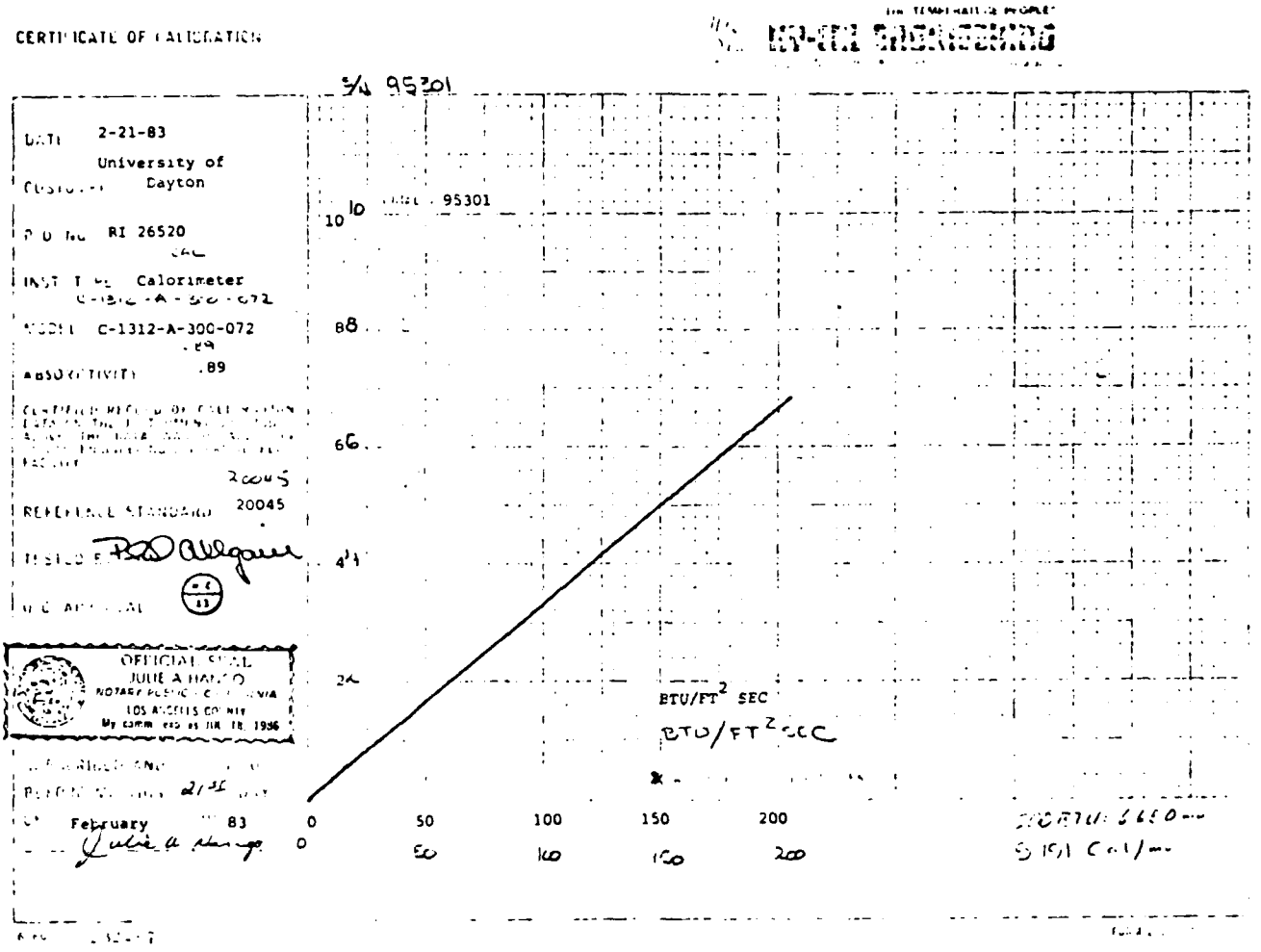

Figure A15.

HY-CAL CALIBRATION CERTIFICATE Sr. no. 95301

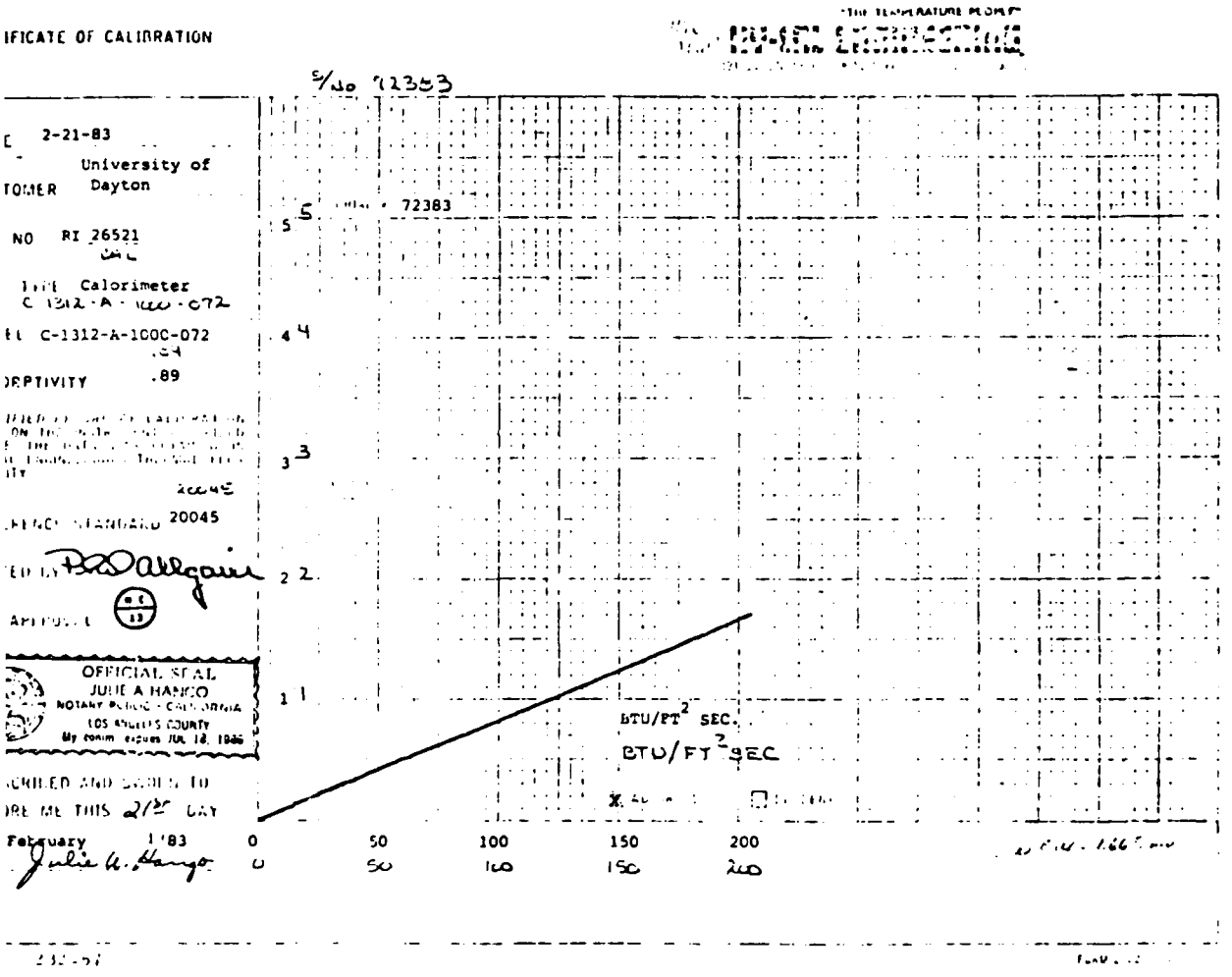

Figure A16.
HY-CAL CALIBRATION CERTIFICATE Sr. no. 72383

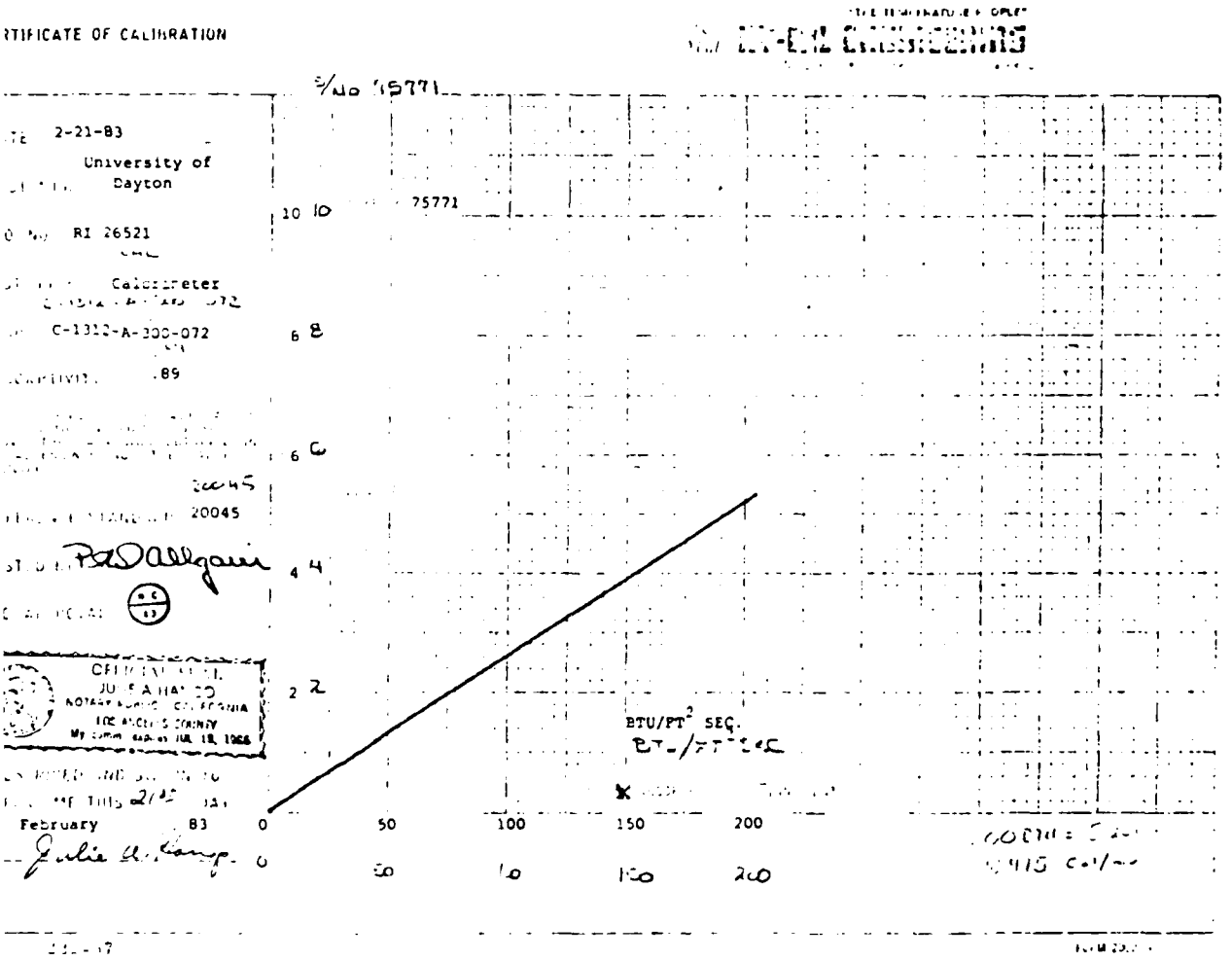

Figure A17.

HY-CAL CALIBRATION CERTIFICATE Sr. no. 75771

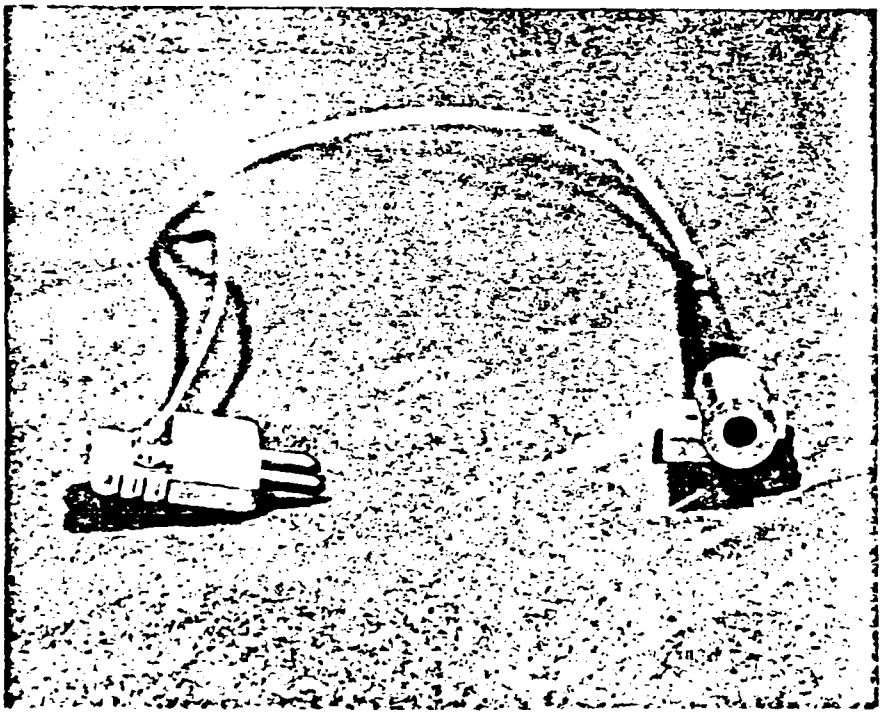

Figure A18.
NULL POINT CALORIMETER ADAPTER

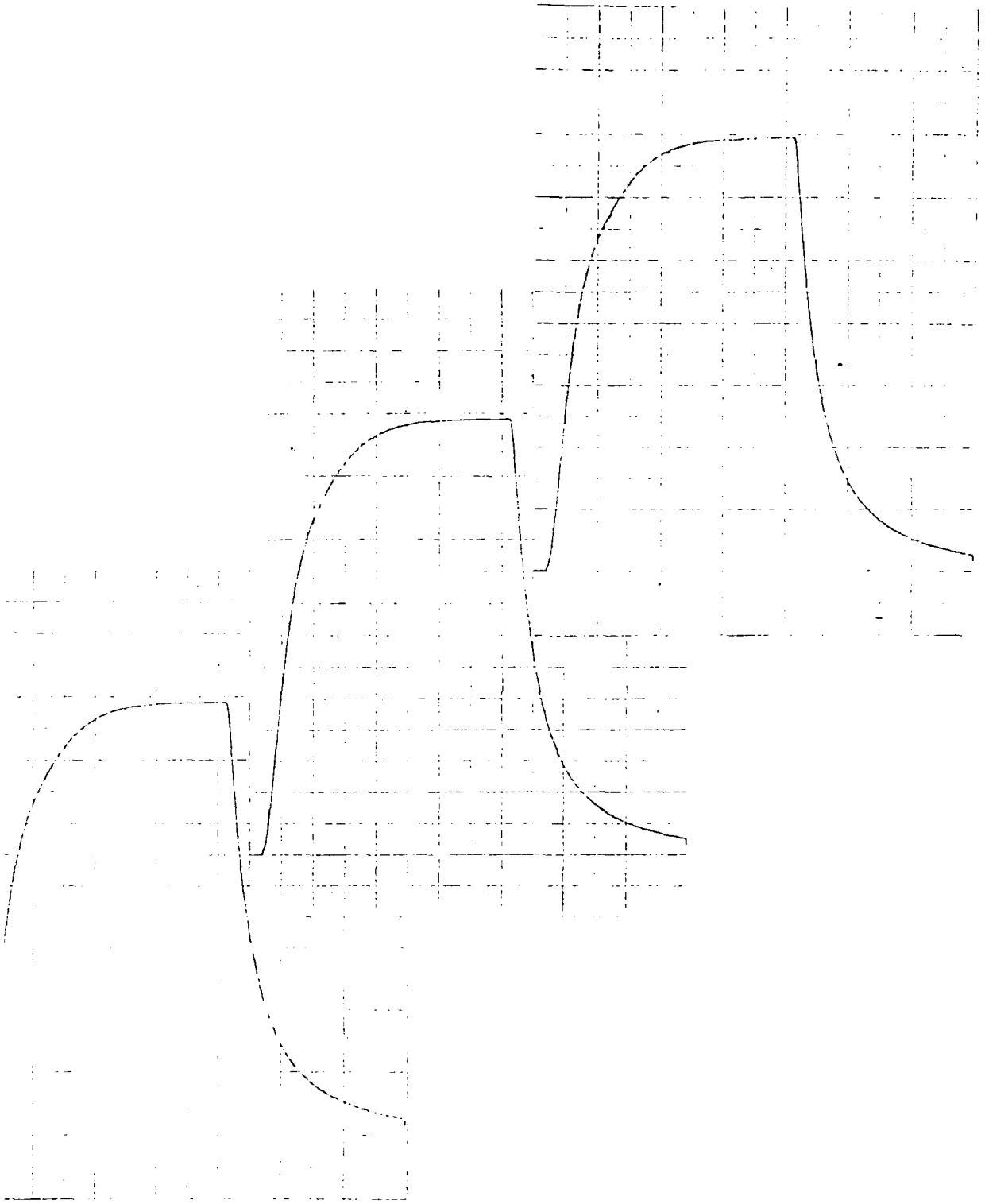

Figure A19. Level 1, Flux, Ser. No. 55199.

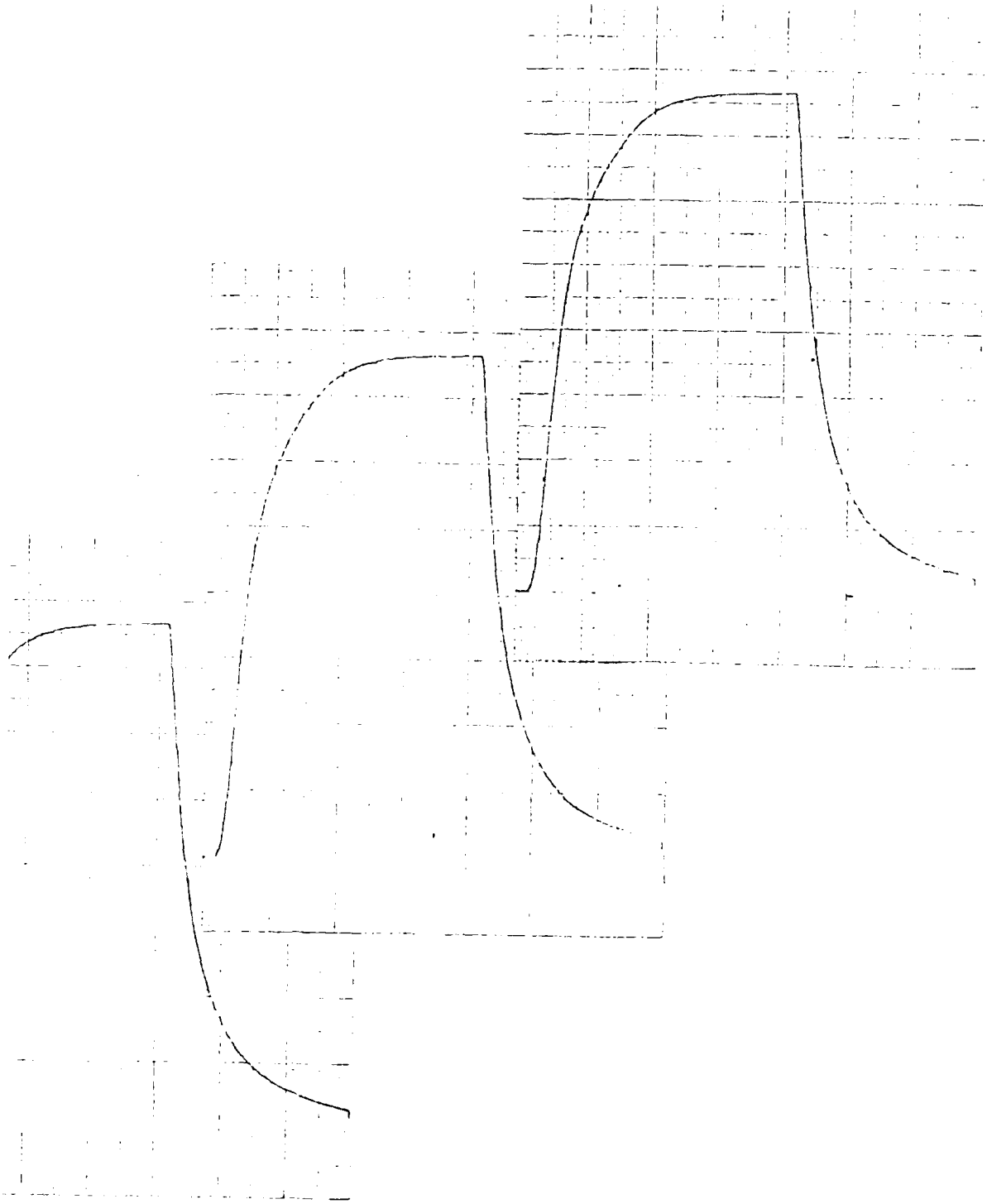

gure A20. Level 1, Flux, Ser. No. 95301.

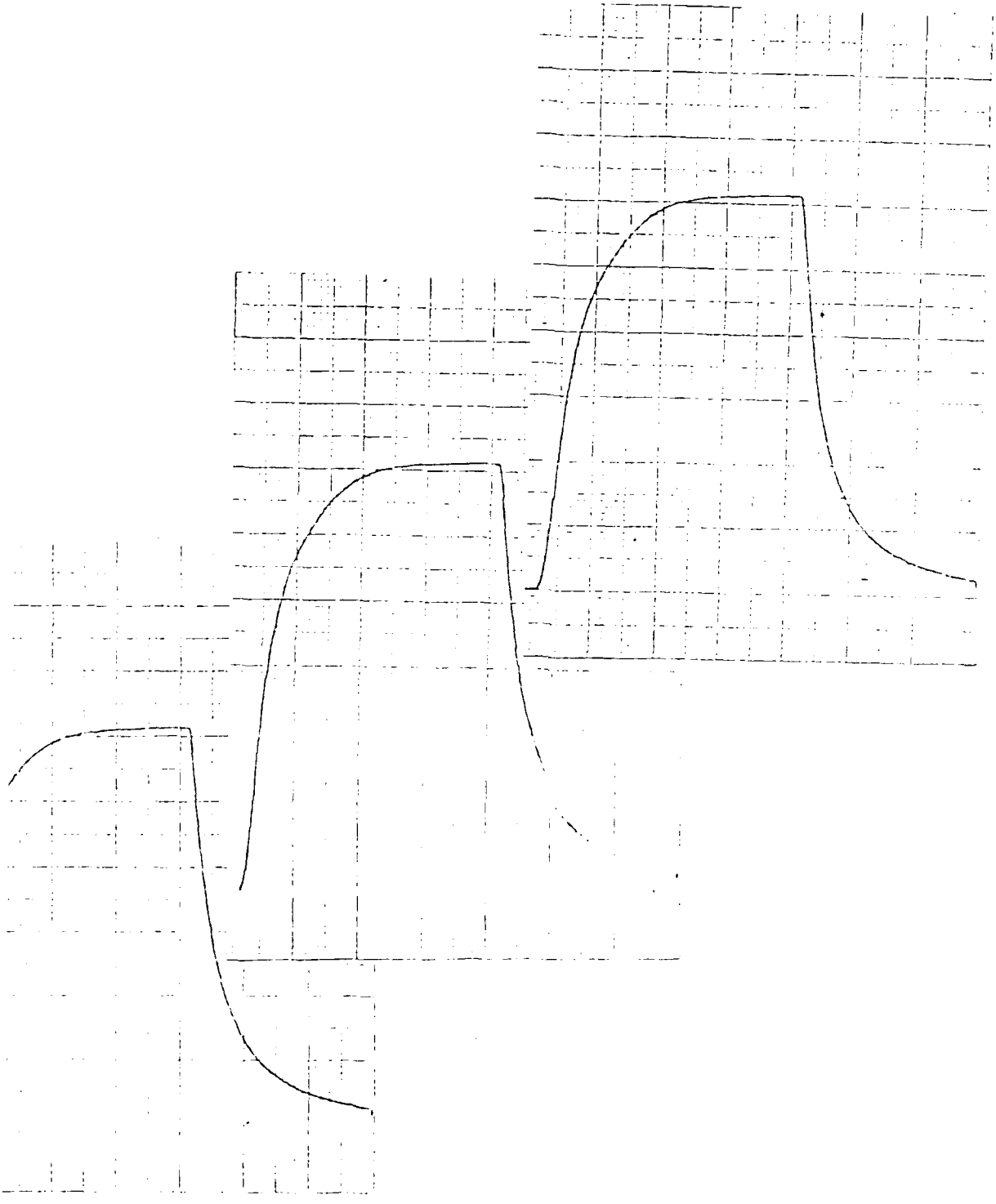

Figure A21. Level 1, Flux, Ser. No. 75771.

AD-A156 852 HIGH FLUX CALORIMETRY(U) SCIENCE APPLICATIONS 2/2
INTERNATIONAL CORP MCLEAN VA M MCDONNELL ET AL.
05 MAY 84 SAIC-84/1104 DNA-TR-84-183 DNA001-82-C-0185
UNCLASSIFIED F/G 14/2 NL

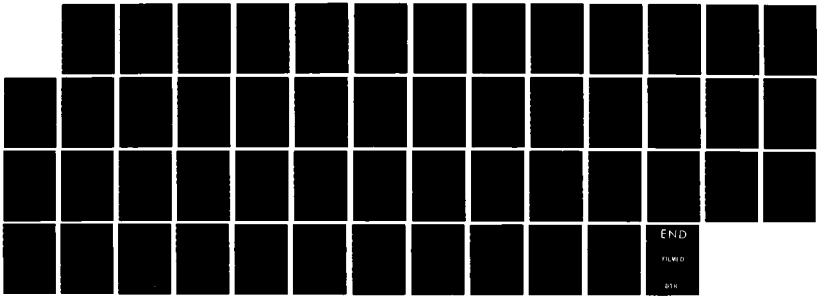

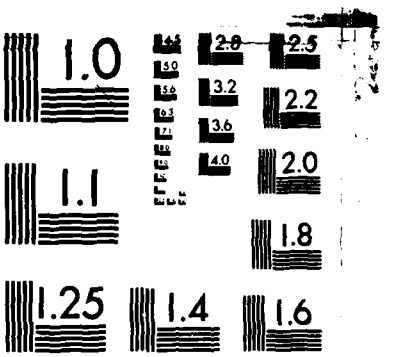

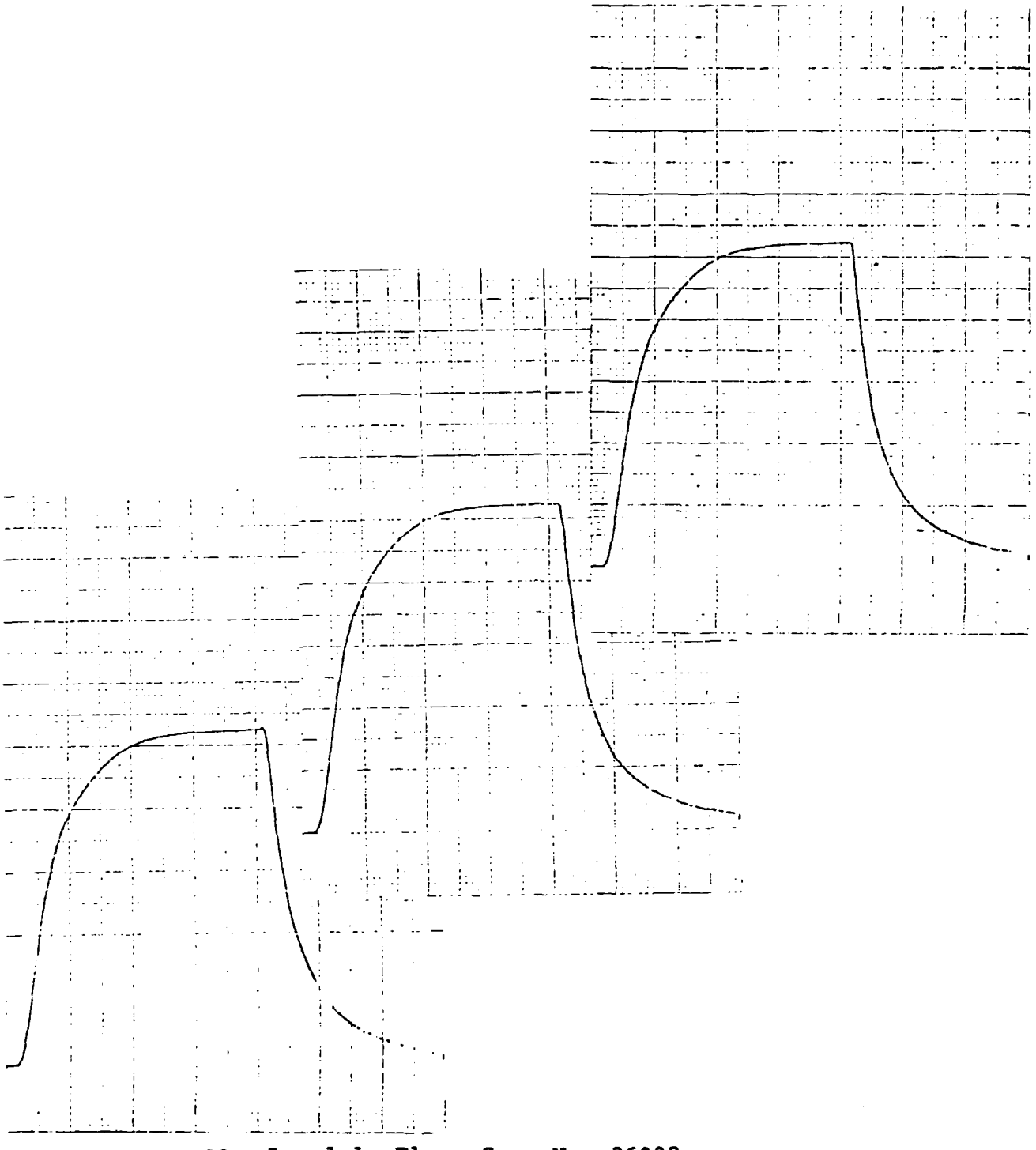

Figure A22. Level 1, Flux, Ser. No. 36002.

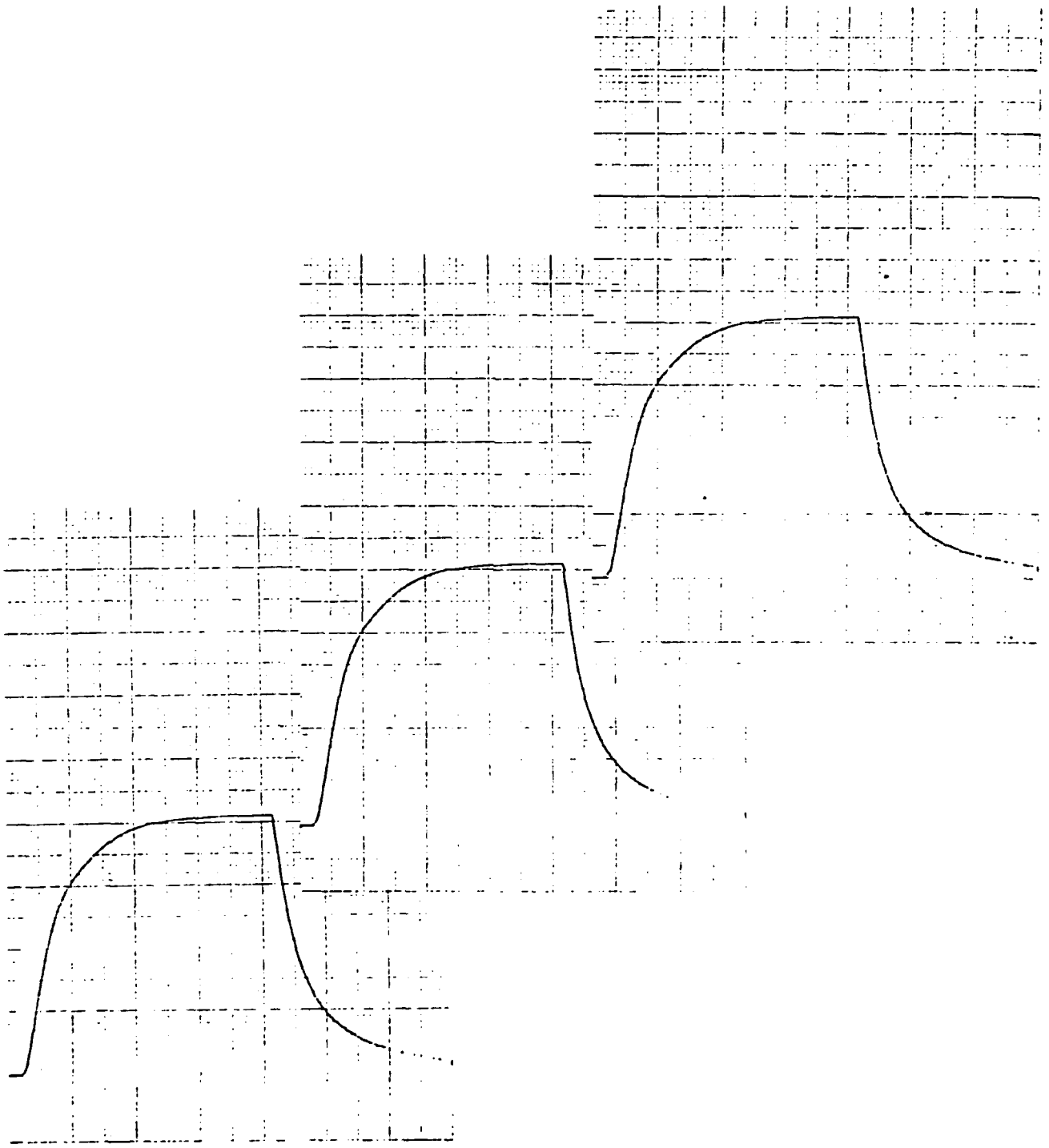

Figure A23. Level 1, Flux, Ser. No. 72383.

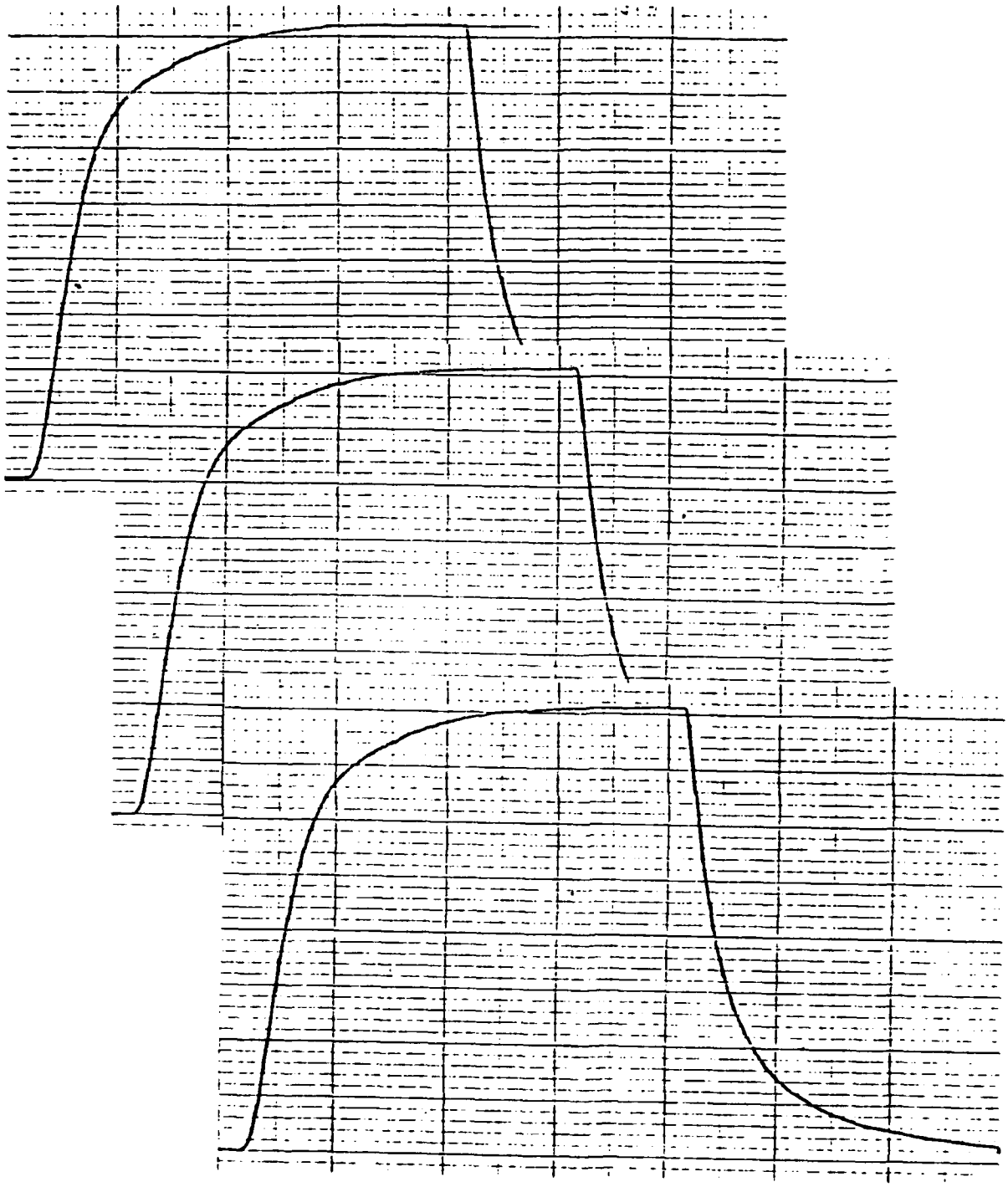

Figure A24. Level 2, Flux, Ser. No. 55199.

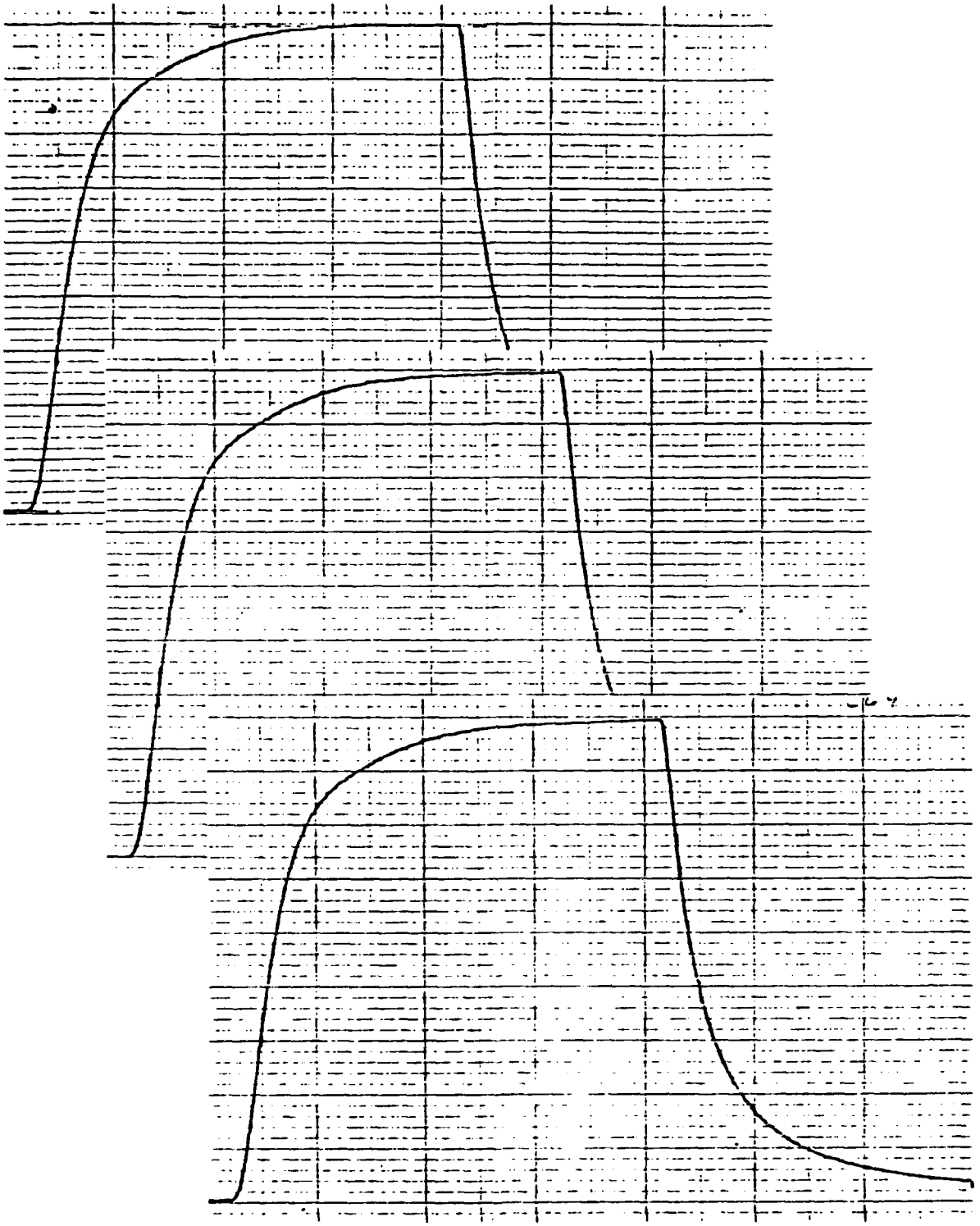

Figure A25. Level 2, Flux, Ser. No. 95301.

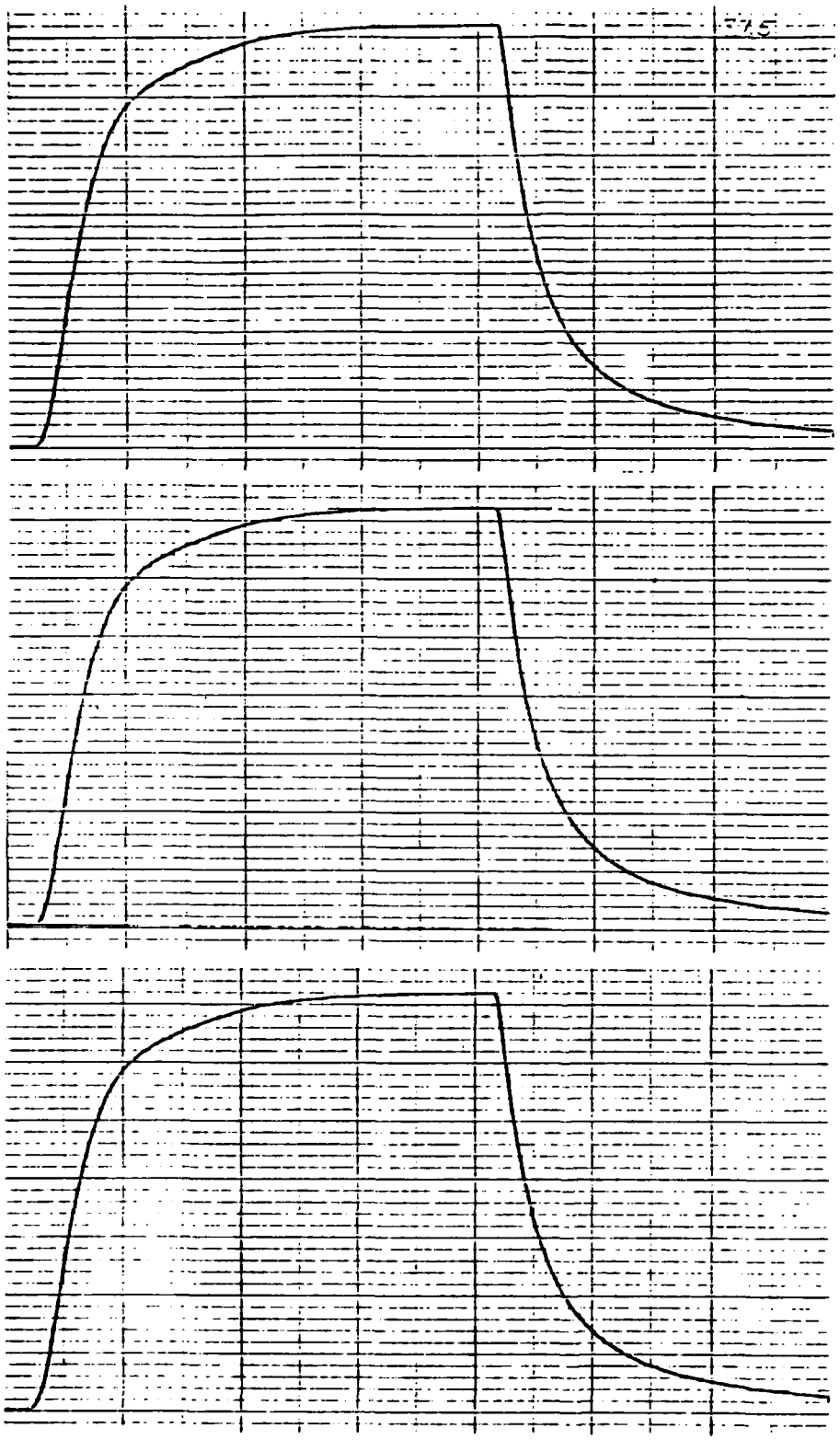

Figure A26. Level 2, Flux, Ser. No. 75771.

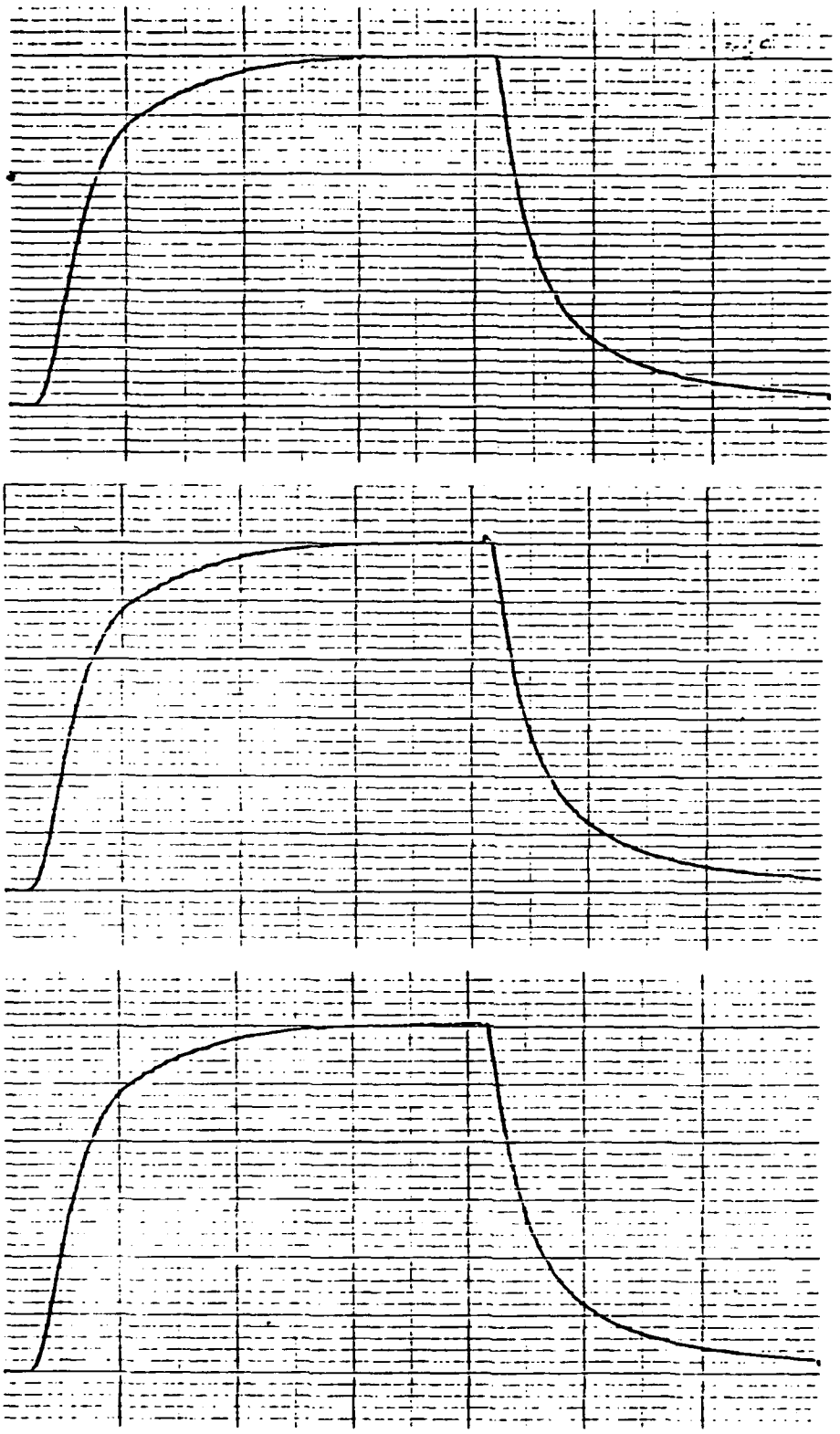

Figure A27. Level 2, Flux, Ser. No. 36002.

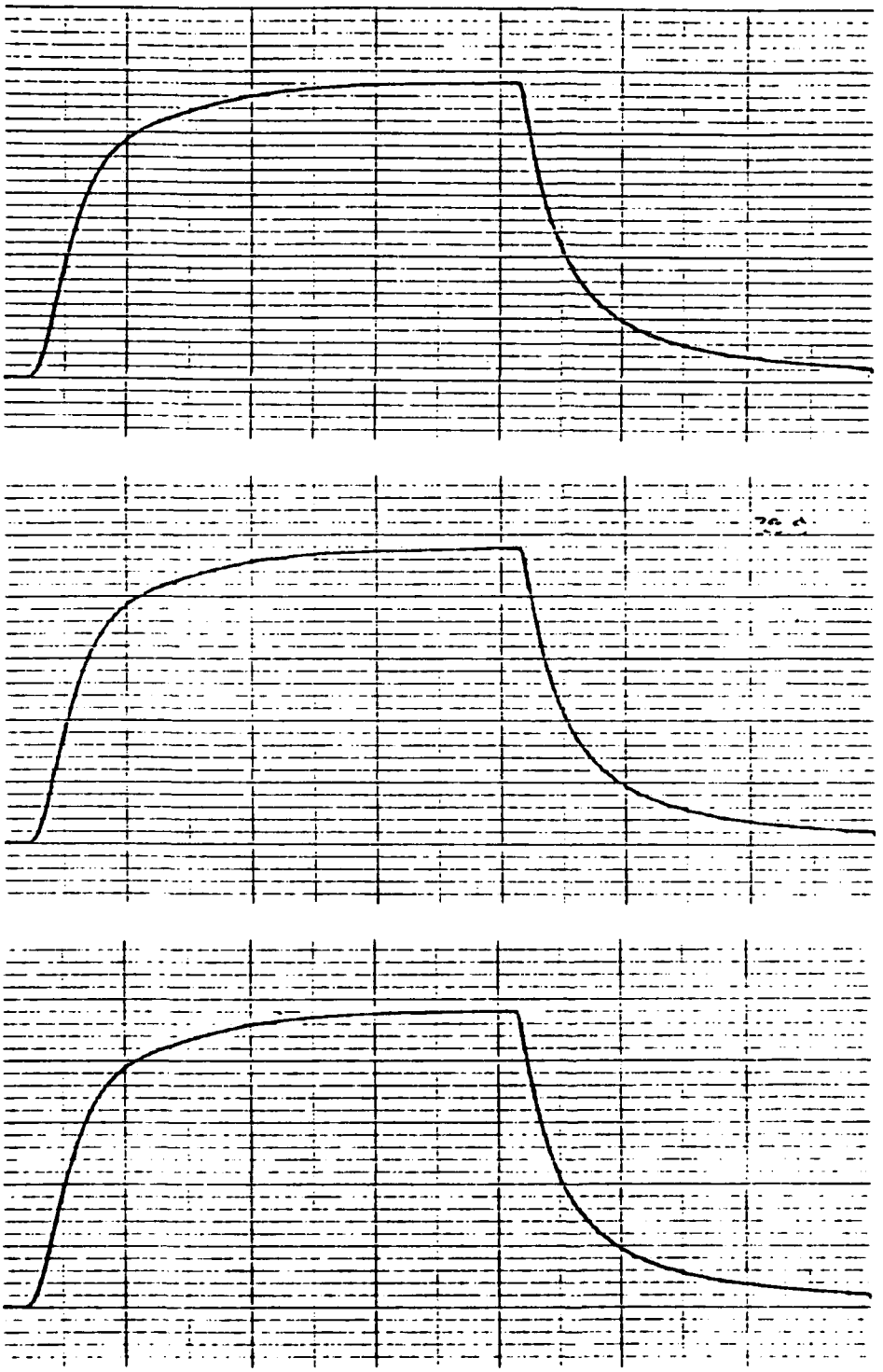

Figure A28. Level 2, Flux, Ser. No. 72383.

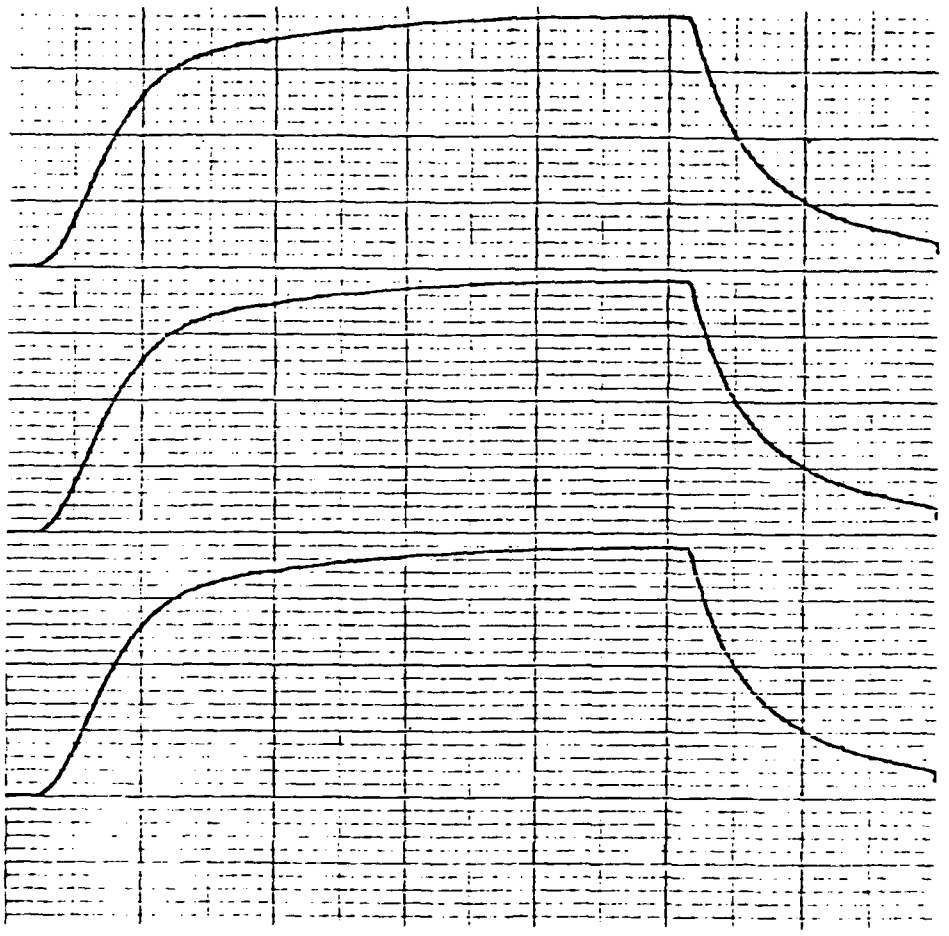

Figure A29. Level 3, Flux, Ser. No. 55199.

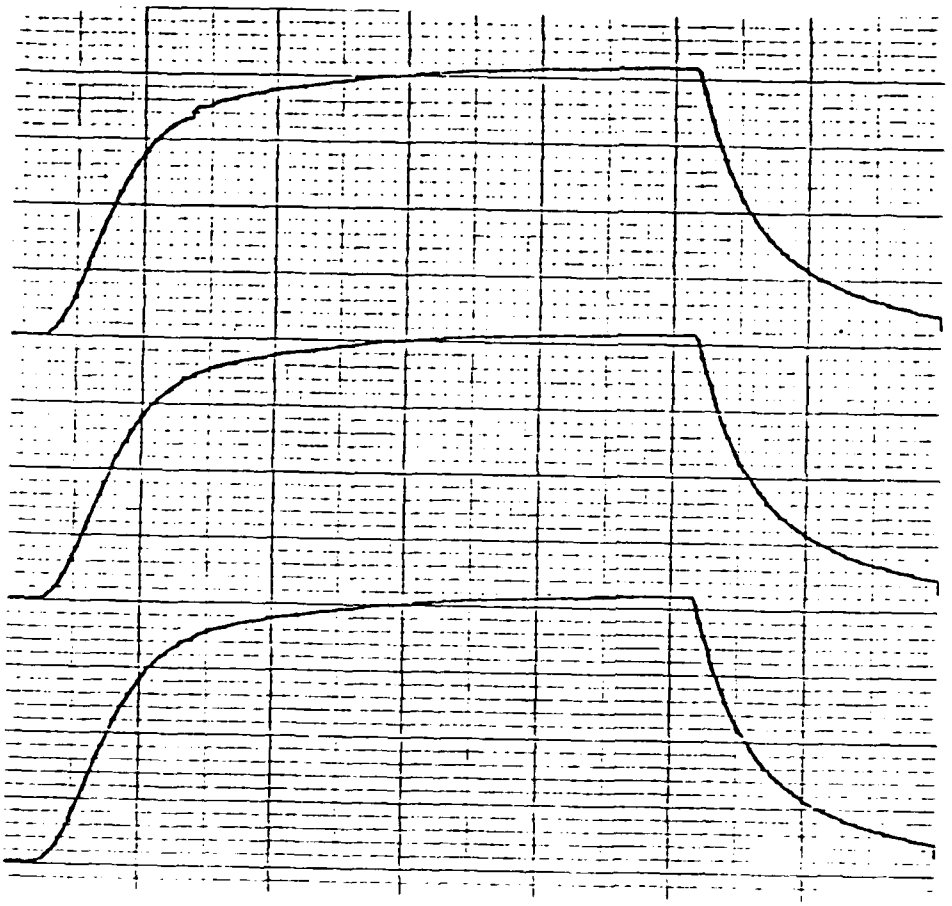

Figure A30. Level 3, Flux, Ser. No. 95301.

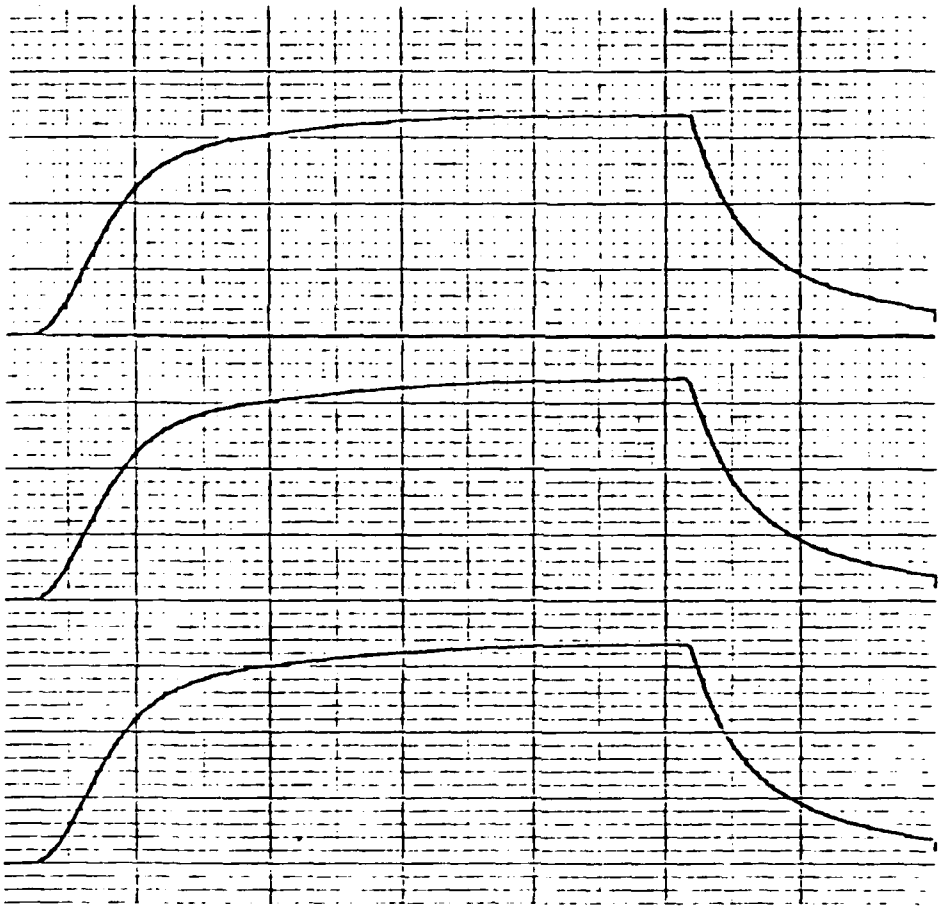

Figure A31. Level 3, Flux, Ser. No. 75771.

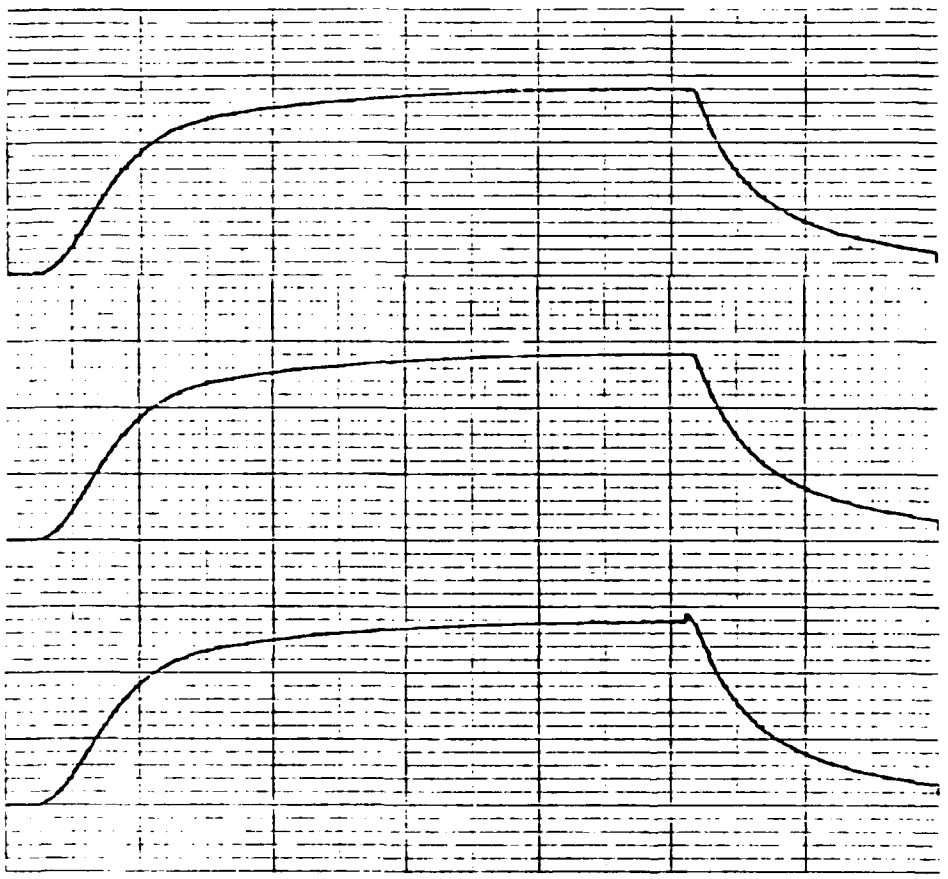

Figure A32. Level 3, Flux, Ser. No. 36002.

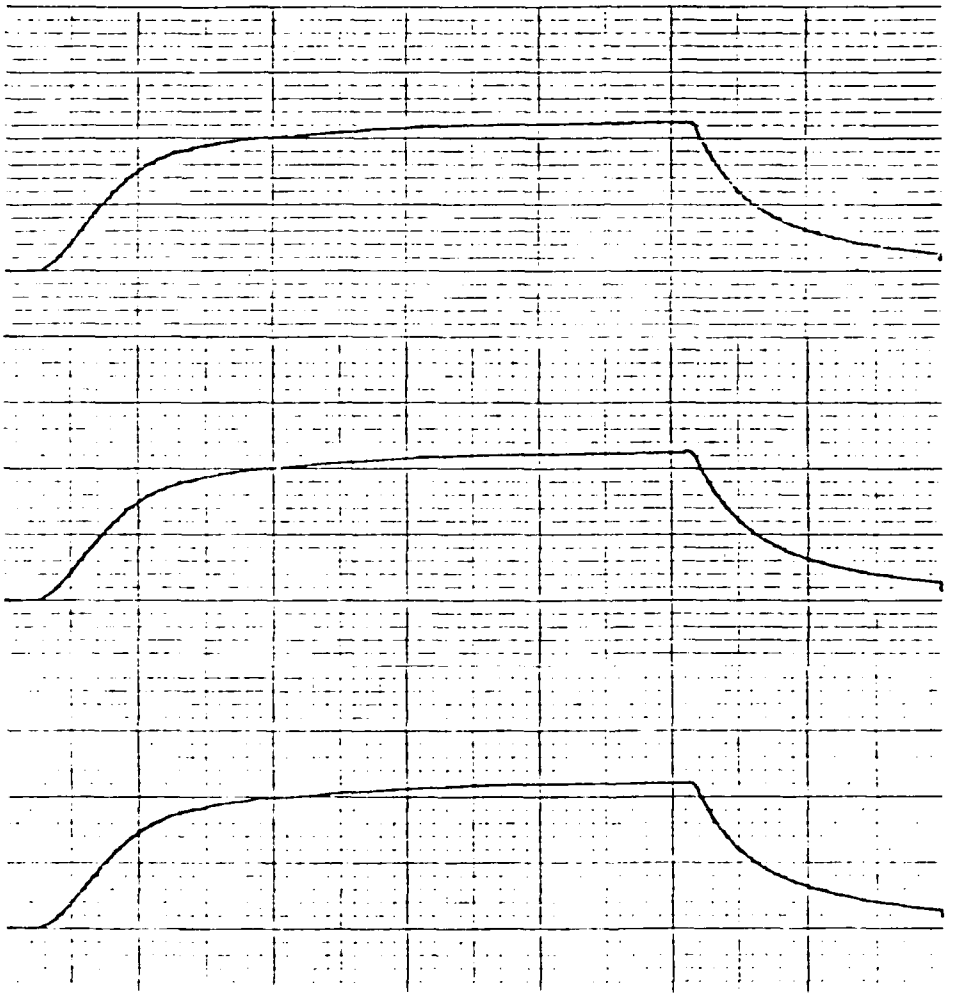

Figure A33. Level 3, Flux, Ser. No. 72383.

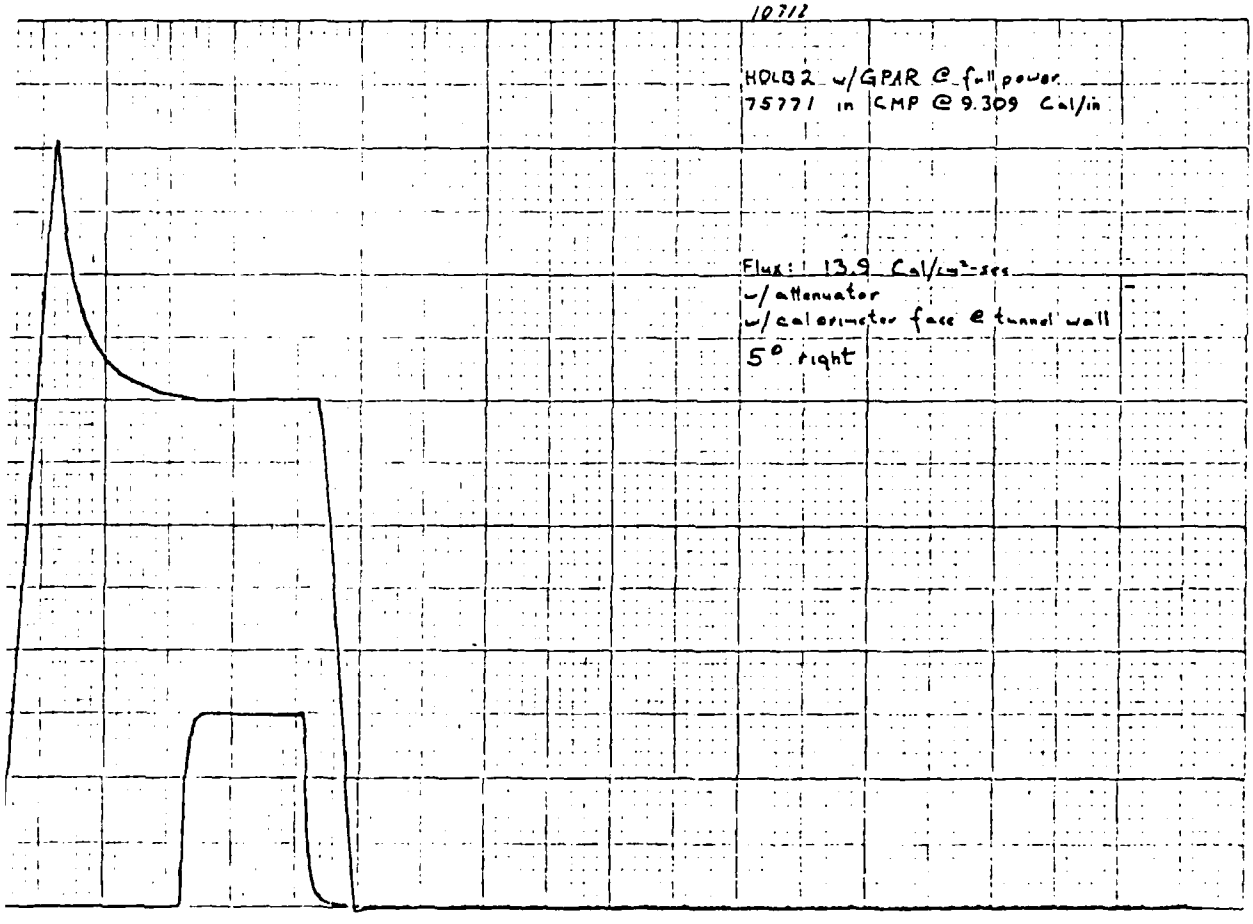

Figure A47. Flux w/Attenuator Offplane, 5° Right.

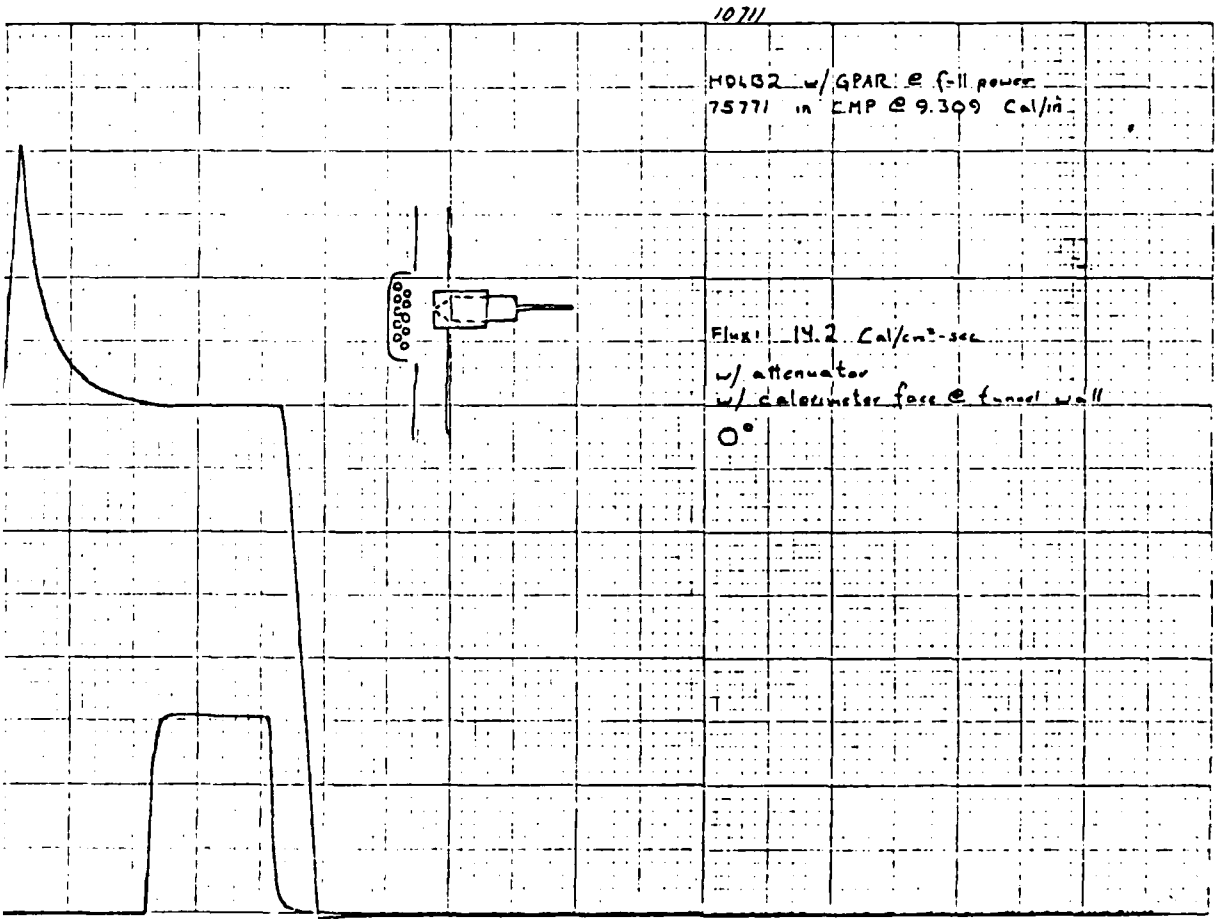

Figure A46. Flux w/Attenuator Offplane, 0°.

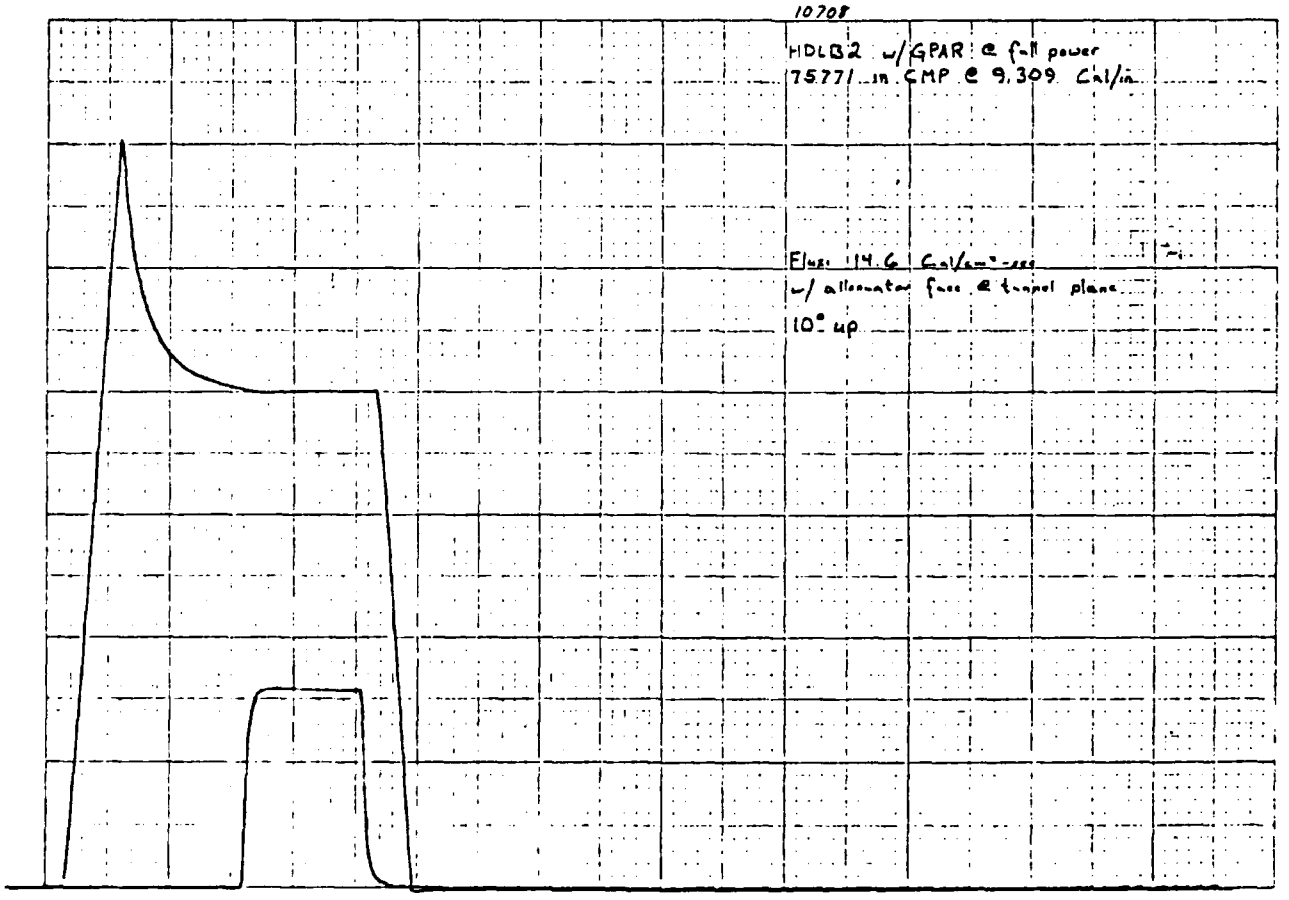

Figure A45. Flux w/Attenuator @ Plane, 10° Up.

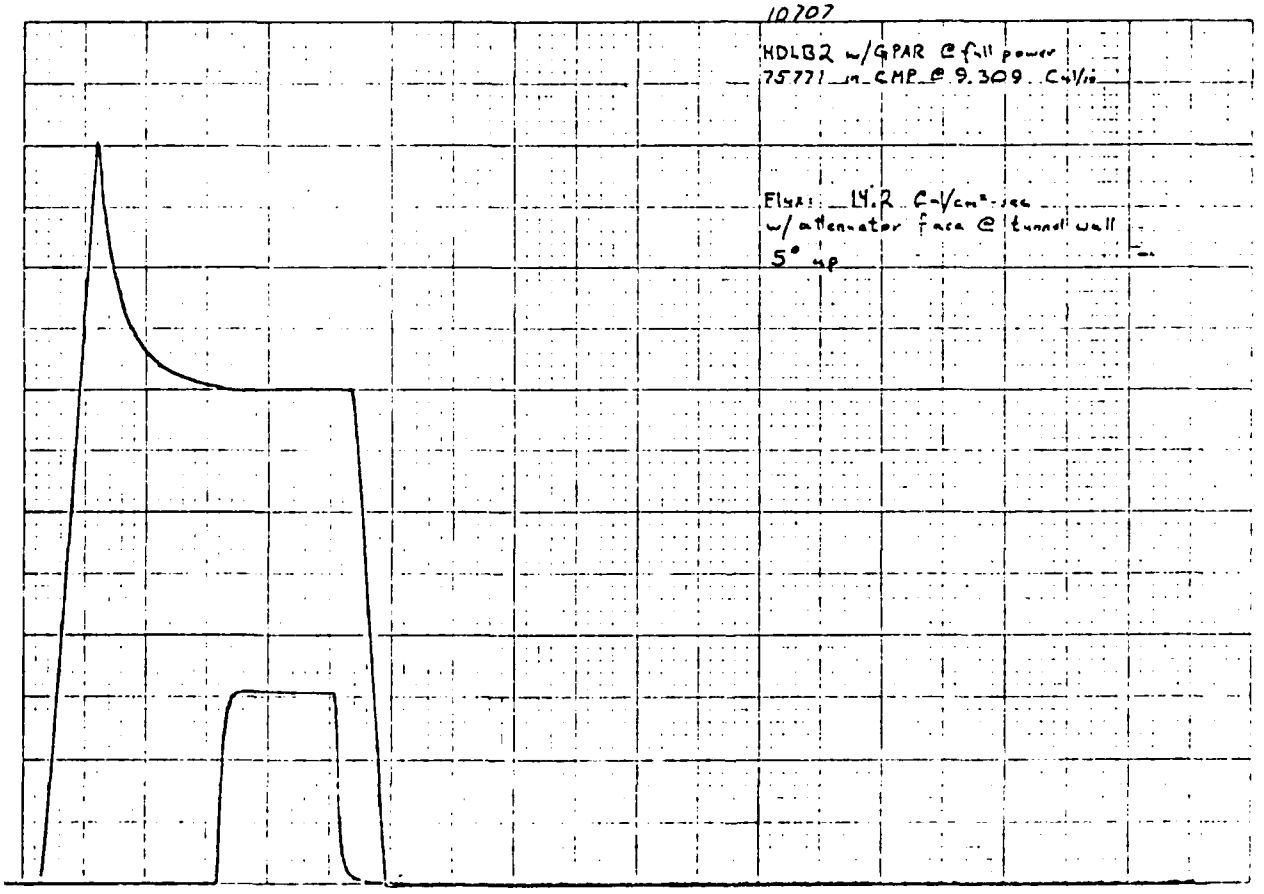

Figure A44. Flux w/Attenuator @ Plane, 5° Up.

46 0780

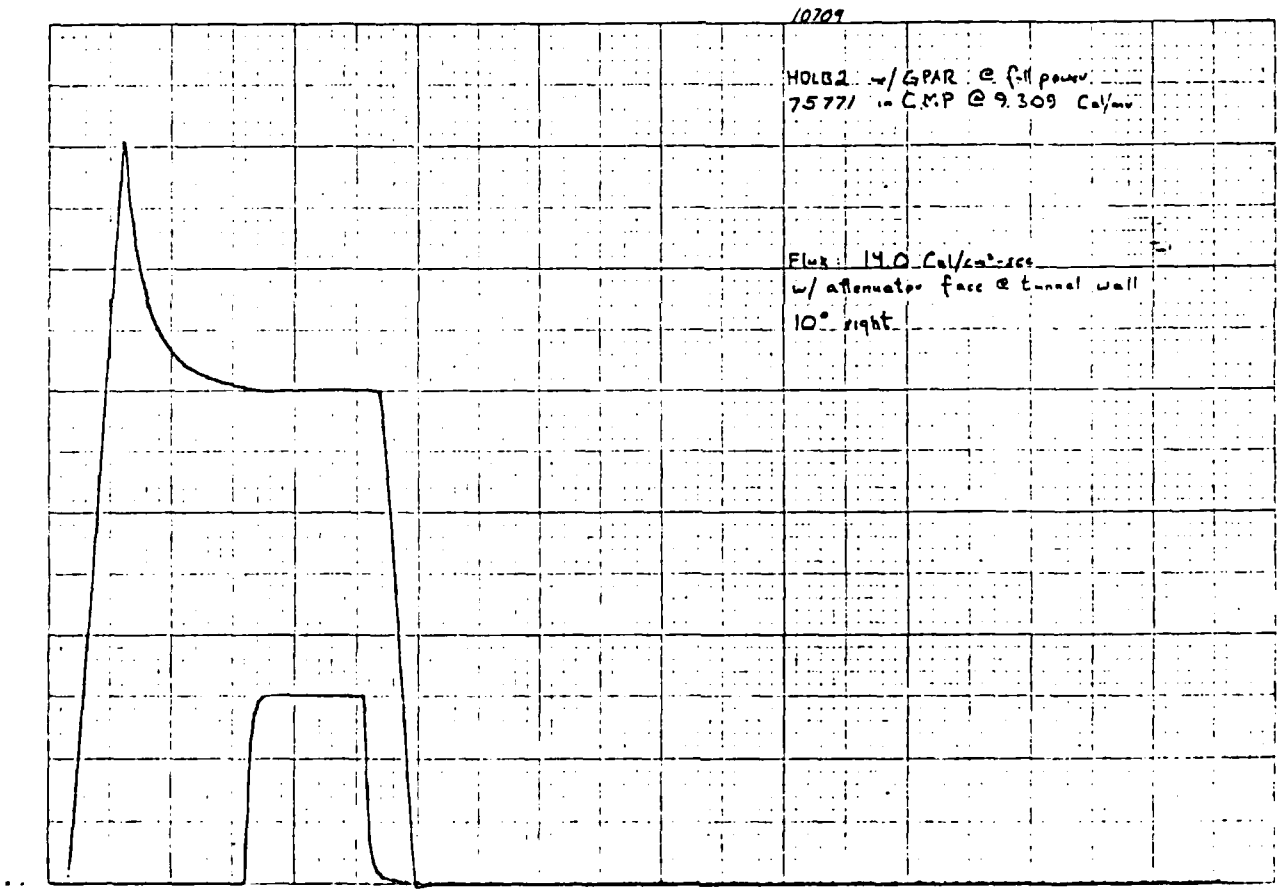

Figure A43. Flux w/Attenuator @ Plane, 10° Right.

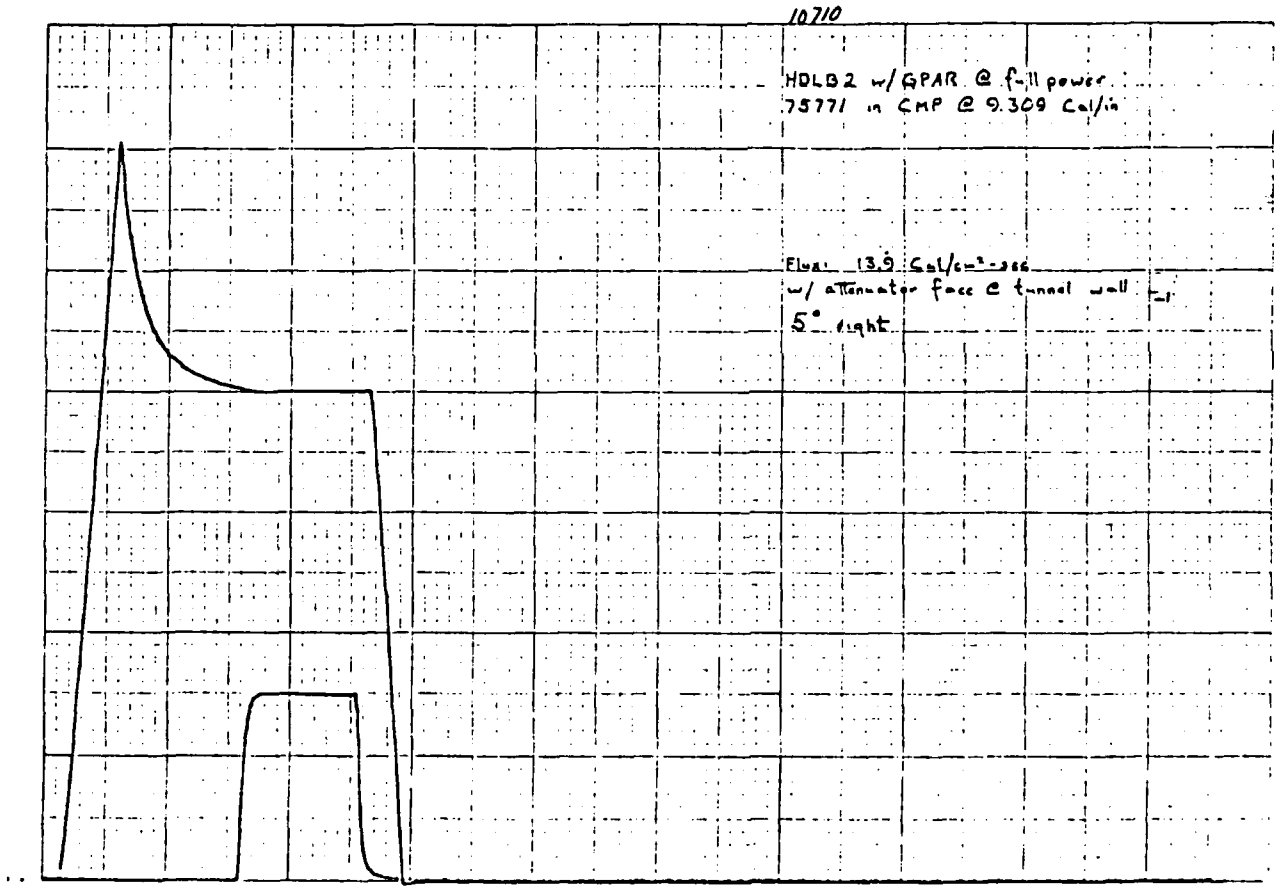

Figure A42. Flux w/Attenuator @ Plane, 5° Right.

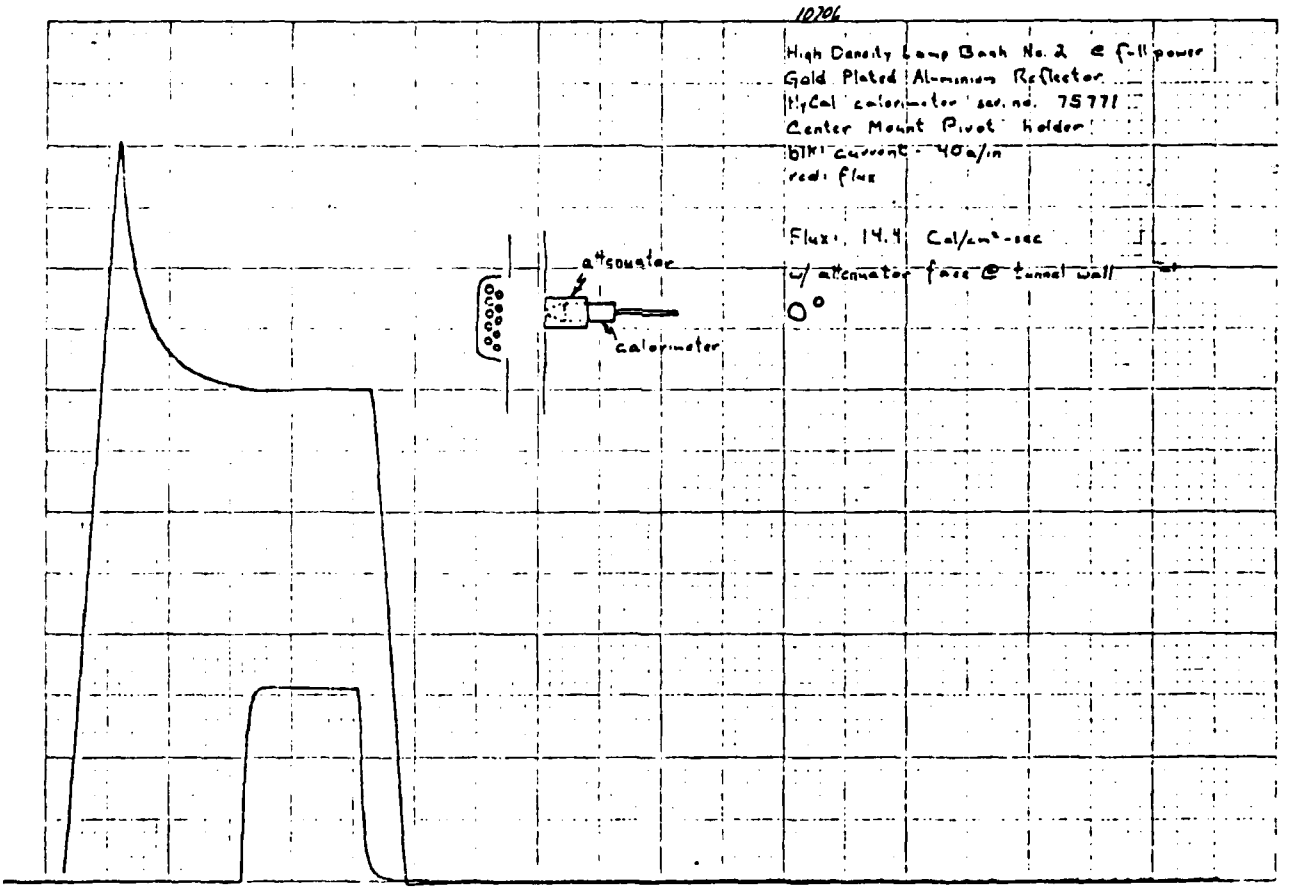

Figure A41. Flux w/Attenuator @ Plane, 0°.

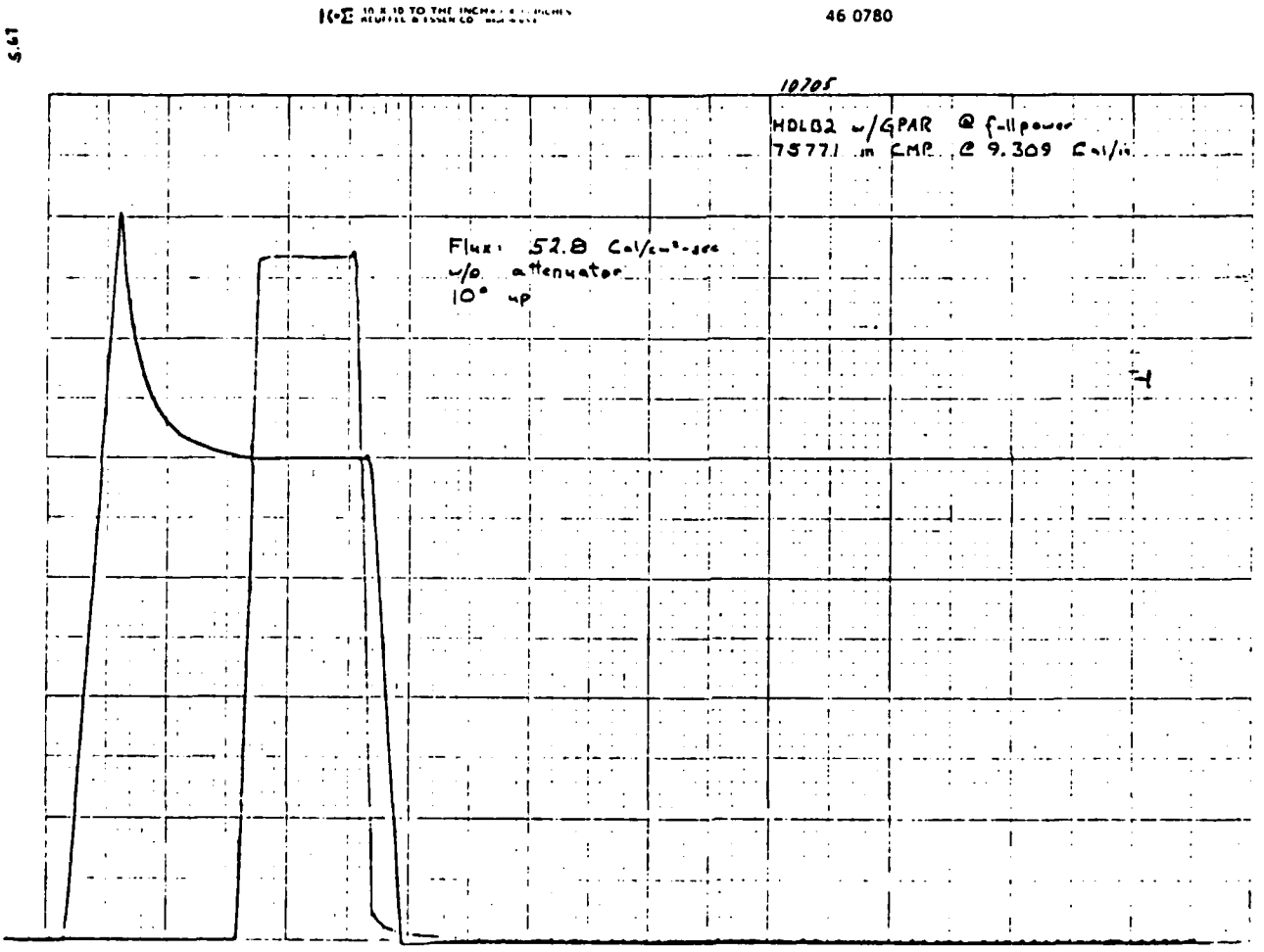

Figure A40. Flux w/o Attenuator, 10° Up.

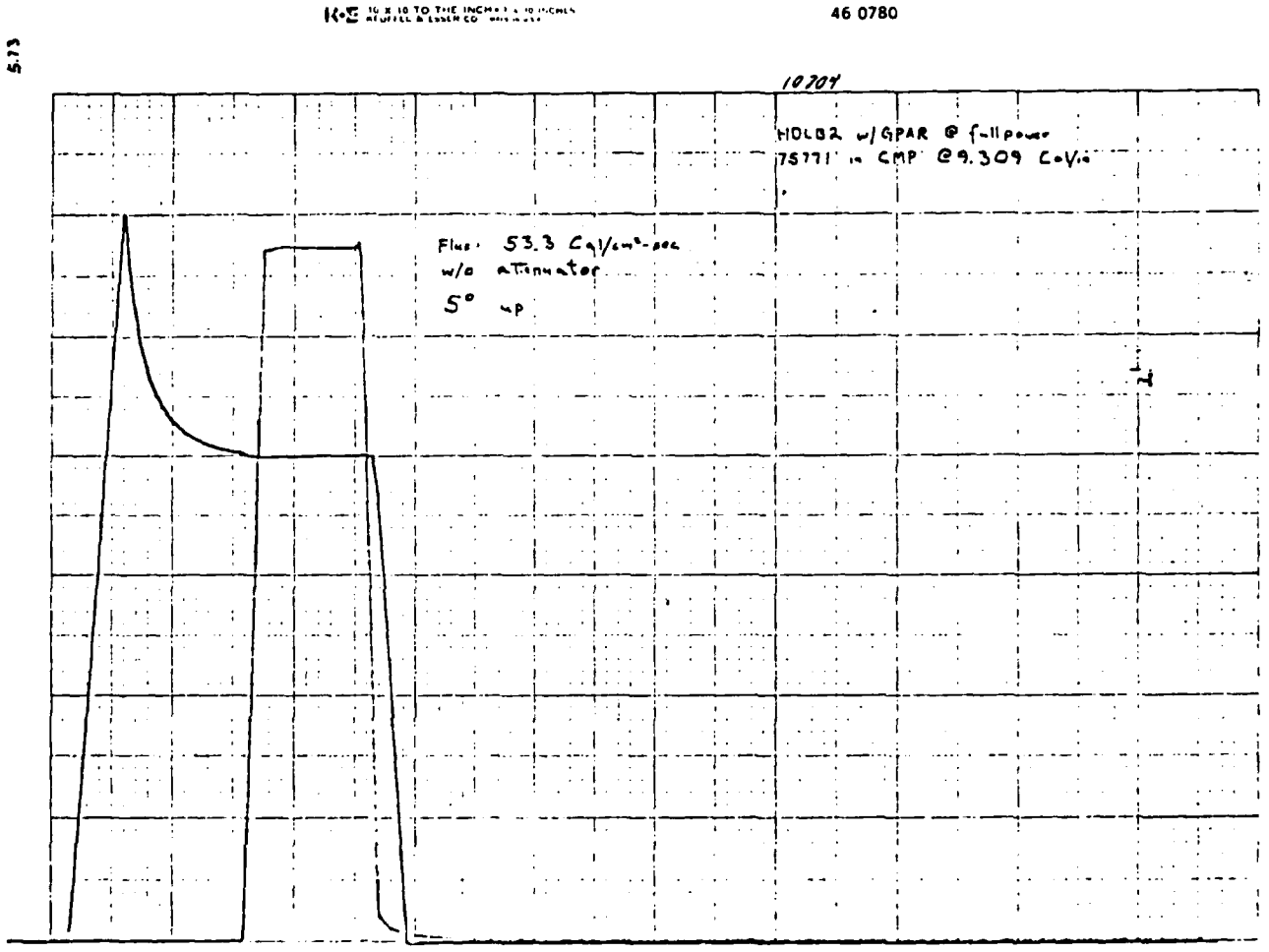

Figure A39. Flux w/o Attenuator, 5° Up.

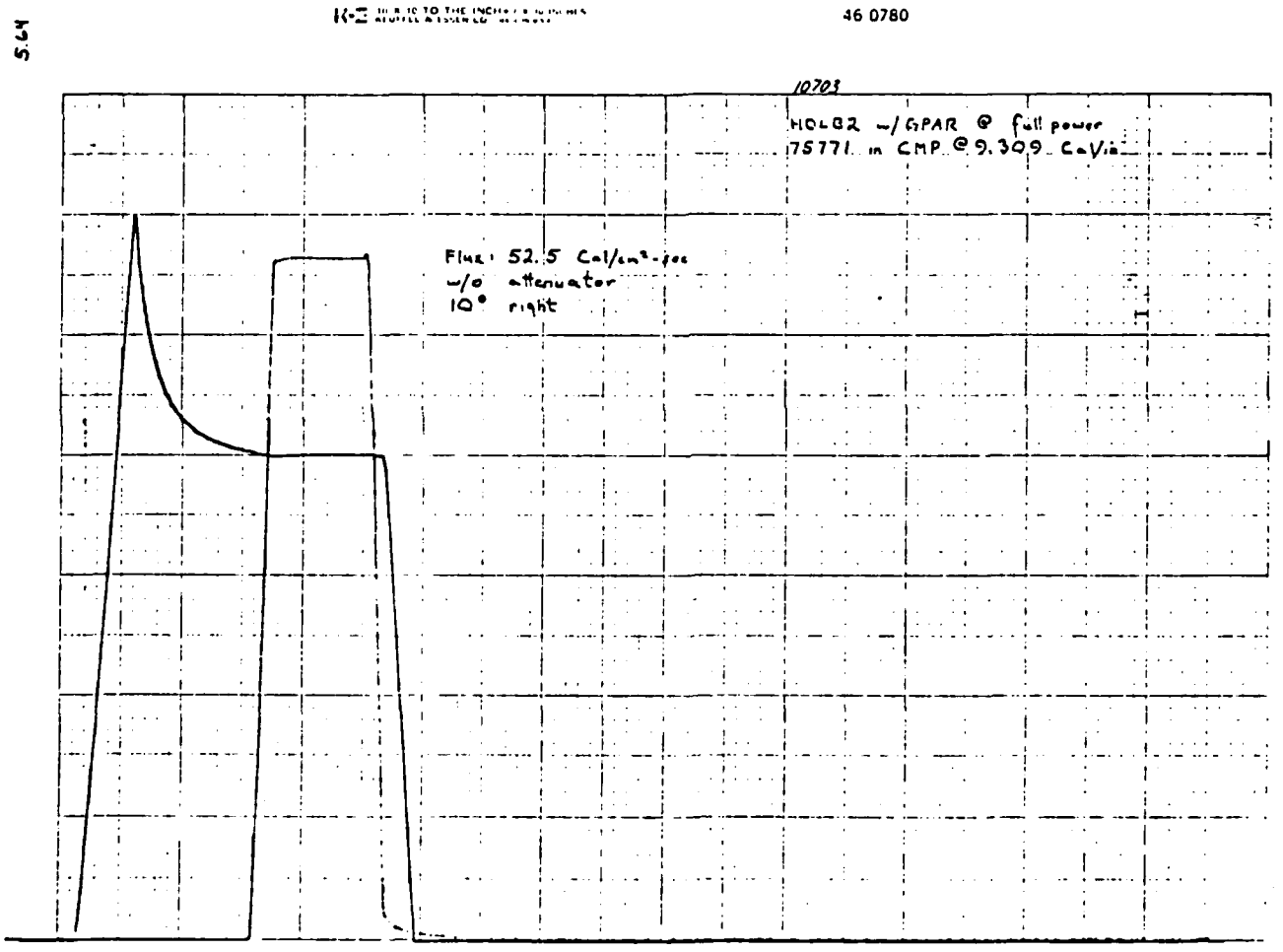

Figure A38. Flux w/o Attenuator, 10° Right.

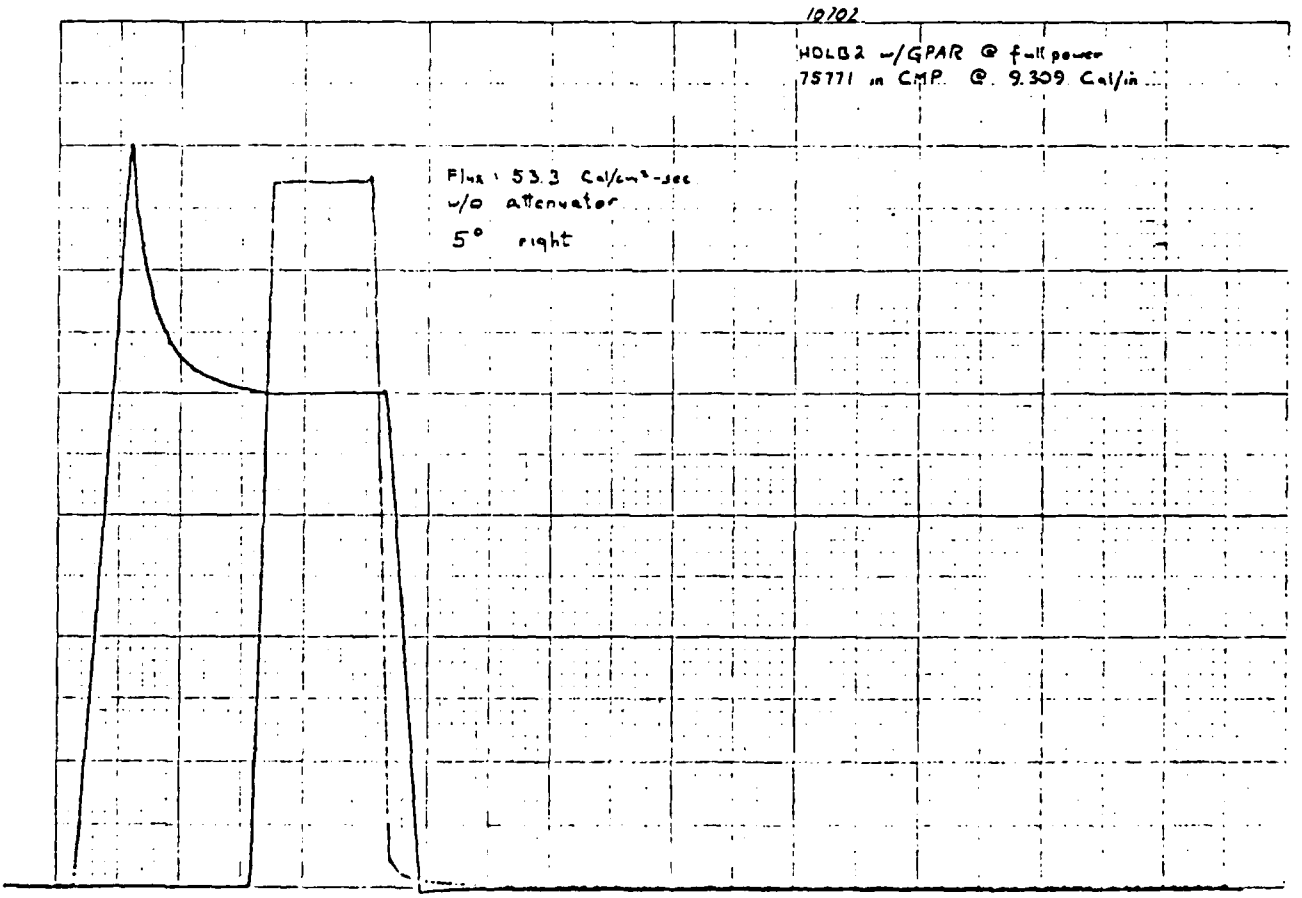

Figure A37. Flux w/o Attenuator, 5° Right.

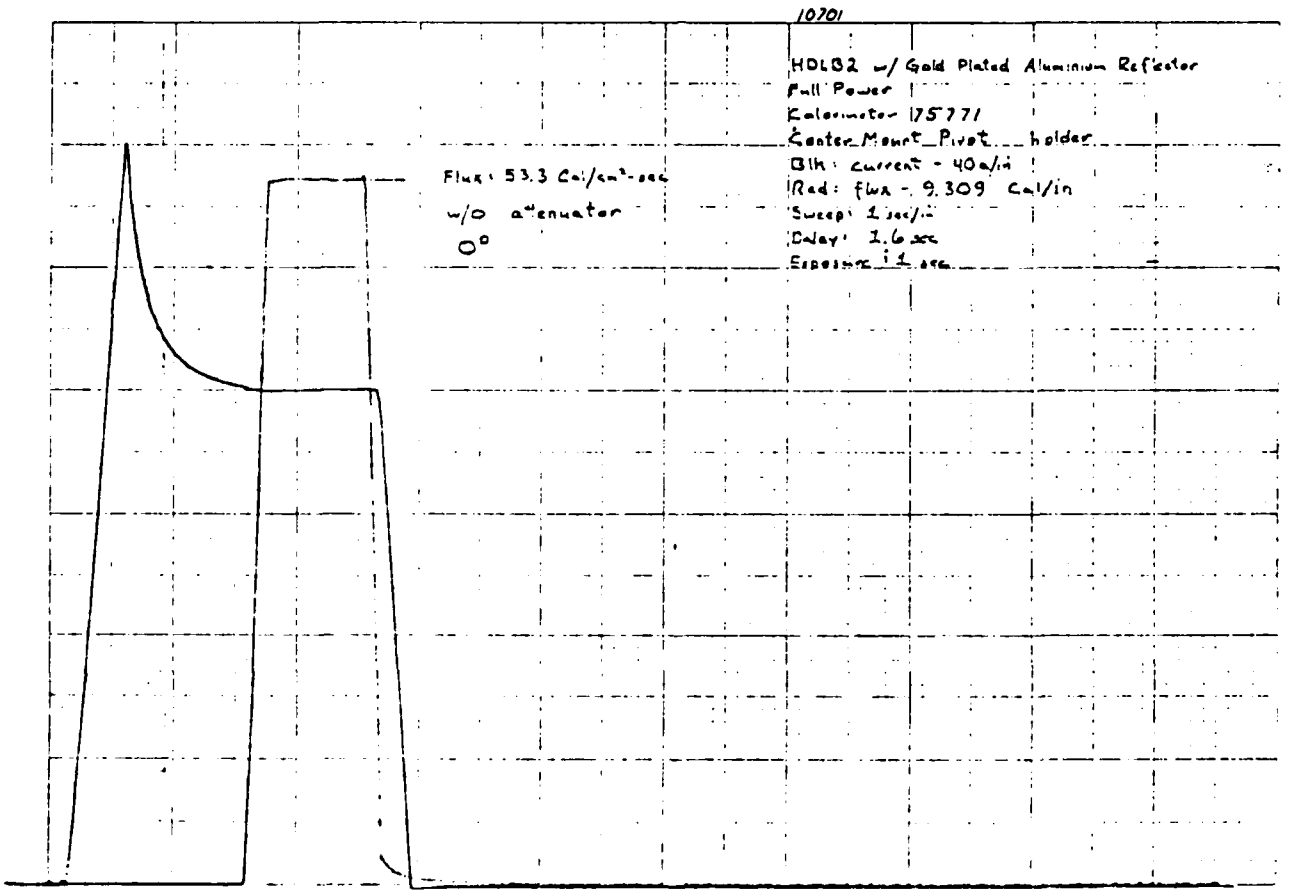

Figure A36. Flux w/o Attenuator, 0°.

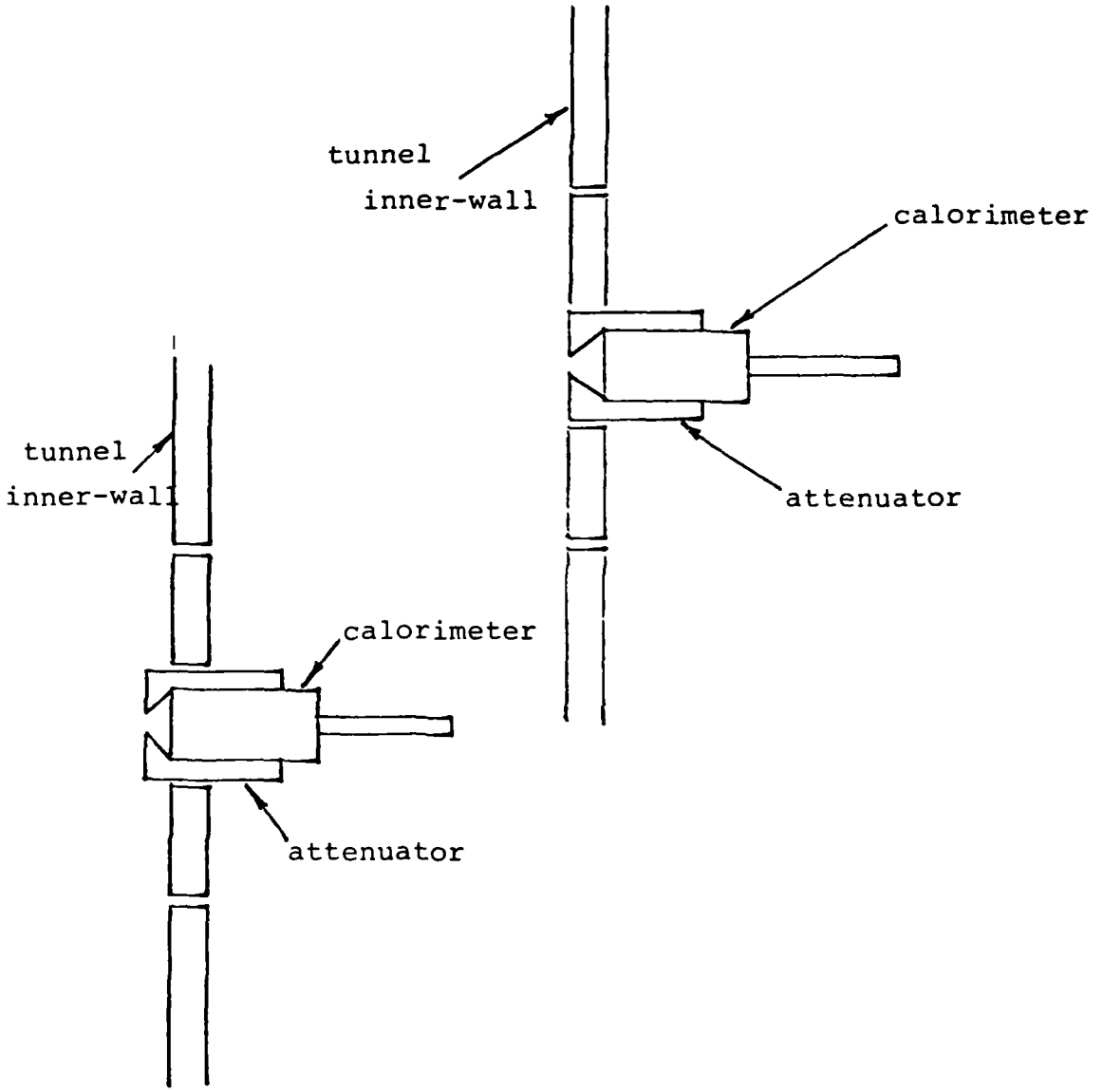

Figure A35.

CALORIMETER/ATTENUATOR/TUNNEL WALL

PIN HOLE COLLIMATOR DESIGN & CONSTRUCTION

Machine a block of aluminum to fit a 5/8" diameter Hycal calorimeter leaving a conical cavity above the Hycal face. The cone angle α can be selected to permit ease of machining (45 deg suggested). The inner surface of the conical cavity and the outer face of the collimator must be polished. Try to achieve an input aperture (πa^2) to output aperture (πA^2) area ratio of 1 to 10. An exact ratio is not important but careful measurement of the finished dimensions plus calibration experiments with the Hycal in place should be used to determine the actual area ratio. Make at least two pinhole collimators. Note any changes in the input aperture with use.

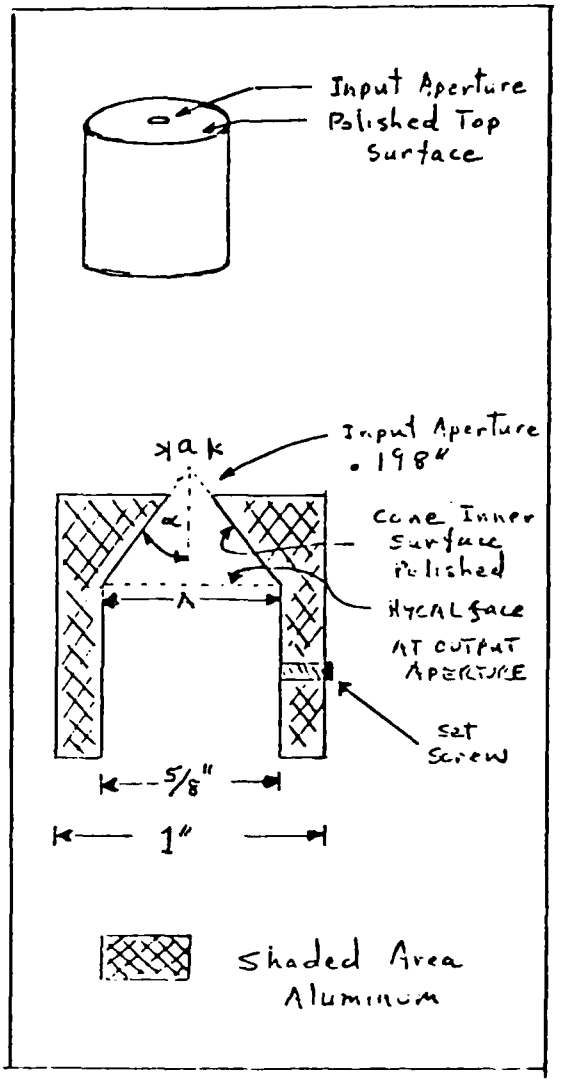

Figure A34.
PIN HOLE COLLIMATOR
DESIGN & CONSTRUCTION

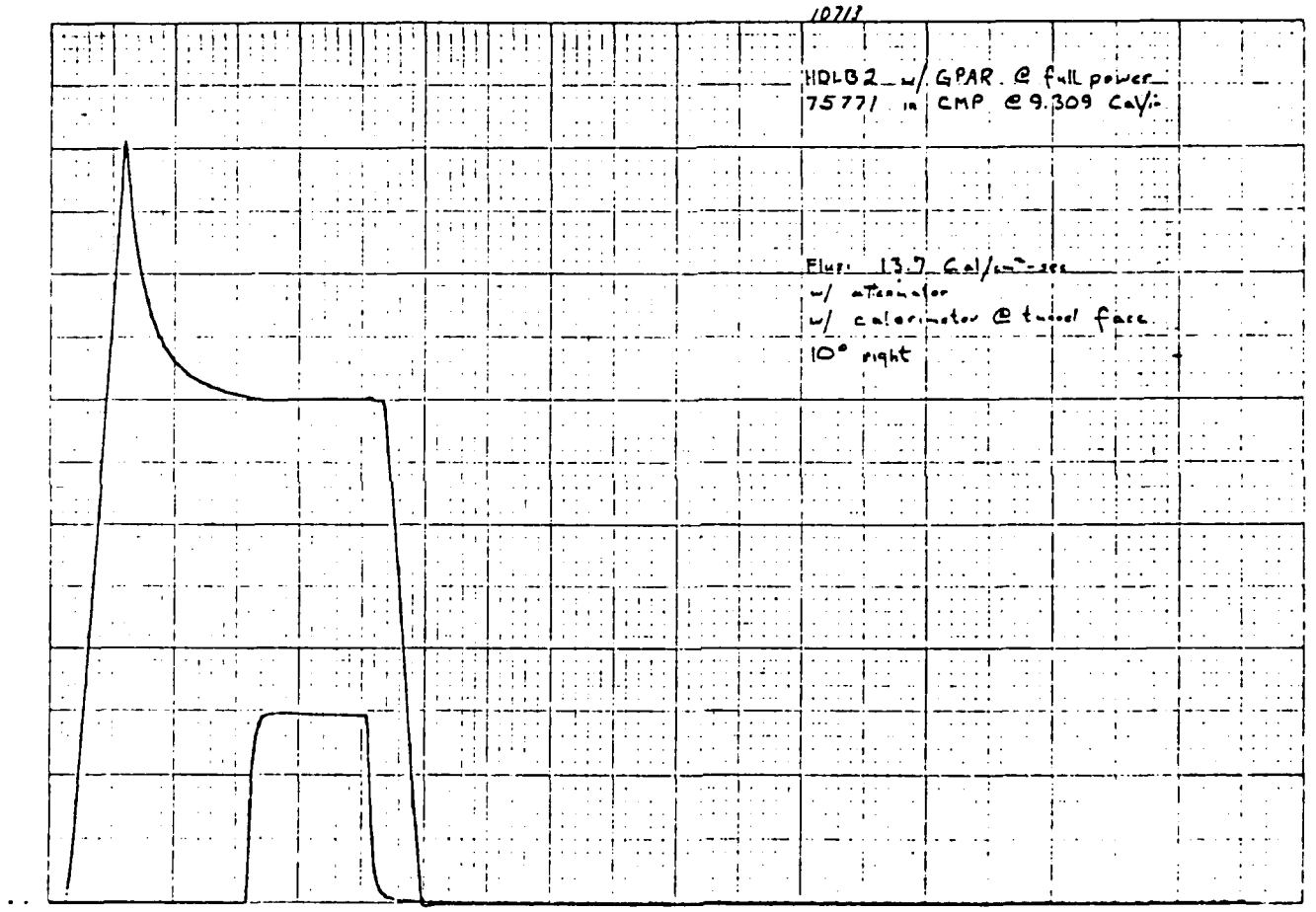

Figure A48. Flux w/Attenuator Offplane, 10° Right.

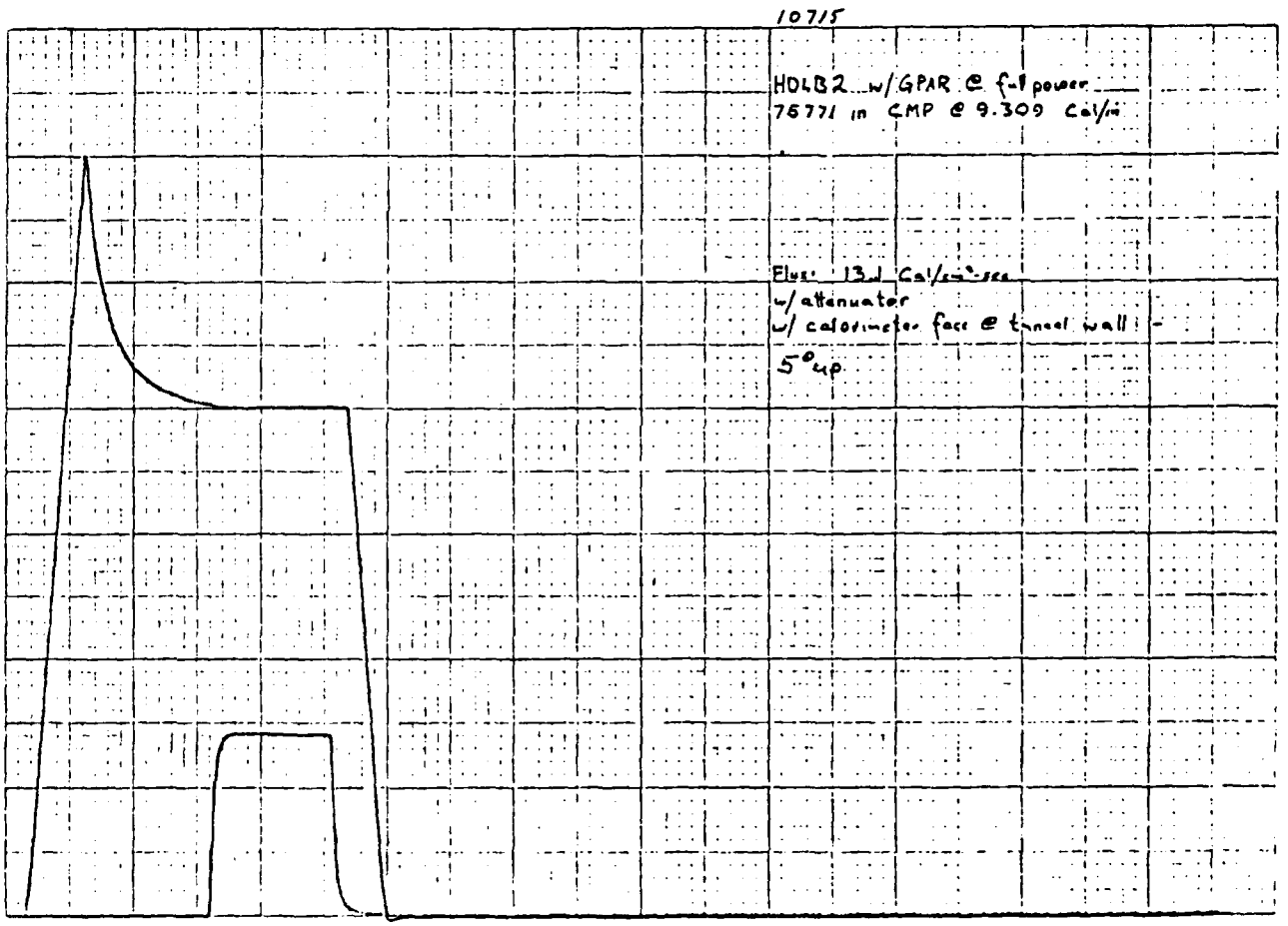

Figure A49. Flux w/Attenuator Offplane, 5° Up.

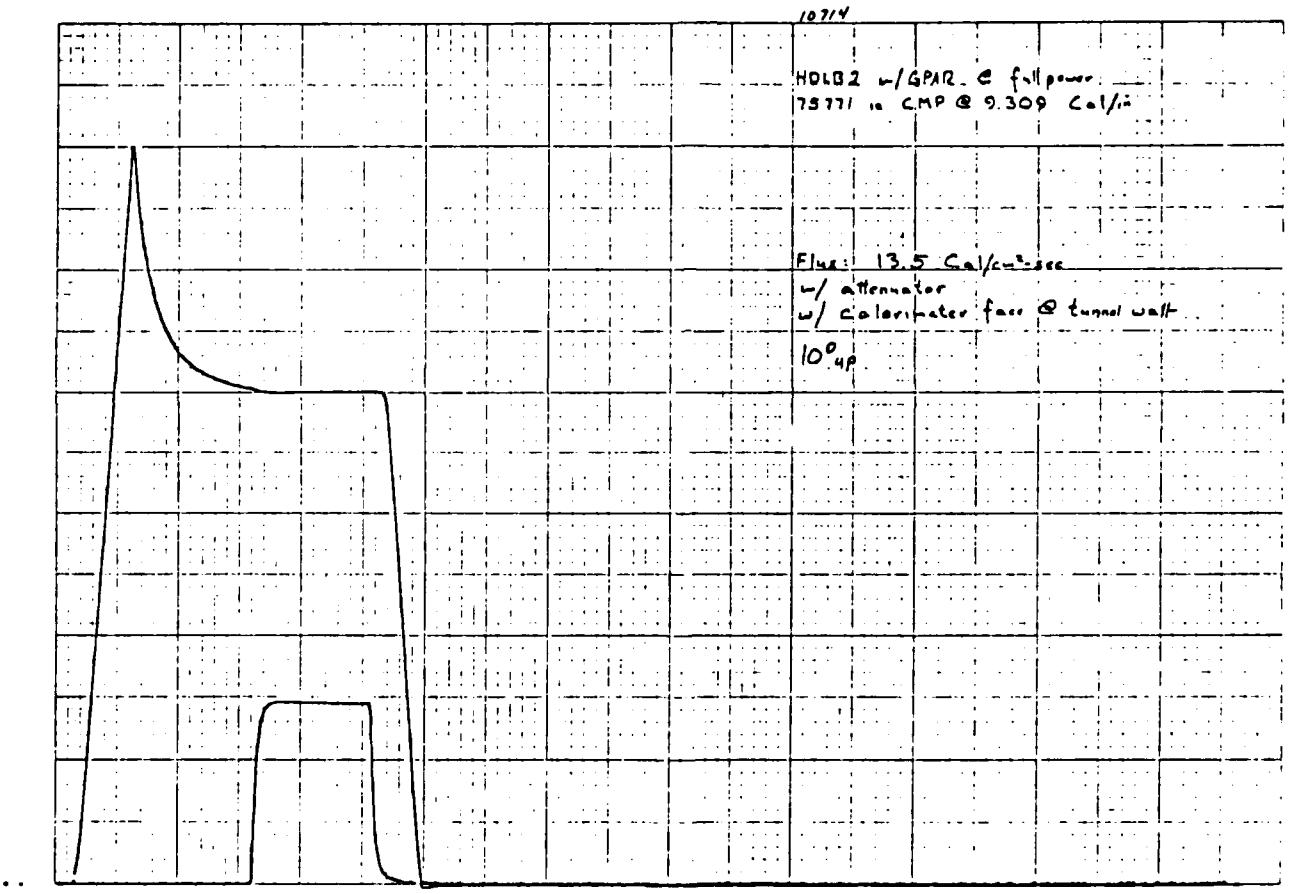

Figure A50. Flux w/Attenuator Offplane, 10° Up.

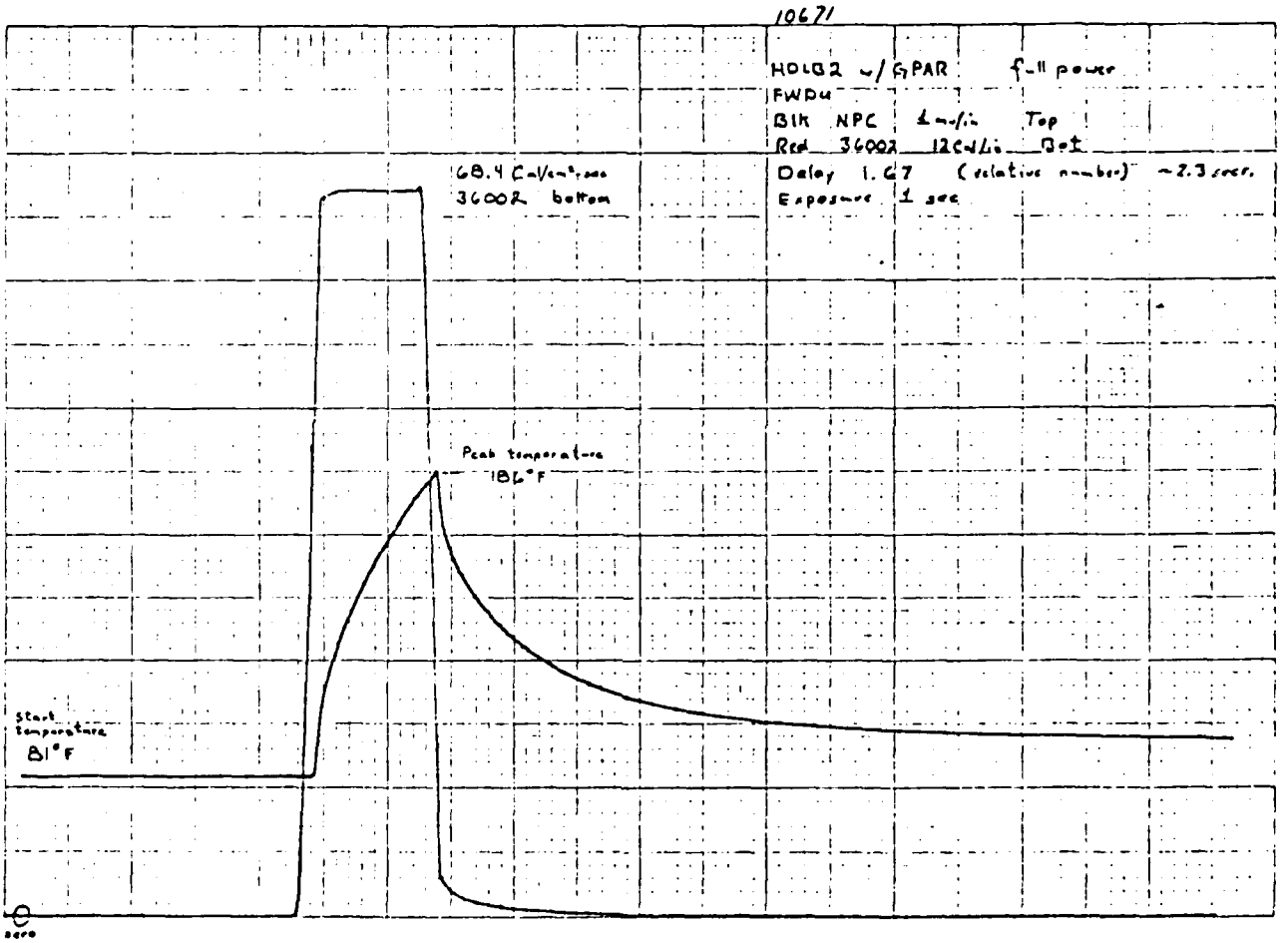

Figure A51. NPC Over Hy-Cal, Hi Flux, 1 Sec.

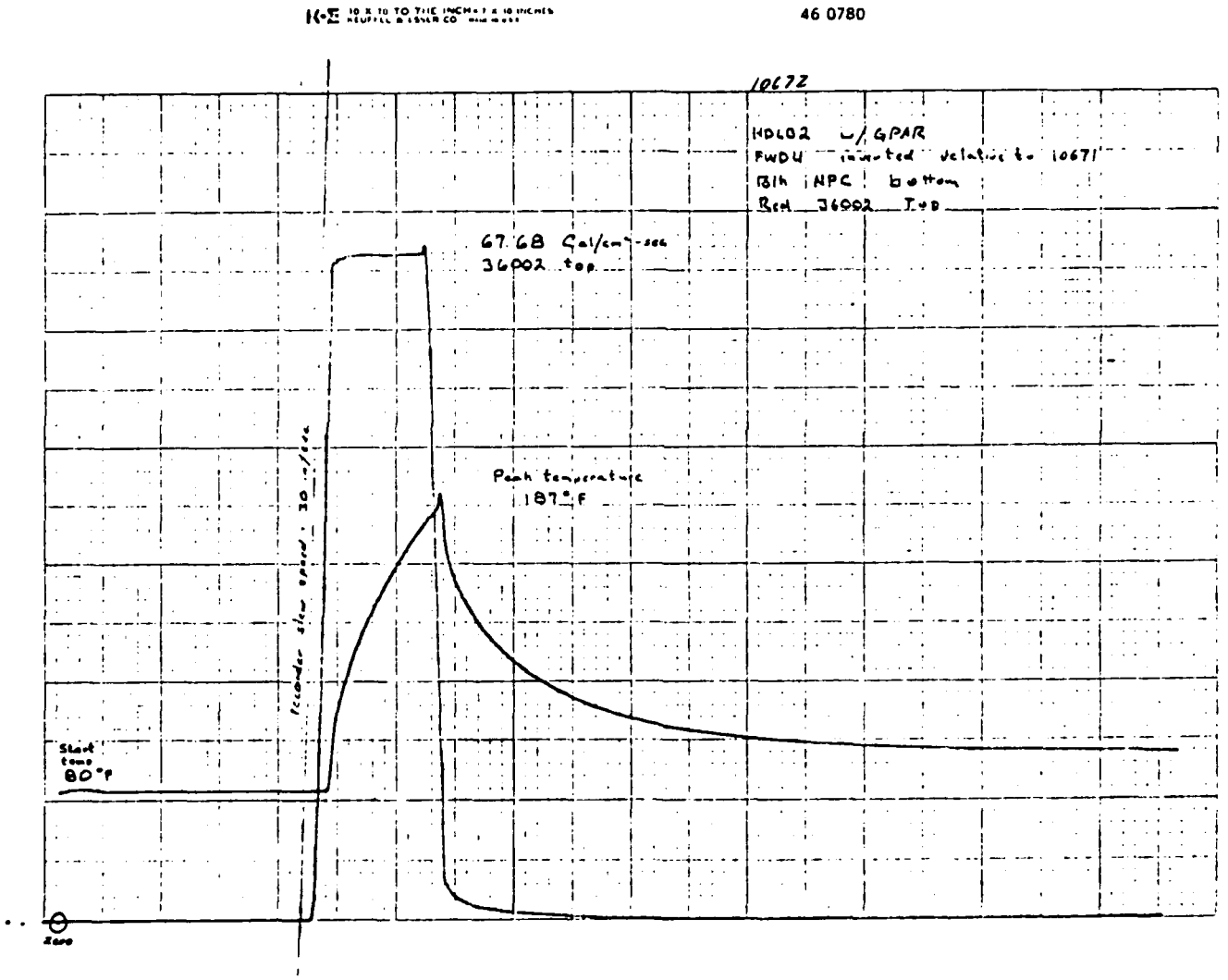

Figure A52. Hy-Cal Over NPC, Hi Flux, 1 Sec.

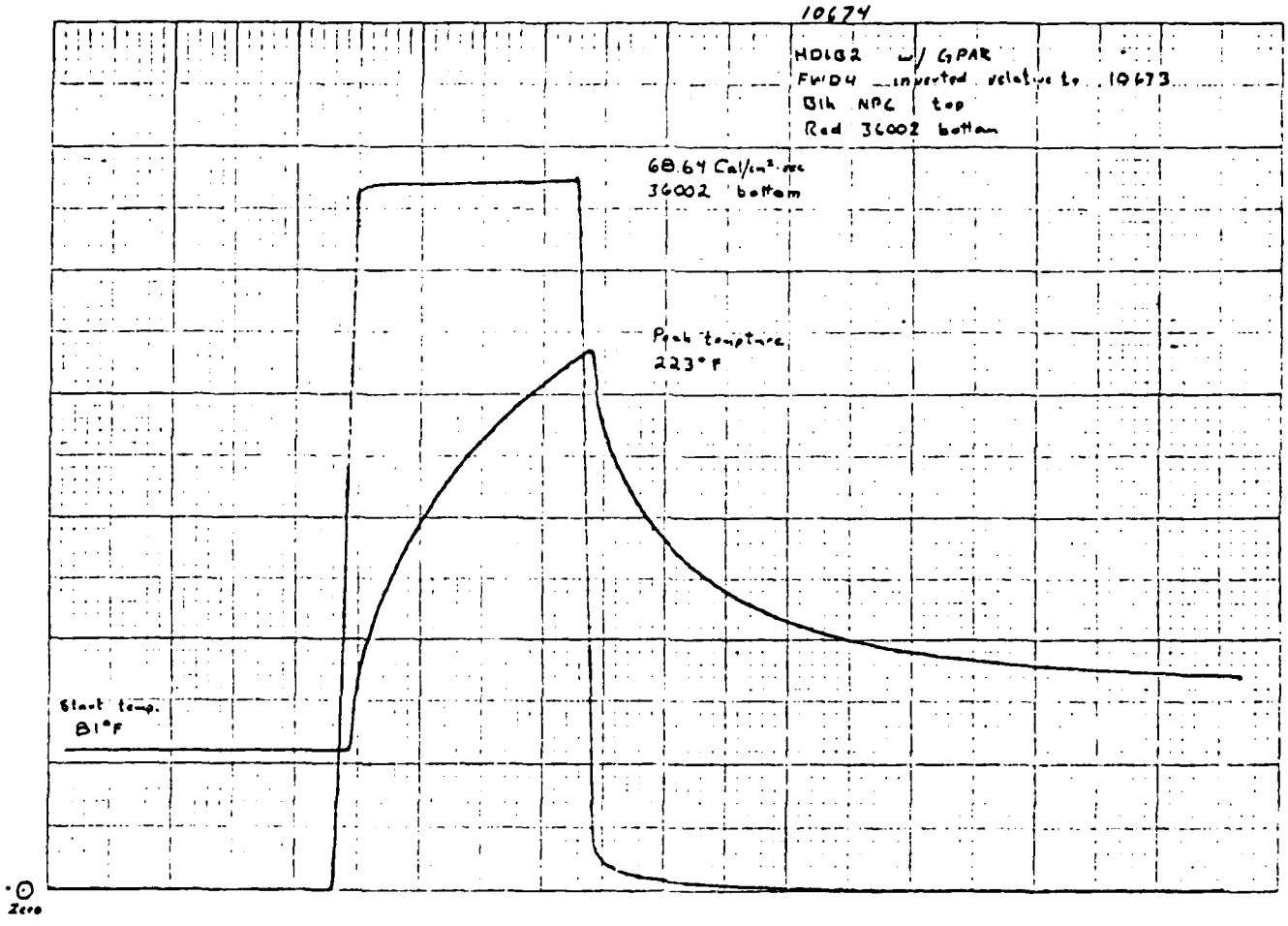

Figure A53. NPC Over Hy-Cal, Hi Flux, 2 Sec.

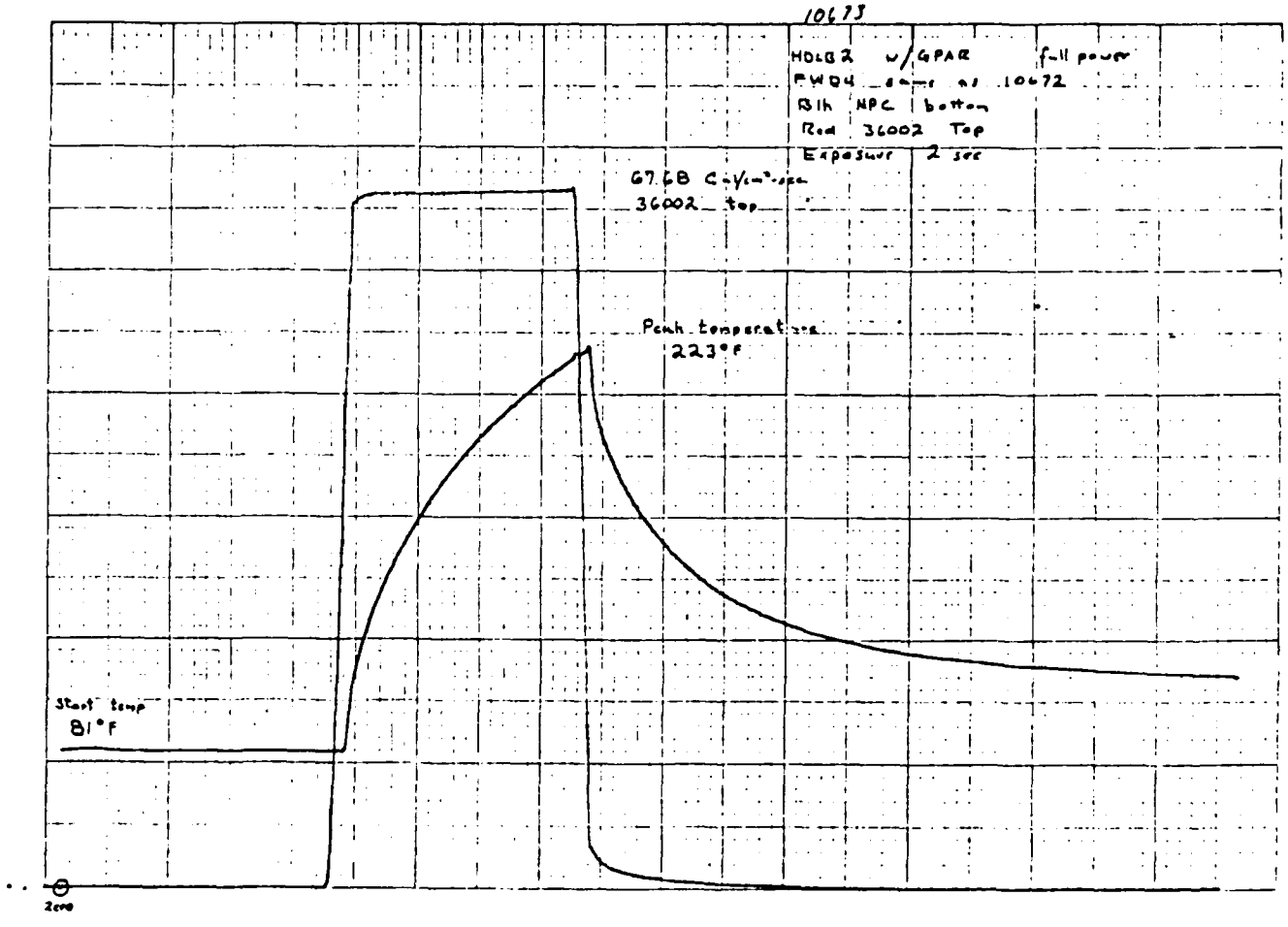

Figure A54. Hy-Cal Over NPC, Hi Flux 2 Sec.

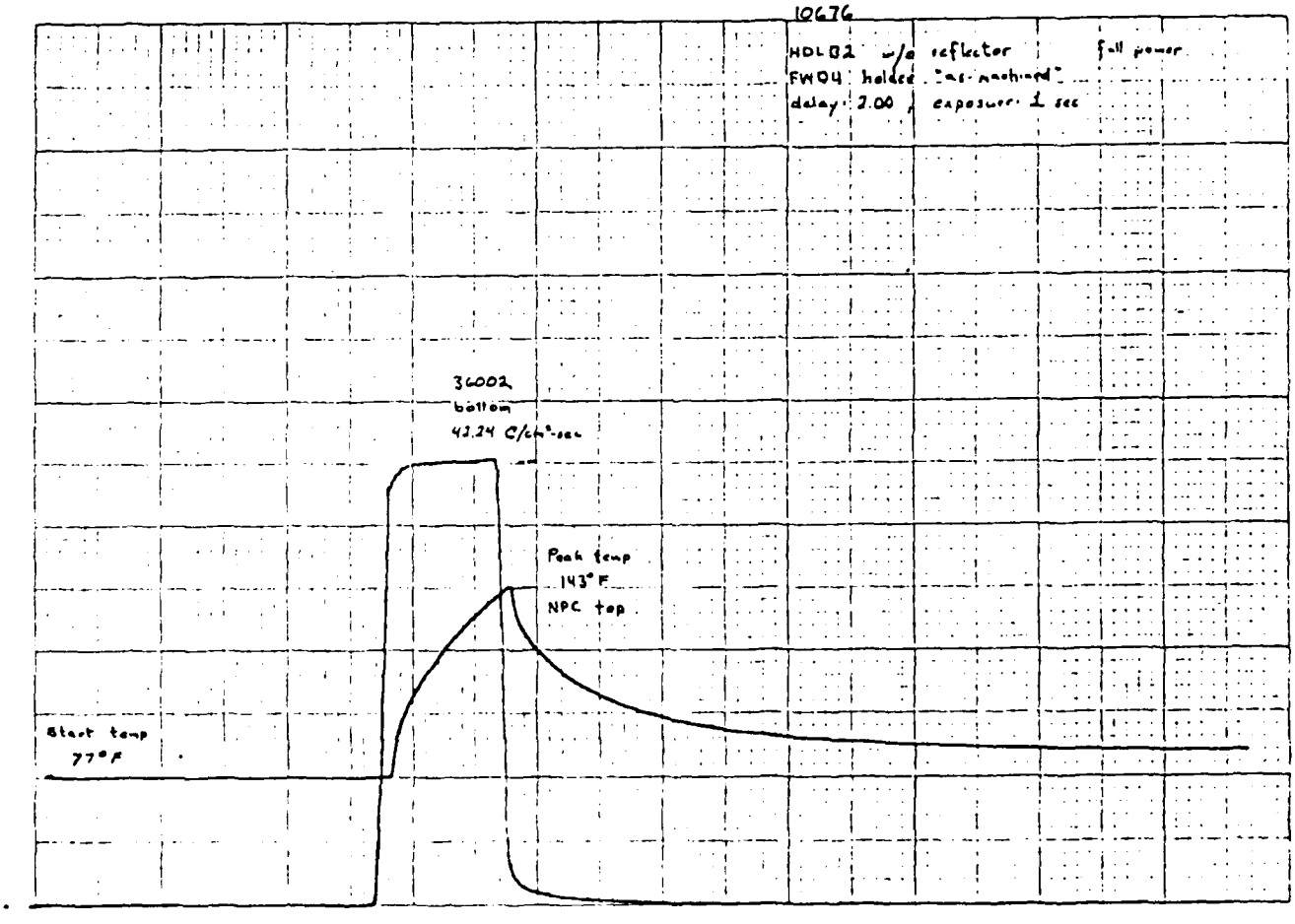

Figure A55. NPC Over Hy-Cal, Low Flux, 1 Sec.

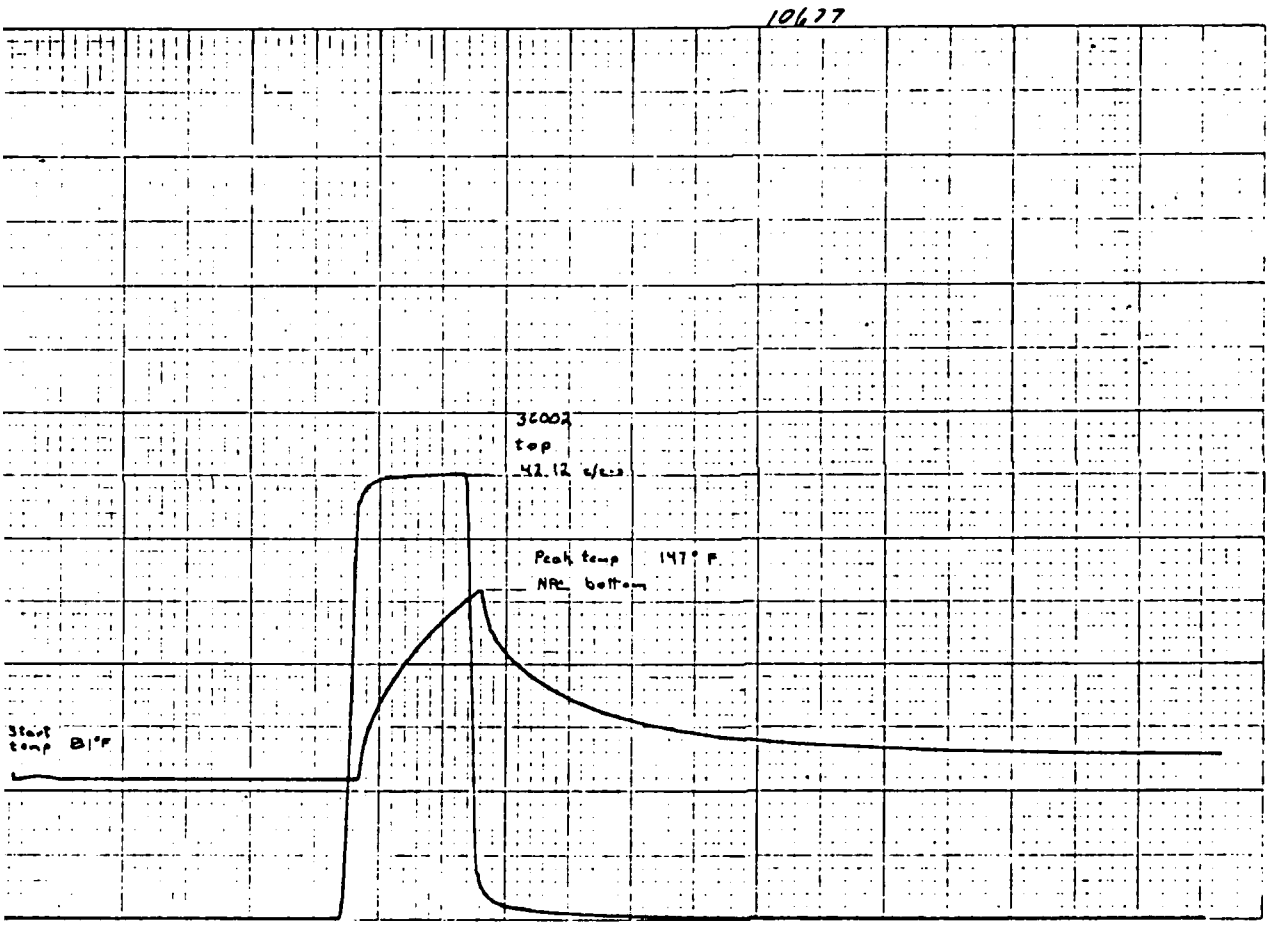

Figure A56. Hy-Cal Over NPC, Low Flux, 1 Sec.

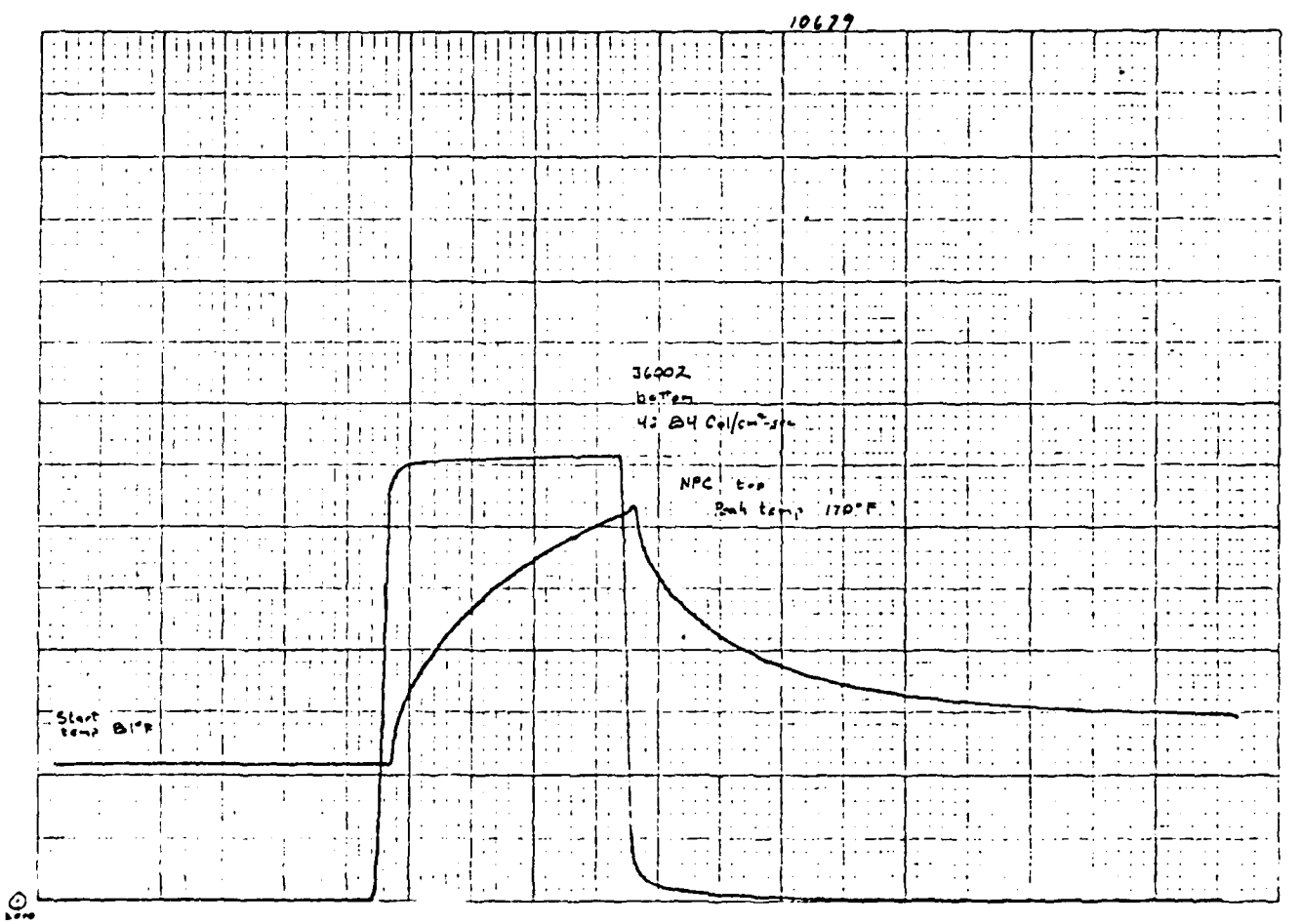

Figure A57. NPC Over Hy-Cal, Low Flux, 2 Sec.

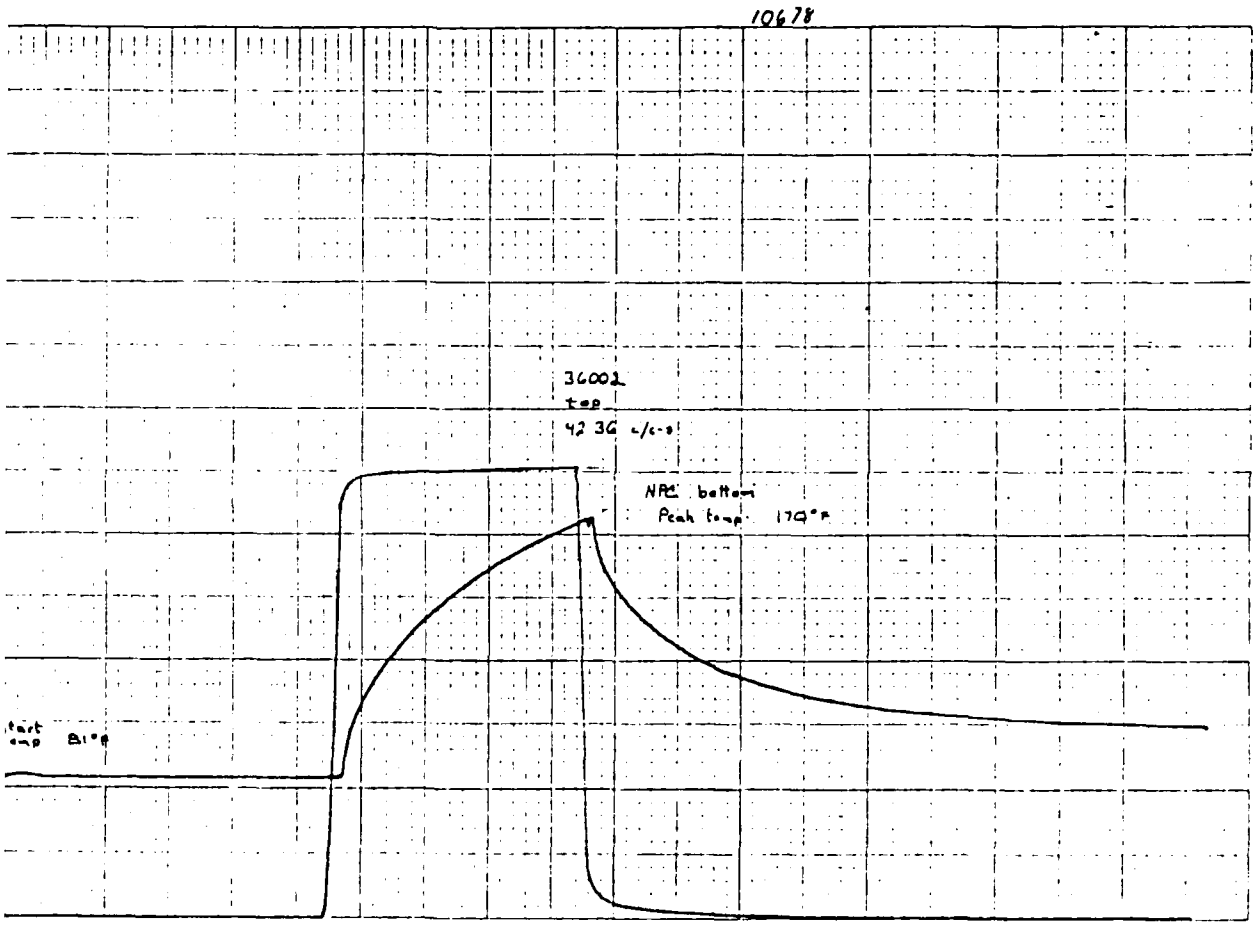

Figure A58. Hy-Cal Over NPC, Low Flux, 2 Sec.

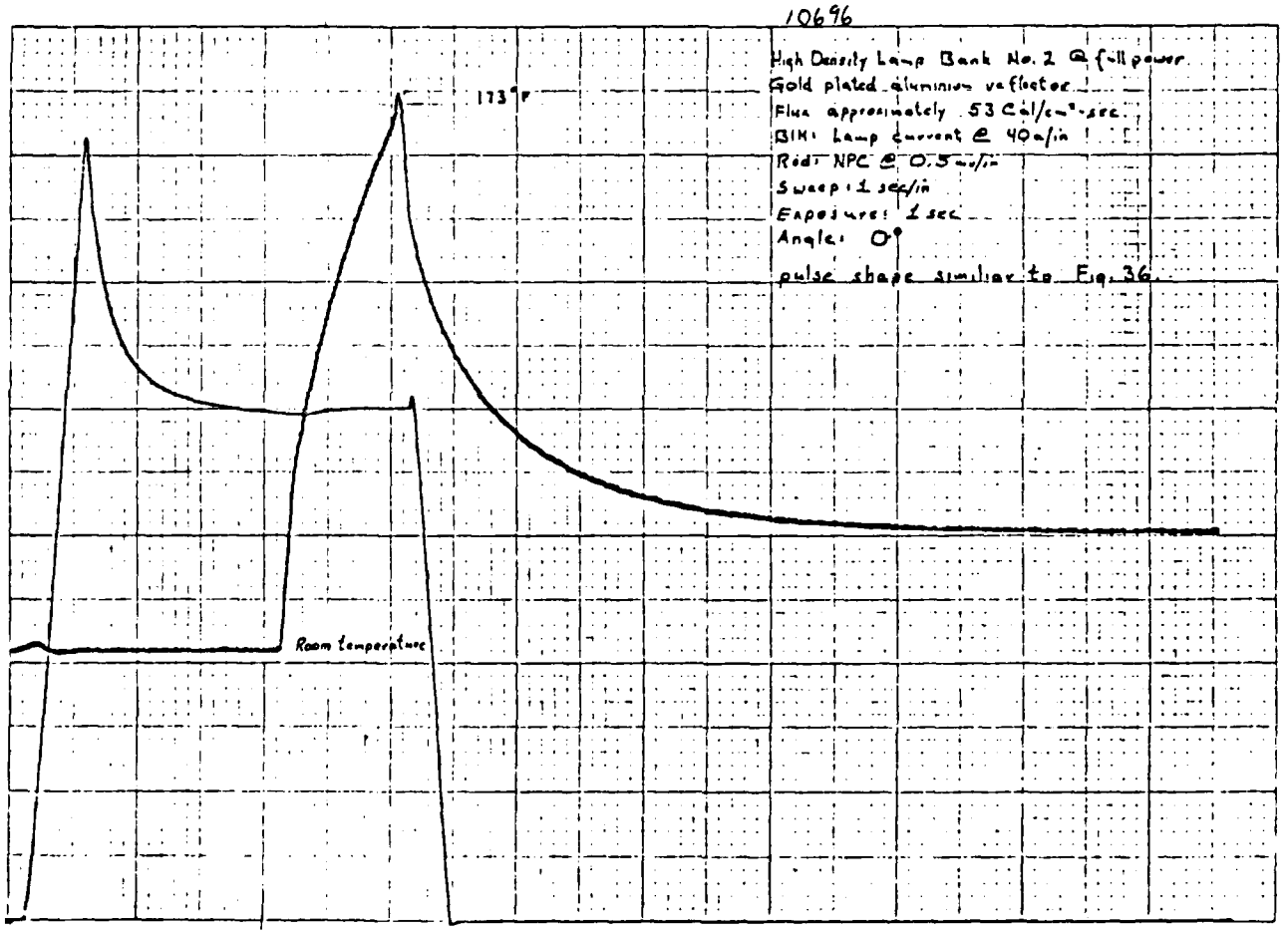

Figure A59. NPC @ 0°.

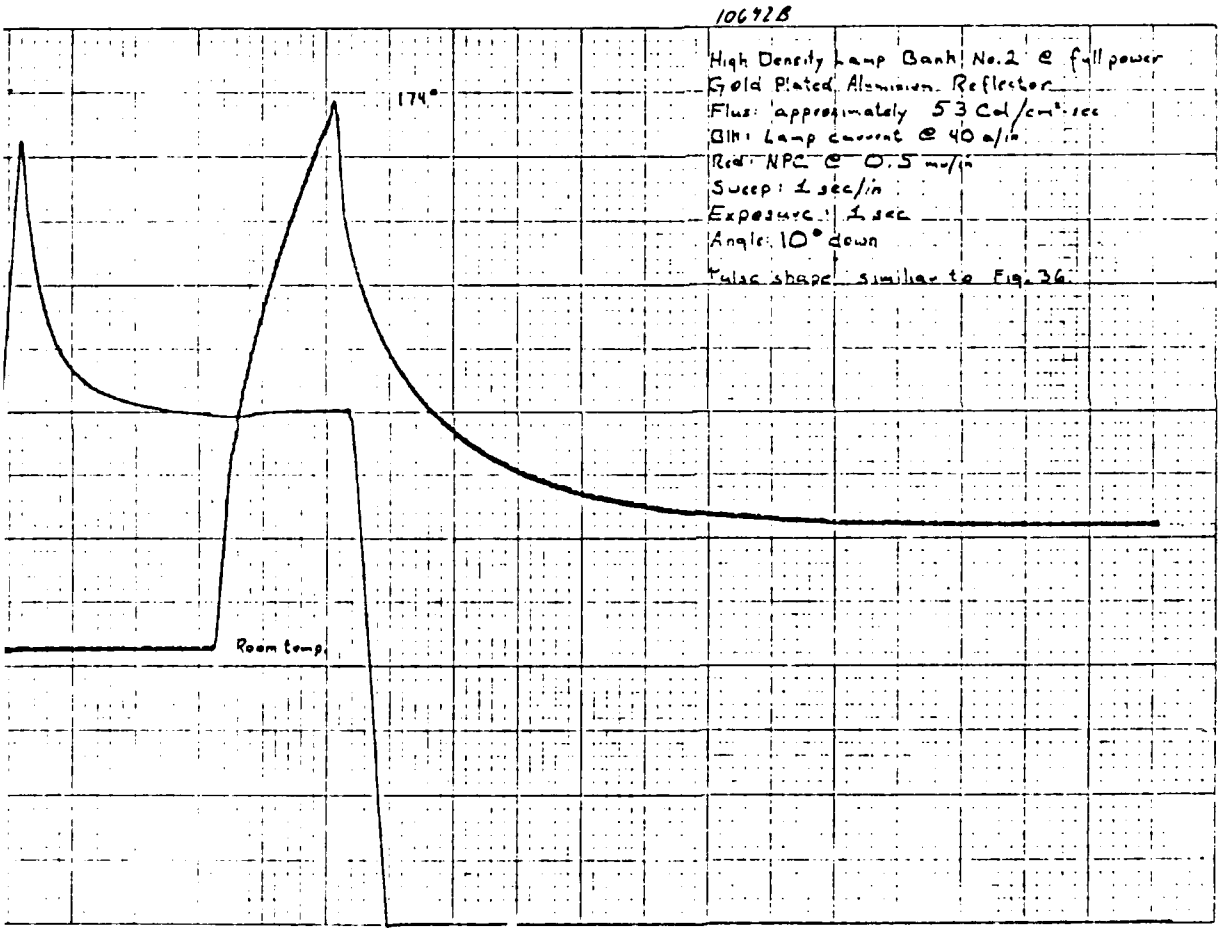

Figure A60. NPC @ 10° Down.

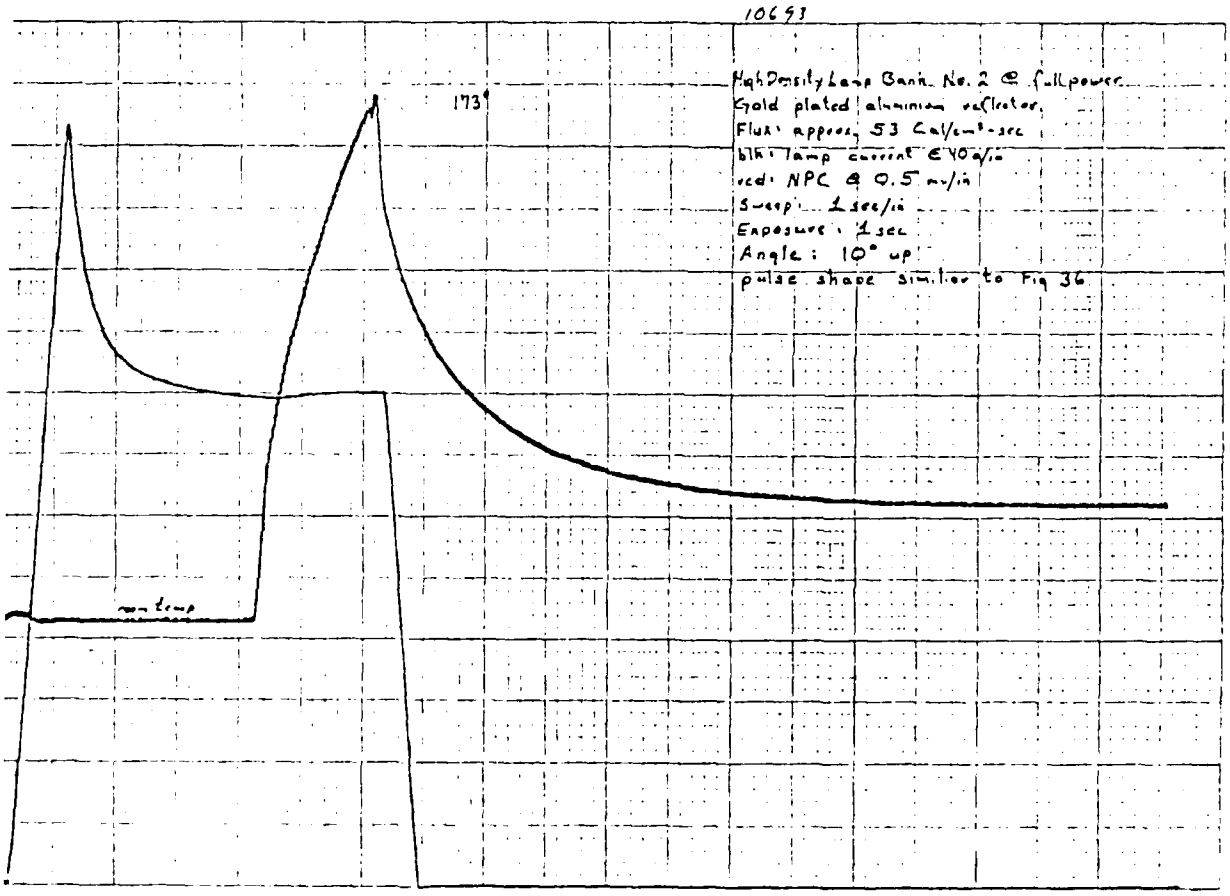

Figure A61. NPC @ 10° Up.

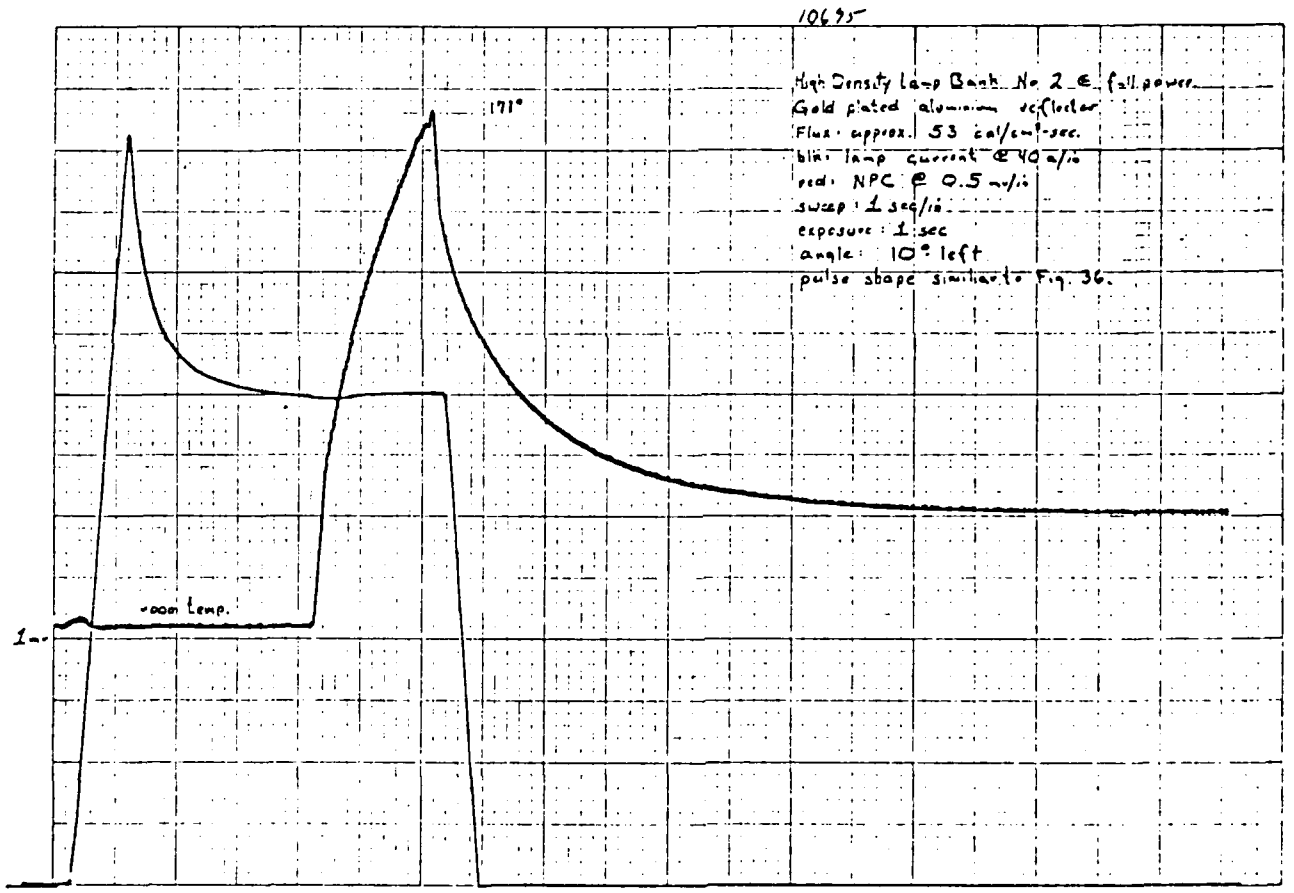

Figure A62. NPC @ 10° Left.

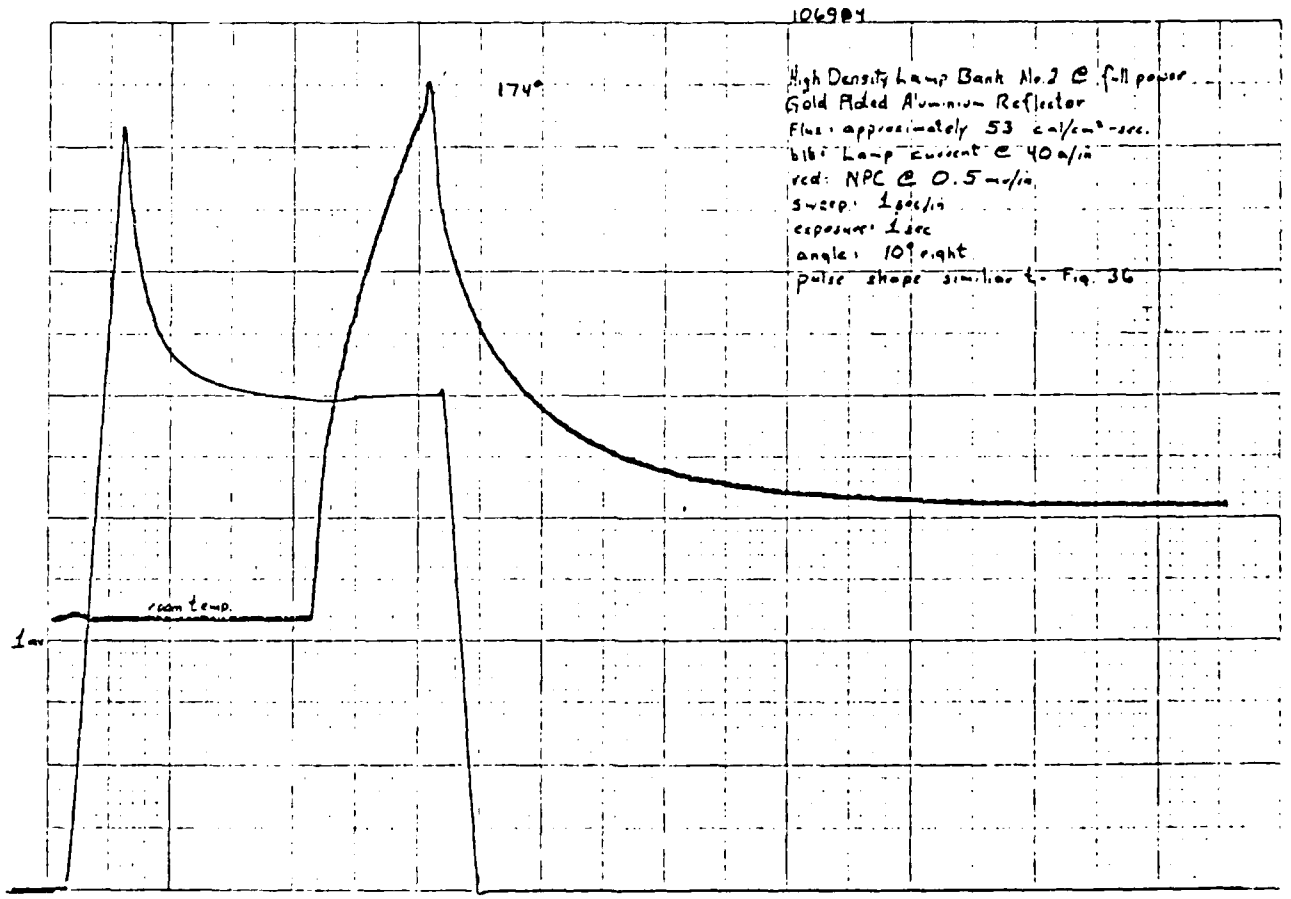

Figure A63. NPC @ 10° Right.

APPENDIX B
NULL POINT ANALYSIS

The Hycal calorimeter and the Null Point calorimeter are significantly different instruments. The Hycal calorimeter measures a differential signal based on the difference in temperature between the front face and the temperature of a coolant water supply. The Null Point calorimeter measures the temperature behind a mass exposed to radiant energy. The Accurex Null Point calorimeter uses a ½" long, ⅝" diameter Cu slug with black Cu Oxide on the front surface. A thin, type K (Chromel-Alumel) thermocouple is attached to the Cu Slug 10 to 12 mils from the front face and in the center of the slug. According to heat conduction theory the thermocouple within the Null point calorimeter will register a temperature history identical to that of the front face if the thermocouple tip is spaced a distance from the front face equal to the diameter of the hollow shaft containing the thermocouple. The flux history on the face of the Null point calorimeter has to be deconvolved from the temperature history at the thermocouple tip.

Accurex supplies instrumentation and computer programs to perform the deconvolution algorithms. Due to the high cost of the Accurex software this item was not acquired. However, a simple finite element computer program was written to model the Null point calorimeter response.

The simple model treats the absorbing face of the Null Point Calorimeter as a semi-infinite plane (see "Conduction of Heat in Solids", Carslaw and Jaeger) of copper that is heated by incoming radiation with no losses to the surroundings. The model approximates the actual physical construction and mounting of the Null Point Calorimeter which possesses a ⅝" diameter, ½" long copper slug with a 3/32" diameter access shaft drilled to within 10 to 12 mils of front face of the slug. The type K thermocouple wire is attached at the end of the access shaft nearest the front face. The access shaft will cause only small perturbation to heat flow in the copper slug since the cross-sectional area ratio of slug to access shaft is greater than 7 to 1. The Null Point probe was mounted with insulating materials shielding all but the front face from radiation.

The computer simulation divides the copper slug into elements (slices) through which energy is transported. Energy enters through the absorbing face and is assumed to heat the first element, with no losses, to a temperature based upon its thermal mass. This occurs only through a time period based upon the diffusivity of copper: $t=.5*b^2/a$ where b is a characteristic length (element width) and a is defined as the diffusivity of OFHC copper (1.21×10^{-3} ft^2/sec). When this time has elapsed the element loses heat to the next adjacent element through heat conduction driven by the difference in temperature of the two elements. The program computes the above for a constant flux input, total time, and number of elements as selected by the user. A sample program written in Applesoft for an Apple computer is provided.

A plot of the computer model output is shown in Figure B1. It provides a good approximation for Null point calorimeter response. From Figure 8, a 1 to 2 ms time delay is observed between the arrival of radiant flux and the beginning of response for both the Hycal and the Null Point calorimeters. This time delay theoretically is closely related to the time of thermal transport from the front face to the sensing element for both detectors. With appropriate analysis the flux histroy at the front face of the Null Point calorimeter can be determined but not in "real time". Null point data from Figure 7 has been replotted to the same scale as shown in Figure B1 and presented in Figure B2. The simulated response shown in Figure B1 closely follows the actual data but begins to deviate after .1 seconds. To improve the model additional terms accounting for leakage of energy out of the calorimeter would have to be added. It is not clear how much resolution such analysis can reveal. The Hycal calorimeter gives a "real time" response degraded by less thermal inertia. The time constant for the Hycal calorimeter response probably could also be corrected with more theoretical work.

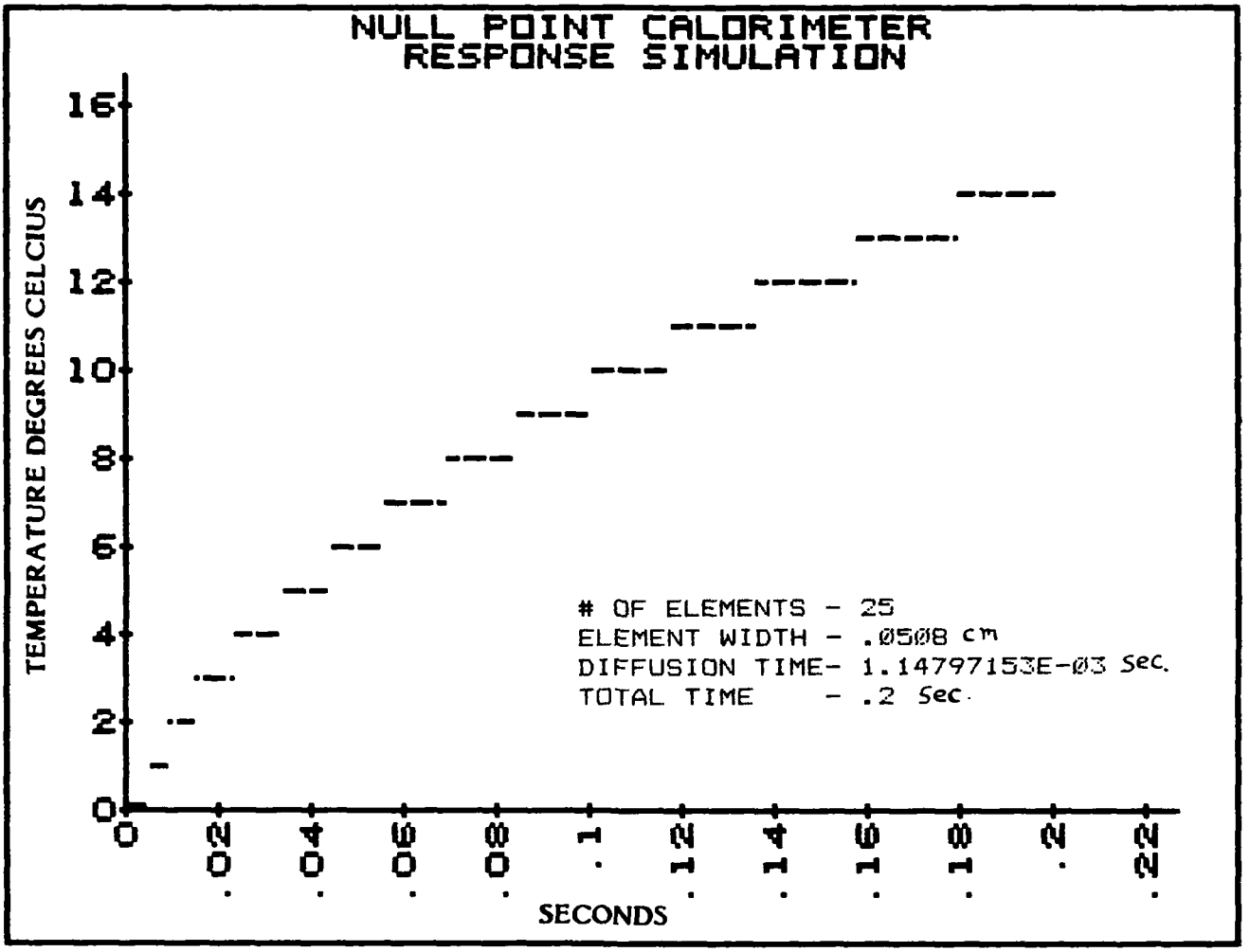

Figure B1. Simulated Response of Null Point Calorimeter to a 33 Cal/Cm^2/sec Thermal Flux Input

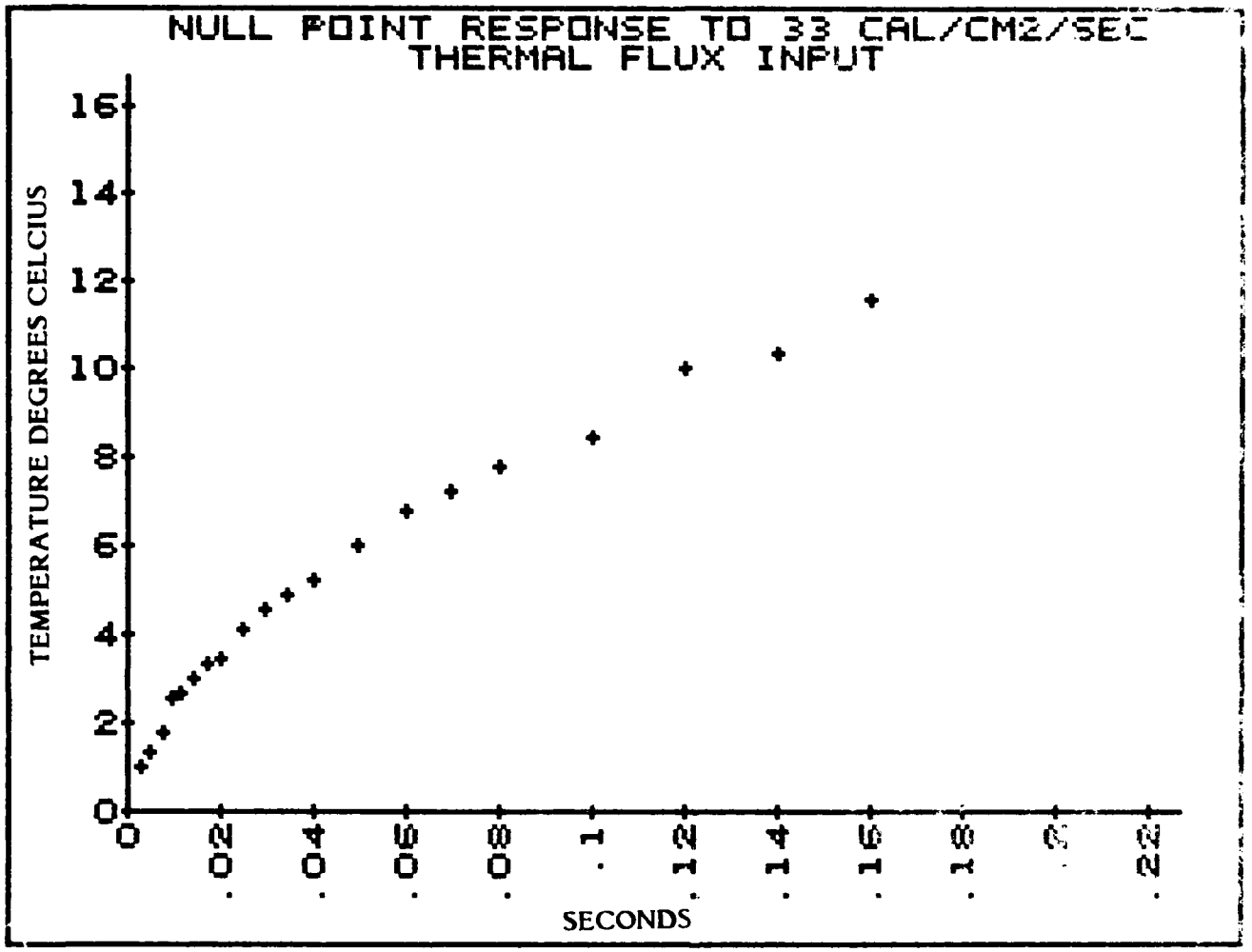

Figure B2. Actual response of Null Point Calorimeter to a 33 Cal/Cm^2/sec Thermal Flux Input

NULL POINT CALORIMETER SIMULATION PROGRAM

```
]LIST

5 D$ =  CHR$ (4): REM  OUTPUT CON
    TROL
10  INPUT "ENTER NUMBER OF FINITE
     ELEMENTS ";Q
15 A = 1.092: REM   ABSORPTANCE/(
    SPECIFIC HEAT * DENSITY
16 B = 1.109: REM  THERMAL COND./
    (SPECIFIC HEAT * DENSITY)
20 X = 1.27 / Q: REM  CALCULATE #
     OF ELEMENTS
21 D = .5 * (X ^ 2) / 1.124: REM
     CALCULATE TIME FOR HEAT TRA
    NSPORT ACROSS ELEMENT
30  INPUT "ENTER TOTAL TIME FOR D
    ATA ACQ ";R
40 S =  INT (R / D): REM  TOTAL #
     OF SAMPLES
50  DIM T(S + 1,Q + 1)
70  INPUT "ENTER FLUX LEVEL IN CA
    L/CM2/SEC ";F
73  PRINT
75  PRINT "ARRAY SIZE = ";S * Q
77  PRINT
80  INPUT "ENTER INITITAL AMBIENT
     ELEMENT TEMPERATURE ";Q1
85  FOR I = 0 TO Q:T(0,I) = Q1: NEXT
    I
89  REM  CALCULATE TEMPERATURE FO
    R ELEMENTS IN ARRAY
90  FOR I = 1 TO S
100  FOR P = 1 TO Q
110 T(I,0) = A * D * F / X + T(I -
    1,0) - (T(I - 1,0) - T(I - 1
    ,1)) * (B * D / (X ^ 2))
115  IF P = Q THEN 125
120 T(I,P) = (T(I - 1,P - 1) - T(
    I - 1,P)) * B * D / (X ^ 2) +
    T(I - 1,P) - (T(I - 1,P) - T
    (I - 1,P + 1)) * B * D / (X ^
    2)
123  GOTO 130
125 T(I,P) = (T(I - 1,P - 1) - T(
    I - 1,P)) * B * D / (X ^ 2) +
    T(I - 1,P)
130  NEXT P
140  NEXT I
145  INPUT "SENT OUTPUT TO PRINTE
    R (Y/N)? ";Z$
146  IF Z$ = "Y" THEN 150
147  IF Z$ <  > "N" THEN 145
148  GOTO 255
149  REM  PRINTER OUTPUT
150  PRINT D$;"PR#1"
155  PRINT "# OF ELEMENTS - ";Q
160  PRINT "ELEMENT WIDTH - ";X
170  PRINT "DIFFUSION TIME- ";D
175  PRINT "TOTAL TIME    - ";R
```

```
180  PRINT : PRINT
190  PRINT "TIME"; SPC( 15);"ELEM
     ENT Ø"; SPC( 5);"ELEMENT 1";
      SPC( 5);"ELEMENT ";Q - 1; SPC(
     5);"ELEMENT ";Q
195  PRINT : PRINT
200  FOR I = Ø TO S
210  PRINT I * D;
220  POKE 36,22: PRINT  INT (T(I,
     Ø));
230  POKE 36,36: PRINT  INT (T(I,
     1));
240  POKE 36,5Ø: PRINT  INT (T(I,
     Q - 1));
245  POKE 36,64: PRINT  INT (T(I,
     Q))
250  NEXT I
252  PRINT D$;"PR#Ø"
254  PRINT : PRINT : PRINT
255  INPUT "SENT OUTPUT TO DISK (
     Y/N)? ";Z$
256  IF Z$ = "N" THEN 5ØØ
257  IF Z$ <  > "Y" THEN 255
3ØØ  PRINT D$;"OPEN NULL"
310  PRINT D$;"WRITE NULL"
320  FOR I = Ø TO 255
325  IF I > Q THEN T(I,1) = Ø
330  PRINT  INT (T(I,1))
340  NEXT I
350  PRINT D$;"CLOSE NULL"
5ØØ  END
```

DISTRIBUTION LIST

DEPARTMENT OF DEFENSE

Assistant to the Secy of Def, Atomic Energy
ATTN: Executive Assistant

Defense Advanced Rsch Proj Agency
ATTN: COL A. Lowery
ATTN: Dir, Strat Tech Off
ATTN: NMRO

Defense Communications Agency
ATTN: Code 510
ATTN: C670

Defense Intelligence Agency
ATTN: DB-4C, P. Johnson
ATTN: DI-7D
ATTN: DT-1C
ATTN: DT-2

Defense Nuclear Agency
ATTN: NASD
ATTN: NASF
ATTN: NATF
ATTN: NAWE
ATTN: RAAE
ATTN: RAEE
ATTN: RAEV
ATTN: SPAS
ATTN: SPSS
ATTN: SPTD
ATTN: STNA
ATTN: STRA
ATTN: STSP
4 cy ATTN: STTI-CA

Defense Technical Information Center
12 cy ATTN: DD

Field Command, DNA, Det 1
Lawrence Livermore National Lab
ATTN: FC-1

Field Command, Defense Nuclear Agency
ATTN: FCPR
ATTN: FCT
ATTN: FCTT
ATTN: FCTT, W. Summa
ATTN: FCTXE

Joint Chiefs of Staff
ATTN: GD10, J-5 Nuc & Chem Div
ATTN: GD50, J-5 Force Plng & Prog Div
ATTN: SAGA

Joint Data System Support Ctr
ATTN: C-610

Under Secy of Def for Rsch & Engrg
ATTN: Engr Tech, J. Persh
ATTN: Strat & Space Sys (OS)

DEPARTMENT OF THE ARMY

Atmospheric Sciences Laboratory
ATTN: DELAS-EO
ATTN: DELAS-EO, F. Niles

DEPARTMENT OF THE ARMY (Continued)

BMD Advanced Technology Center
ATTN: ATC-T
ATTN: ATC-T, M. Capps

BMD Systems Command
ATTN: BDMSC-H
ATTN: BMDATC-R, W. Dickerson
ATTN: BMDSC-HUL, E. Martz
ATTN: BMDSC-HW, R. DeKalb

Dep Ch of Staff for Rsch, Dev, & Acq
ATTN: DAMA-CSS-N

Harry Diamond Laboratories
ATTN: DELHD-DTSO, 00103
ATTN: DELHD-NW-P, 20240
ATTN: DELHD-NW-P, F. Balicki, 20240
ATTN: DELHD-NW-P, J. Gwaltney, 20240
ATTN: DELHD-TA-L, 81100, Tech Library

Research & Dev Center
ATTN: Commander

Test Measurement & Diagnostic Sys
ATTN: Project Manager

US Army Armament Rsch Dev & Cmd
ATTN: Commander
ATTN: DRDAR-LC
ATTN: DRDAR-LCE
ATTN: DRDAR-LCN
ATTN: DRDAR-LCS-W
ATTN: DRDAR-LCW

US Army Ballistic Research Labs
ATTN: DRDAR-BLA-S, Tech Library
ATTN: DRDAR-BLE
ATTN: DRDAR-BLT
ATTN: DRDAR-BLT, Dr Celmins
ATTN: DRDAR-BLT, J. Keefer
ATTN: DRDAR-BLT, W. Kitchens
ATTN: DRDAR-BLT, W. Schuman
ATTN: DRDAR-BLV-A, R. Mayerhofer

US Army Engr Waterways Exper Station
ATTN: WESGH
ATTN: WESGR
ATTN: WESNV
ATTN: WESSA
ATTN: WESSA, W. Flathau
ATTN: WESSD
ATTN: WESSE
ATTN: WESSS

US Army Material & Mechanics Rsch Ctr
ATTN: Commander
ATTN: DRXMR-HH

DEPARTMENT OF THE NAVY

David Taylor Naval Ship R&D Ctr
ATTN: Code 17
ATTN: Commander
ATTN: Structures Dept

DEPARTMENT OF THE NAVY (Continued)

Dir Cmd Control Planning & Programing Div, OP-940
ATTN: OP-981-N1

Joint Cruise Missiles Project Ofc
ATTN: Director

Naval Material Command
ATTN: Commander
ATTN: MAT-0323

Naval Ocean Systems Center
ATTN: Code 8122, W. Flanigan
ATTN: Commander
ATTN: W. Shaw

Naval Research Laboratory
ATTN: Commander

Naval Sea Systems Command
ATTN: SEA-0352
ATTN: SEA-3221

Naval Surface Weapons Center
ATTN: Code K06

Naval Surface Weapons Center
ATTN: Commander

Naval Weapons Center
ATTN: Commander

DEPARTMENT OF THE AIR FORCE

Aeronautical Systems Division
ATTN: ASD/ENSG, CPT J. Greneczho
ATTN: ASD/ENSSA
ATTN: ASD/ENSSS, D. Ward

Air Force Engineering & Services Ctr
ATTN: Commander

Air Force Institute of Technology
ATTN: Library

Air Force Weapons Laboratory
ATTN: NT, COL S. Tyler
ATTN: NTE
ATTN: NTO
ATTN: SAB
ATTN: SUL

Air Force Wright Aeronautical Lab
Flight Dynamics Laboratory
ATTN: Commandant
ATTN: FIMG

Air Force Wright Aeronautical Lab
Materials Laboratory
ATTN: Commandant
ATTN: LPH
ATTN: MAS
ATTN: MLBC

Air University Library
ATTN: AUL-LSE

Ballistic Missile Office/DAA
ATTN: ENMR

DEPARTMENT OF THE AIR FORCE (Continued)

Deputy Ch of Staff for Rsch, Dev, & Acq
ATTN: AFRD
ATTN: AFRDQI
ATTN: AFRDS, Space Sys & C3 Dir

OTHER GOVERNMENT AGENCY

Federal Emergency Management Agency
ATTN: Ofc of Rsch/NP, D. Bensen

FOREIGN AGENCIES

British Defence Staff, British Embassy
ATTN: ACOW
ATTN: AWRE, Mr Samuels

Bundes ministerium de Verteidigung
ATTN: E. Hentschel

Defense Research Establishment, Suffield
ATTN: R. Heggie

Ernst-Mach-Institut
ATTN: H. Reichenbach

Inqeniur En Chef De L'Armement DRET/SDNBC
ATTN: COL Raphael Amat

Technologisch Laboratorium (TNO)
ATTN: Director

Wehrwissenschaftliche Dienststelle der
Bundeswehr fur ABC-Schutz
ATTN: H. Kruger

DEPARTMENT OF ENERGY CONTRACTORS

University of California
Lawrence Livermore National Lab
ATTN: Director
ATTN: L-125, J. Keller
ATTN: L-262, J. Knox
ATTN: L-8, P. Chrzanowski

Los Alamos National Laboratory
ATTN: J. Hopkins
ATTN: MS 670/T&V

Oak Ridge National Laboratory
ATTN: Civ Def Res Proj, Mr Kearny

Sandia National Laboratories
ATTN: Dept 1100, T. Dowler

DEPARTMENT OF DEFENSE CONTRACTORS

Aerospace Corp
ATTN: R. Crolius

Analytic Services, Inc (ANSER)
ATTN: J. Selig

AVCO Systems Division
ATTN: Document Control

Boeing Co
ATTN: M/S 85/20, E. York
ATTN: R. Holmes

DEPARTMENT OF DEFENSE CONTRACTORS (Continued)

Boeing Co
ATTN: M/S 13-13, R. Dyrdahl

Calspan Corp
ATTN M. Holden

Carpenter Research Corp
ATTN: H. Carpenter

University of Colorado Seminary, Denver
ATTN: Sec Officer for J. Wisotski
ATTN: Sec Officer for L. Brown

EG&G, Inc
ATTN: R. Ward

Electro-Mech Systems, Inc
ATTN: R. Shunk

General Research Corp
ATTN: T. Stathacopoulos

Institute for Defense Analyses
ATTN: Classified Library

Kaman AviDyne
ATTN: N. Hobbs
ATTN: S. Criscione

Kaman Sciences Corp
ATTN: F. Shelton

Kaman Sciences Corp
ATTN: E. Conrad

Kaman Tempo
ATTN: DASIAC

Kaman Tempo
ATTN: DASIAC

Kaman Tempo
ATTN: E. Bryant

Lockheed Missiles & Space Co, Inc
ATTN: F. Borgardt

Lockheed Missiles & Space Co, Inc
ATTN: R. Walz

Martin Marietta Corp
ATTN: G. Aiello

TRW Electronics & Defense Sector
ATTN: N. Lipner

TRW Electronics & Defense Sector
ATTN: P. Dai
ATTN: R. Mortensen

Weidlinger Assoc, Consulting Engrg
ATTN: T. Deevy

DEPARTMENT OF DEFENSE CONTRACTORS (Continued)

McDonnell Douglas Corp
ATTN: E. Fitzgerald

National Academy of Sciences
ATTN: National Materials Advisory Board

University of New Mexico
New Mexico Engineering Research Institute
ATTN: G. Lane

Northrop Corp
ATTN: D. Hicks

Pan Am World Service, Inc 2
ATTN: AEDC/Library Doc, TRF

PDA Engineering
ATTN: J. McDonald

Physics International Co
ATTN: Tech Library

R&D Associates
ATTN: F. Field
ATTN: P. Haas

Rand Corp
ATTN: P. Davis

Rand Corp
ATTN: B. Bennett

S-CUBED
ATTN: R. Duff

Science Applications Intl Corp
ATTN: W. Layson
2 cy ATTN: M. McDonnell
2 cy ATTN: N. Olson
2 cy ATTN: S. Woods

Science Applications, Inc
ATTN: W. Plows

Science Applications, Inc
ATTN: C. Swain

Science Applications, Inc
ATTN: J. Manship

Southern Research Institute
ATTN: C. Pears

SRI International
ATTN: A. Burns
ATTN: G. Abrahamson
ATTN: H. Lindberg

Teledyne Brown Engineering
ATTN: R. Patrick

Terra TEK, Inc
ATTN: S. Green

END

FILMED

9-85

DTIC